

BSC

Design Calculation or Analysis Cover Sheet

1. QA:QA

2. Page 1

Complete only applicable items.

3. System Monitored Geologic Repository				4. Document Identifier 000-00C-MGR0-04700-000-00A			
5. Title Bias and Range of Applicability Determinations for Commercial Nuclear Fuels							
6. Group Licensing & Nuclear Safety / Preclosure Safety Analysis/ Preclosure Criticality							
7. Document Status Designation <input type="checkbox"/> Preliminary <input checked="" type="checkbox"/> Committed <input type="checkbox"/> Confirmed <input type="checkbox"/> Cancelled/Superseded							
8. Notes/Comments None							
Attachments							Total Number of Pages
Attachment 1: Tables of Statistics Values							4
Attachment 2: Critical Benchmark Pin Maps for LEU-COMP-THERM-007							2
Attachment 3: Critical Benchmark Pin Maps for LEU-COMP-THERM-011							9
Attachment 4: Critical Benchmark Pin Maps for LEU-COMP-THERM-021							2
Attachment 5: List of Files on the Attachment 6 CD							1
Attachment 6: One CD							N/A
RECORD OF REVISIONS							
9. No.	10. Reason For Revision	11. Total # of Pgs.	12. Last Pg. #	13. Originator (Print/Sign/Date)	14. Checker (Print/Sign/Date)	15. EGS (Print/Sign/Date)	16. Approved/Accepted (Print/Sign/Date)
00A	Initial Issue	92	92	W. G. Rhoden <i>W. G. Rhoden</i> 2/21/08	D. M. Vaughn <i>D. M. Vaughn</i> 2/21/08	A. A. Alsaed <i>A. A. Alsaed</i> 2/21/08	M. R. Wisenberg <i>M. R. Wisenberg</i> 2/21/08

DISCLAIMER

The calculations contained in this document were developed by Bechtel SAIC Company, LLC (BSC) and are intended solely for the use of BSC in its work for the Yucca Mountain Project.

CONTENTS	Page
DISCLAIMER	2
ACRONYMS AND ABBREVIATIONS	8
1. PURPOSE	10
1.1 SCOPE	10
1.2 TERMINOLOGY CONSISTENCY	10
2. REFERENCES	10
2.1 PROCEDURES/DIRECTIVES	10
2.2 DESIGN INPUTS	11
2.3 DESIGN CONSTRAINTS	12
2.4 DESIGN OUTPUTS	12
3. ASSUMPTIONS	12
3.1 ASSUMPTIONS REQUIRING VERIFICATION	12
3.2 ASSUMPTIONS NOT REQUIRING VERIFICATION	12
3.2.1 Zn Cross Section Replacement	12
4. METHODOLOGY	13
4.1 QUALITY ASSURANCE	13
4.2 USE OF SOFTWARE	13
4.2.1 MCNP	13
4.2.2 EXCEL	14
4.3 ANALYSIS PROCESS	15
4.3.1 Weighted Single-Sided Tolerance Limit for Normal Data	17
4.3.2 Shapiro-Wilk Test Procedure for Normality	19
4.3.3 Single-Sided Distribution Free Tolerance Limit	20
5. LIST OF ATTACHMENTS	22
6. BODY OF CALCULATION	22
6.1 BENCHMARK DESCRIPTIONS	22
6.1.1 LEU-COMP-THERM-001	23
6.1.2 LEU-COMP-THERM-002	28
6.1.3 LEU-COMP-THERM-007	31
6.1.4 LEU-COMP-THERM-011	39
6.1.5 LEU-COMP-THERM-021	49
6.1.6 LEU-COMP-THERM-034	56
6.2 DETERMINATION OF CRITICAL LIMIT (K_L)	66
6.2.1 Benchmark Results	66
6.2.2 Test for Normality of Benchmark results	67
6.2.3 Single-Sided Distribution Free Tolerance Limit Determination	67
6.3 RANGE OF APPLICABILITY DETERMINATIONS AND COMPARISONS	68
7. RESULTS AND CONCLUSIONS	73

ATTACHMENT 1: TABLES OF STATISTICS VALUES.....	75
ATTACHMENT 2: CRITICAL BENCHMARK PIN MAPS FOR LEU-COMP-THERM-007..	79
ATTACHMENT 3: CRITICAL BENCHMARK PIN MAPS FOR LEU-COMP-THERM-011..	81
ATTACHMENT 4: CRITICAL BENCHMARK PIN MAPS FOR LEU-COMP-THERM-021..	90
ATTACHMENT 5: LIST OF FILES ON THE ATTACHMENT 6 CD	92

FIGURES	Page
Figure 1. Neutron Absorption Cross Sections for ^{63}Cu and Natural Zn	13
Figure 2. Depiction of Fuel Pin Model for LEU-COMP-THERM-001 Benchmark	23
Figure 3. Arrangement of Fuel Pin Clusters for Critical Benchmarks from the LEU-COMP-THERM-001 Benchmark	24
Figure 4. Fuel Pin Model for LEU-COMP-THERM-002	29
Figure 5. Arrangement of Fuel Pin Clusters for Critical Benchmarks from the LEU-COMP-THERM-002 Benchmark	29
Figure 6. Fuel Pin Model for LEU-COMP-THERM-007	32
Figure 7. Elevation View of Basic Benchmark Model for LEU-COMP-THERM-007	35
Figure 8. Fuel Pin Dimensions for LEU-COMP-THERM-011 Benchmark Model	40
Figure 9. Basic Dimensions of the Spacer Grids for LEU-COMP-THERM-011 Benchmark	41
Figure 10. As Modeled Dimensions of the B_4C Absorber Rods for LEU-COMP-THERM-011	42
Figure 11. Basic Axial Configuration of Benchmark Models for LEU-COMP-THERM-011	43
Figure 12. Fuel Pin Dimensions for LEU-COMP-THERM-021 Benchmark Model	50
Figure 13. Axial Depiction of Benchmark Model for LEU-COMP-THERM-021	52
Figure 14. Axial Views of the as-modeled Experimental Setup for LEU-COMP-THERM-034	58
Figure 15. Fuel Pin Assembly Arrangement for LEU-COMP-THERM-034	60
Figure 16. Pin Maps for Cases 1 through 6 for LEU-COMP-THERM-007	79
Figure 17. Pin Maps for Cases 7 through 10 for LEU-COMP-THERM-007	80
Figure 18. Pin Map for Case 1 of LEU-COMP-THERM-011	81
Figure 19. Pin Map for Case 2 of LEU-COMP-THERM-011	82
Figure 20. Pin Map for Cases 3 through 9 of LEU-COMP-THERM-011	83
Figure 21. Pin Map for Case 10 of LEU-COMP-THERM-011	84
Figure 22. Pin Map for Case 11 of LEU-COMP-THERM-011	85
Figure 23. Pin Map for Case 12 of LEU-COMP-THERM-011	86
Figure 24. Pin Map for Case 13 of LEU-COMP-THERM-011	87
Figure 25. Pin Map for Case 14 of LEU-COMP-THERM-011	88
Figure 26. Pin Map for Case 15 of LEU-COMP-THERM-011	89
Figure 27. Case 1 Pin Map for LEU-COMP-THERM-021	90
Figure 28. Case 2 Pin Map for LEU-COMP-THERM-021	90
Figure 29. Case 3 Pin Map for LEU-COMP-THERM-021	91

TABLES	Page
Table 1. Single-Sided Lower Tolerance Factors (U)	19
Table 2. Values of m for a Single-Sided Distribution Free Tolerance Limit.....	21
Table 3. Non-Parametric Margins.....	22
Table 4. Fuel Pin Material Specifications for LEU-COMP-THERM-001 Benchmark.....	25
Table 5. Water Material Specification	27
Table 6. Acrylic Material Specification for LEU-COMP-THERM-001	27
Table 7. Fuel Pin Material Specifications for LEU-COMP-THERM-002 Benchmark.....	30
Table 8. Fuel Pin Model Geometry Data for LEU-COMP-THERM-007	33
Table 9. Critical Benchmark Model Information for LEU-COMP-THERM-007	34
Table 10. Fuel Material Specifications for LEU-COMP-THERM-007	37
Table 11. Material Specification for Z2CN18-10 Stainless Steel for LEU-COMP-THERM-007	38
Table 12. Expected k_{eff} and Estimated Experimental Uncertainties for LEU-COMP-THERM-007	39
Table 13. Fuel Pin Model Geometry Data for LEU-COMP-THERM-011	40
Table 14. Benchmark Model Critical Information for LEU-COMP-THERM-011	44
Table 15. Fuel Pin Material Specifications for LEU-COMP-THERM-011 Benchmark.....	46
Table 16. Atom Densities for the Water/Borated Water Moderator for LEU-COMP-THERM-011	47
Table 17. Material Specification for B ₄ C for LEU-COMP-THERM-011	47
Table 18. Expected Experimental k_{eff} and Estimated Experimental Uncertainties for LEU-COMP-THERM-011	48
Table 19. Fuel Pin Model Geometry Data for LEU-COMP-THERM-021	49
Table 20. Benchmark Model Critical Parameters for LEU-COMP-THERM-021	51
Table 21. Fuel Pin Material Specifications for LEU-COMP-THERM-021 Benchmark.....	53
Table 22. Material Specification for Borated Water for LEU-COMP-THERM-021	54
Table 23. Material Specification for Steel 3 for LEU-COMP-THERM-021	54
Table 24. Material Specification for Aluminum D1 Alloy for LEU-COMP-THERM-021	55
Table 25. Expected k_{eff} and Estimated Experimental Uncertainties for LEU-COMP-THERM-021	55
Table 26. Fuel Pin Model Geometry Data for LEU-COMP-THERM-034	59
Table 27. Benchmark Critical Parameters for LEU-COMP-THERM-034	61
Table 28. Fuel Material Specifications for LEU-COMP-THERM-034	62
Table 29. Water Material Specification	63
Table 30. Boral B ₄ C+Al Material Specification for LEU-COMP-THERM-034	63
Table 31. Borated Steel Material Specification for LEU-COMP-THERM-034	64
Table 32. Expected k_{eff} and Estimated Experimental Uncertainties for LEU-COMP-THERM-034	65
Table 33. Benchmark Results	66
Table 34. Parameter Values and Ranges for the MCNP Modeled Critical Benchmarks and Selected Commercial Nuclear Fuel Models.....	70
Table 35. Significant MCNP Models of Commercial Nuclear Fuel from the Criticality Safety Analysis.....	71
Table 36. Estimated Boron Worth in Selected MCNP Models	73
Table 37. Range of Applicability for Commercial Fuel Modeled with MCNP.....	74
Table 38. Lower Tail Values of W for n experiments at the 95% Confidence Level	75

Table 39. Values of α_j for the Shapiro-Wilks Test for Normality	76
Table 40. Values of α_j for the Shapiro-Wilks Test for Normality	76
Table 41. Values of α_j for the Shapiro-Wilks Test for Normality	77
Table 42. Values of α_j for the Shapiro-Wilks Test for Normality	78

ACRONYMS AND ABBREVIATIONS

Acronyms

AENCF	average energy of neutron causing fission
CD	compact disc
DIRS	document input reference system
EALF	energy of average lethargy of neutron causing fission
ENDF	evaluated nuclear data file
EROA	extending range of applicability
GROA	geologic repository operations area
LEU	Low Enriched Uranium
MCNP	Monte Carlo N-Particle
MPC	multi-purpose canister
NEA	Nuclear Energy Agency
NPM	non-parametric margin
OD	outer diameter
PNL	pacific northwest laboratories
PWR	pressurized water reactor
ROA	range of applicability
ROP	range of parameters
USL	upper subcritical limit
WHF	Wet Handling Facility

Abbreviations

°C	degrees Celsius
COMP	Compound
cm	centimeter
cm ³	cubic centimeters
g	grams
K	degrees Kelvin
k _{eff}	effective neutron multiplication factor
L	liter
mg	milligram

mm	millimeter
Ref.	reference
THERM	Thermal
wt. %	weight percent

1. PURPOSE

The purpose of this calculation is to apply the process described in the *Preclosure Criticality Analysis Process Report* (Ref. 2.2.12) to establish the bias for k_{eff} calculations performed for commercial nuclear fuels using the MCNP code system. This bias will be used in criticality safety analyses as part of the basis for establishing the upper subcritical limit (USL). This calculation also defines the range of applicability (ROA) for which the bias may be used directly without need to consider additional penalties on the USL. In addition, the range of parameters (ROP) is determined for those MCNP models of commercial nuclear fuels that are expected to be relied upon to form the criticality safety basis for the geologic repository operations area (GROA). The comparison of the ROP of the MCNP models of commercial nuclear fuels and the ROA of the modeled critical benchmarks is used as the basis for determining the need for any additional penalties on the USL.

MCNP is used throughout this document to refer specifically to version 4B2 as described in Section 4.2.1.

1.1 SCOPE

The scope of this calculation is limited to evaluating the bias that is specifically applicable to the MCNP code as given in Section 4.2.1 and the MCNP modeling of commercial nuclear fuels for determining values of k_{eff} . This bias determination does not include any credit for burnup and is specifically designed for calculations that take no credit for fuel burnup (i.e., model fresh fuel). This calculation also evaluates the need for additional penalties on the USL.

1.2 TERMINOLOGY CONSISTENCY

The terminology used in the benchmark reports referenced by this document is not always consistent. This document uses consistent terminology throughout and therefore, at times, will not exactly match the terminology utilized in the benchmark reports. In most cases translation between the terminology used herein and that used in the benchmark reports will be obvious (e.g., fuel pin versus fuel rod). In those cases where it may not be obvious the correlation between terminologies will be noted.

2. REFERENCES

This section presents the references used in this calculation. Where applicable, the document input reference system (DIRS) number is in parentheses at the end of the reference.

2.1 PROCEDURES/DIRECTIVES

- 2.1.1 EG-PRO-3DP-G04B-00037, *Calculations and Analyses*, Rev. 10, Las Vegas, Nevada: Bechtel SAIC Company, ACC: ENG.20071018.0001.
- 2.1.2 LS-PRO-0201, *Preclosure Safety Analysis Procedure*, Rev. 5, Las Vegas, Nevada: Bechtel SAIC Company, ACC: ENG.20071010.0021.
- 2.1.3 IT-PRO-0011, *Software Management*, Rev. 7, Las Vegas, Nevada: Bechtel SAIC Company, ACC: DOC.20070905.0007.

- 2.1.4 QA-DIR-10, *Quality Management Directive*, Rev. 2, Las Vegas, Nevada: Bechtel SAIC Company, ACC: DOC.20080103.0002.
- 2.1.5 IT-PRO-0012, *Qualification of Software*, Rev. 4, Las Vegas, Nevada: Bechtel SAIC Company, ACC: DOC.20070319.0014.

2.2 DESIGN INPUTS

- 2.2.1 ANSI/ANS-8.17-2004. 2004. *American National Standard, Criticality Safety Criteria for the Handling, Storage and Transportation of LWR Fuel Outside Reactors*. La Grange Park, Illinois: American Nuclear Society. TIC: 257593 (DIRS 176225)
- 2.2.2 ANSI/ANS-8.24-2007. 2007. *American National Standard, Validation of Neutron Transport Methods for Nuclear Criticality Safety Calculations*. La Grange Park, Illinois: American Nuclear Society. TIC: 259483 (DIRS 182309)
- 2.2.3 Dean, J.C. and Tayloe, R.W., Jr. 2001. *Guide for Validation of Nuclear Criticality Safety Calculational Methodology*. NUREG/CR-6698. Washington, D.C.: U.S. Nuclear Regulatory Commission. TIC: 254004 (DIRS 161786)
- 2.2.4 Briesmeister, J.F., ed. 1997. *MCNP-A General Monte Carlo N-Particle Transport Code. LA-12625-M, Version 4B*. Los Alamos, New Mexico: Los Alamos National Laboratory. ACC: MOL.19980624.0328 (DIRS 103897).
- 2.2.5 CRWMS M&O 1998. *Software Qualification Report for MCNP Version 4B2, A General Monte Carlo N-Particle Transport Code*. CSCI: 30033 V4B2LV. DI: 30033-2003, Rev. 01. Las Vegas, Nevada: CRWMS M&O. ACC: MOL.19980622.0637 (DIRS 102836).
- 2.2.6 NEA (Nuclear Energy Agency) 2006. *International Handbook of Evaluated Criticality Safety Benchmark Experiments*. September 2006 Edition. NEA/NSC/DOC(95)03. [Paris, France]: Nuclear Energy Agency, Organisation for Economic Co-Operation and Development. TIC: 259708 (DIRS 182629)
- 2.2.7 Baum, E.M.; Knox, H.D.; and Miller, T.R. 2002. *Nuclides and Isotopes*. 16th edition. [Schenectady, New York]: Knolls Atomic Power Laboratory. TIC: 255130. (DIRS 175238).
- 2.2.8 Lide, D.R., ed. 2006. *CRC Handbook of Chemistry and Physics*. 87th Edition. Boca Raton, Florida: CRC Press. ISBN: 0-8493-0487-3. TIC: 258634 (DIRS 178081).
- 2.2.9 Natrella, M.G. 1963. *Experimental Statistics*. National Bureau of Standards Handbook 91. Washington, D.C.: U.S. Department of Commerce, National Bureau of Standards. TIC: 245911 (DIRS 103886)
- 2.2.10 BSC (Bechtel SAIC Company) 2002, *Software Baseline Request, MCNP V4B2LV, LV-2002-270*. Software Tracking Number: 10437-4B2LV-00. Las Vegas, Nevada: Bechtel SAIC Company ACC: MOL.20030312.0066 (DIRS 183325)
- 2.2.11 MCNP V.4B2LV.2002. WINDOWS 2000.STN: 10437-4B2LV-00 (DIRS 163407)

- 2.2.12 BSC (Bechtel SAIC Company) 2008. *Preclosure Criticality Analysis Process Report*. TDR-DS0-NU-000001, Rev. 03, Las Vegas, Nevada: Bechtel SAIC Company. ACC : ENG.20080220.0001 (DIRS 185056)
- 2.2.13 D'Agostino, R.B. and Stephens, M.A., eds. 1986. *Goodness-Of-Fit Techniques*. Statistics, Textbooks and Monographs Volume 68. New York, New York: Marcel Dekker. TIC: 253256. ISBN: 0824774876 (DIRS 160320)
- 2.2.14 BSC (Bechtel SAIC Company) 2007. *Nuclear Criticality Calculations for the Wet Handling Facility*. 050-00C-WH00-00100-000-00A. Las Vegas, Nevada: Bechtel SAIC Company. ACC: ENG.20071212.0001. (DIRS 182101)

2.3 DESIGN CONSTRAINTS

None.

2.4 DESIGN OUTPUTS

- 2.4.1 BSC (Bechtel SAIC Company) 2008. *Preclosure Criticality Safety Analysis*. TDR-MGR-NU-000002, Las Vegas, Nevada: Bechtel SAIC Company.

3. ASSUMPTIONS

3.1 ASSUMPTIONS REQUIRING VERIFICATION

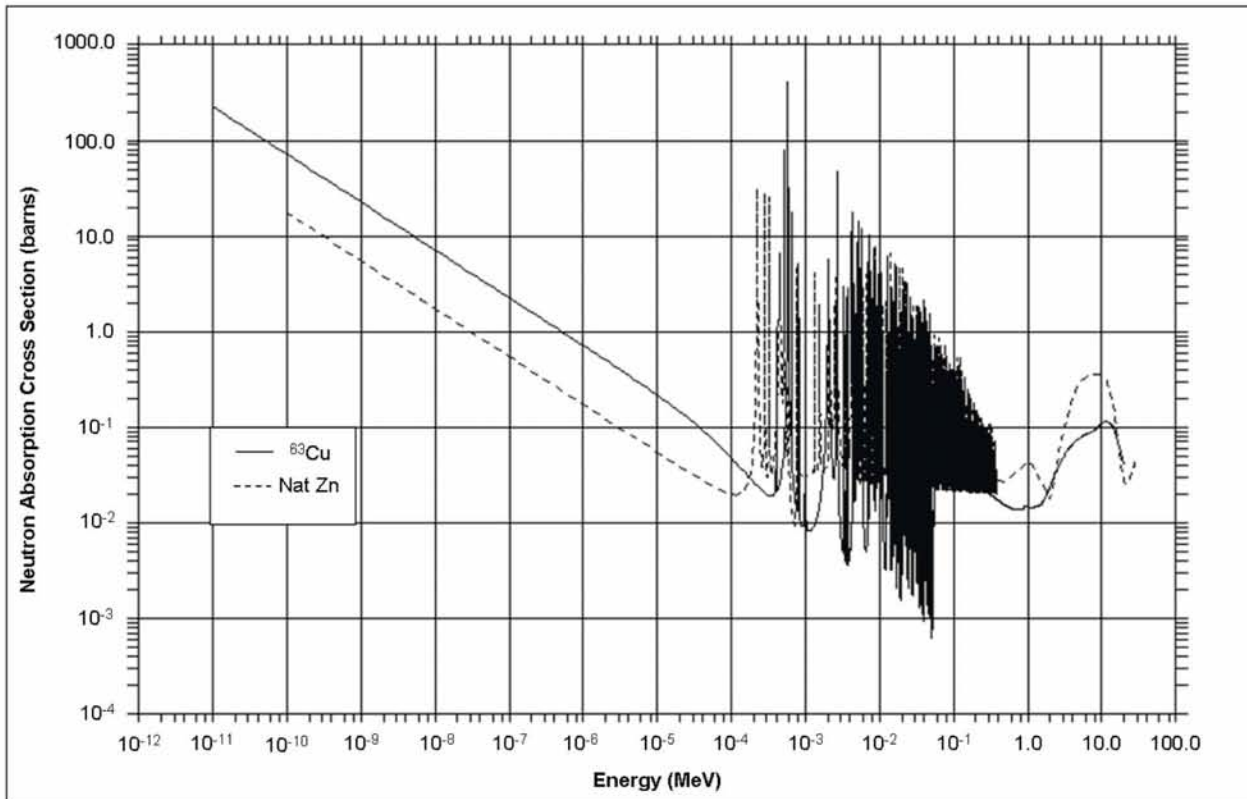
There are no assumptions that require verification in this calculation.

3.2 ASSUMPTIONS NOT REQUIRING VERIFICATION

3.2.1 Zn Cross Section Replacement

Assumption-No ENDF V or ENDF VI zinc cross sections exist for use in MCNP therefore, the ENDF VI ^{63}Cu cross section from MCNP will be used in place of Zn used in the material specifications listing Zn as part of its constituents for the critical benchmark models described in Section 6.1. The ^{63}Cu will be added to the material separately and with the same atom density as Zn.

Rationale-The ^{63}Cu cross section is larger than the Zn cross section as can be seen from Figure 1. This figure is generated by the plot functions of MCNP and is based upon an older MCNP cross section for zinc and the ENDF VI based cross section for ^{63}Cu used throughout this calculation. *Nuclides and Isotopes* (Ref. 2.2.7) shows that the thermal cross section of zinc is 1.1 barns and the resonance integral is 2.8 barns. *Nuclides and Isotopes* (Ref. 2.2.7) also shows that the thermal cross section of ^{63}Cu is 4.5 barns and the resonance integral is 5.0 barns. This shows that ^{63}Cu has, in general, a larger cross section than Zn and its use in replacing Zn in these validation models is conservative.



Source: Original to this document (as generated by MCNP)

Figure 1. Neutron Absorption Cross Sections for ^{63}Cu and Natural Zn

Use in the Calculation-Used in MCNP models as noted in the material specifications given in Section 6.1.

4. METHODOLOGY

4.1 QUALITY ASSURANCE

This calculation is prepared in accordance with EG-PRO-3DP-G04B-00037, *Calculations and Analyses* (Ref. 2.1.1) and LS-PRO-0201, *Preclosure Safety Analysis Procedure* (Ref. 2.1.2). Therefore, the approved record version is designated as QA:QA. This calculation is subject to the applicable requirements of QA-DIR-10, *Quality Management Directive* (Ref. 2.1.4).

4.2 USE OF SOFTWARE

4.2.1 MCNP

The baselined Monte MCNP code (Ref. 2.2.11) was used to calculate the effective neutron multiplication factor (k_{eff}) for various critical benchmarks. The software specifications are as follows:

- Software Title: MCNP
- Version/Revision Number: Version 4B2LV
- Status/Operating System: Qualified/Microsoft Windows 2000 Service Pack 4

- Software Tracking Number: 10437-4B2LV-00
- Computer Type: Dell OPTIPLEX GX260 and GX270 Workstations.

The input and output files for the MCNP calculations are contained on a compact disc attachment to this calculation (Attachment 6) as described in Section 5. The MCNP software has been validated as being appropriate for use in modeling a range of radiation transport problems as documented in *Software Qualification Report for MCNP Version 4B2, A General Monte Carlo N-Particle Transport Code* (Ref. 2.2.5). This range of validated problems includes using MCNP to determine k_{eff} of systems containing fissile material. The use of MCNP Version 4B2 was qualified for use under the Windows 2000 operating system by *Software Baseline Request, MCNP V4B2LV* (Ref. 2.2.10). The use of MCNP in determining k_{eff} values is further documented in *MCNP-A General Monte Carlo N-Particle Transport Code* (Ref. 2.2.4). The MCNP software was obtained from Software Configuration Management in accordance with the appropriate procedure IT-PRO-0011, *Software Management* (Ref. 2.1.3).

The software qualification report *Software Qualification Report for MCNP Version 4B2, A General Monte Carlo N-Particle Transport Code* (Ref. 2.2.5) was performed prior to the effective date of IT-PRO-0012, *Qualification of Software* (Ref. 2.1.5), however, MCNP Version 4B2 was qualified software in the centralized baseline as of the effective date of IT-PRO-0012, *Qualification of Software* (Ref. 2.1.5) and is therefore considered acceptable and part of the established software baseline available for level 1 usage (*Qualification of Software*, Ref. 2.1.5, Paragraph 1.2.3).

4.2.2 EXCEL

- Software Title: Excel
- Version/Revision number: Microsoft® Excel 2000 SP-3 (on OPTIPLEX GX260 Workstation)
- Version/Revision number: Microsoft® Excel 2003 SP-2 (on OPTIPLEX GX620 Workstation)
- Computer Environment for Microsoft® Excel 2000: Software is installed on a DELL OPTIPLEX GX260 personal computer, running Microsoft Windows 2000, Service Pack 4.
- Computer Environment for Microsoft® Excel 2003: Software is installed on a DELL OPTIPLEX GX620 personal computer, running Microsoft Windows XP Professional, Version 2002, Service Pack 2.

Microsoft Excel for Windows is used in calculations and analyses to process results using standard mathematical expressions, operations, and functions. It is also used to tabulate and chart results. The user-defined formulas, inputs, and results are documented in sufficient detail to allow an independent repetition of computations. Thus, Microsoft Excel is used only as a worksheet and not as a software routine. The use of Excel in this calculation constitutes Level 2 software usage (Ref. 2.1.3, Attachment 12) and does not require qualification of the software in accordance with IT-PRO-0012 (Ref. 2.1.5).

The spreadsheet files for the Excel calculations are documented in Attachment 5. The Excel calculations and graphical presentations were verified by hand calculations and visual inspection.

4.3 ANALYSIS PROCESS

This calculation is performed as part of the criticality safety analysis process described in the *Preclosure Criticality Analysis Report* (Ref. 2.2.12).

The determinations of the bias and ROA are performed in accordance with the basic requirements associated with code validation from *Criticality Safety Criteria for the Handling, Storage and Transportation of LWR Fuel Outside Reactors* (Ref. 2.2.1) and *Validation of Neutron Transport Methods for Nuclear Criticality Safety Calculations* (Ref. 2.2.2). The basic process used for the bias determination and the mathematical techniques utilized come from *Guide for Validation of Nuclear Criticality Safety Computational Methodology* (Ref. 2.2.3) with changes as noted in the below discussion. The code bias and ROA are needed to determine the upper subcritical limit (USL) applicable to a specific set of pertinent parameter ranges. The relationship of these items is shown in the following equation;

$$\text{USL} = 1.0 - \text{bias} - \Delta k_{\text{EROA}} - \Delta k_m \quad (\text{Eq. 1})$$

Where

bias = the difference between the calculated k_{eff} of a modeled critical experiment and the experimentally determined k_{eff} of the critical experiment (1.0 by definition). Determined statistically and includes uncertainty in the bias and experimental uncertainties (when known)

Δk_{EROA} = penalty for extending the range of applicability

Δk_m = an administrative margin ensuring subcriticality, turning the critical limit function into an USL function

A value for Δk_{EROA} is determined based on a comparison between the ROA of the modeled critical benchmarks and the ROP of selected MCNP models of commercial nuclear fuels. Details of the determination of Δk_{EROA} can be found in Section 6.3.

A value for Δk_m is not determined in this calculation since it is dependent upon other factors (e.g., control parameters) which are particular to the specific operations and/or physical arrangements being evaluated.

The bias is a statistically determined measure of the calculation method's ability (in this case MCNP's) to properly predict k_{eff} values for known critical configurations. This statistical determination is based on a population of modeled critical benchmarks with similar characteristics to the configurations to which the USL is expected to be applied. The selection of critical experiments is based on identifying parameters important to criticality safety for the configurations to which the USL is expected to be applied and then using these parameters as a guide to identify applicable critical experiments. The range of these identified parameters for the selected critical benchmarks becomes the ROA.

The bias is a measure of the differences between MCNP's k_{eff} predictions and the experimental k_{eff} determinations which would be expected to follow a normal distribution. Specifically, the bias is the difference between the average k_{eff} determined by MCNP and the experimentally determined k_{eff} . For critical benchmark experiments, the experimental k_{eff} is, by definition, 1.0. However, as a result of experimental uncertainties and biases, a “critical benchmark” can be slightly subcritical or supercritical. This possibility has been evaluated in the *International Handbook of Evaluated Criticality Safety Benchmark Experiments* (Ref. 2.2.6) from which the critical benchmarks used in this analysis have been taken. In those cases where the critical benchmark has been determined to be slightly subcritical, the k_{eff} value for these benchmarks will conservatively be assumed to be 1.0. For those cases in which the experimental k_{eff} values of the critical benchmarks are slightly supercritical, the MCNP determined k_{eff} values for these benchmarks will be adjusted based upon the following equation;

$$k_{\text{adj}} = k_{\text{MCNP}} - (k_{\text{exp}} - 1) \quad (\text{Eq. 2})$$

Where,

k_{adj} = Adjusted k_{eff} value to be used as k_{MCNP}

k_{MCNP} = Original MCNP estimated k_{eff} for the critical benchmark

k_{exp} = Estimated k_{eff} from the critical experiment with a value that is greater than 1

The average MCNP determined k_{eff} is an average weighted by the combined calculation and experimental uncertainties.

The combined calculation and experimental uncertainty is given by;

$$\sigma_t = \sqrt{\sigma_{\text{calc}}^2 + \sigma_{\text{exp}}^2} \quad (\text{Eq. 3})$$

Where,

σ_{calc} = uncertainty associated with the determination of k_{eff} by MCNP

σ_{exp} = estimated experimental uncertainty from critical experiment

The weighted mean k_{adj} for the MCNP determined k_{eff} values is given by;

$$\bar{k}_{adj} = \frac{\sum \left[\frac{1}{\sigma_{t_i}^2} k_{adj_i} \right]}{\sum \frac{1}{\sigma_{t_i}^2}} \quad (\text{Eq. 4})$$

where,

\bar{k}_{adj} = weighted mean of the MCNP calculated k_{eff} values

$\sigma_{t_i}^2$ = total variance for the i^{th} critical experiment based on Eq. 3

k_{adj_i} = MCNP determined k_{adj} for the i^{th} critical experiment

A weighted single-sided tolerance limit method applicable to normally distributed data will be used to determine the bias. The use of this method requires that the data be normally distributed. This assertion will be verified through the use of the Shapiro-Wilk test for normality. Should the data be shown not to be normally distributed, then a distribution free statistical treatment will be utilized to determine the bias.

4.3.1 Weighted Single-Sided Tolerance Limit for Normal Data

The weighted single-sided tolerance limit method for normally distributed data is based upon the procedure given in *Guide for Validation of Nuclear Criticality Safety Computational Methodology* (Ref. 2.2.3). The Shapiro-Wilk test procedure used to demonstrate normality in the data is also taken from *Guide for Validation of Nuclear Criticality Safety Computational Methodology* (Ref. 2.2.3). The Shapiro-Wilk test is described in Section 4.3.2.

A weighted single-sided lower tolerance limit (K_L) is a single lower limit above which a defined fraction of the MCNP determined k_{eff} values is expected to lie, with a prescribed confidence for modeled critical benchmarks that are within the ROA. For normally distributed data this becomes the bias given in Eq. 1. The term “weighted” refers to a specific statistical technique where the inverse of the combined MCNP and experimental uncertainties (σ_t from Eq. 3) associated with the k_{adj} value are used to weight the data point when determining values such as the weighted mean k_{adj} value per Eq. 4.

The other quantities that need to be determined for the weighted single-sided lower tolerance limit are;

$$s^2 = \frac{\frac{1}{n-1} \sum \frac{1}{\sigma_{t_i}^2} (k_{adj_i} - \bar{k}_{adj})^2}{\frac{1}{n} \sum \frac{1}{\sigma_{t_i}^2}} \quad (\text{Eq. 5})$$

$$\overline{\sigma_t}^2 = \frac{n}{\sum \frac{1}{\sigma_{t_i}^2}} \quad (\text{Eq. 6})$$

$$S_P = \sqrt{s^2 + \overline{\sigma_t}^2} \quad (\text{Eq. 7})$$

Where,

s^2 = variance about the mean

n = number of modeled critical experiments

k_{adj_i} = k_{adj} value for the i^{th} experiment

$\overline{k_{adj}}$ = weighted mean k_{adj} per Eq. 4

$\overline{\sigma_t}^2$ = average total variance

$\sigma_{t_i}^2$ = total variance for the i^{th} critical experiment based on Eq. 3

S_P = square root of the pooled variance

The square root of the pooled variance (S_P) is used as the mean bias uncertainty for this single-sided tolerance limit method. The bias determined by this single-sided tolerance method is K_L and is given by;

$$K_L = \overline{k_{adj}} - US_P \quad (\text{Eq. 8})$$

Where,

U = single-sided lower tolerance factor

If $\overline{k_{adj}}$ is greater than 1, then

$$K_L = 1 - US_P \quad (\text{Eq. 9})$$

This is done in order not to take credit for a positive bias which may be considered non-conservative. The values of U to give a tolerance limit such that 95% of the data lies above K_L with a confidence of 95% per *Guide for Validation of Nuclear Criticality Safety Computational Methodology* (Ref. 2.2.3) are given in Table 1.

Table 1. Single-Sided Lower Tolerance Factors (U)

# of Experiments (n)	U
10	2.911
11	2.815
12	2.736
13	2.670
14	2.614
15	2.566
16	2.523
17	2.486
18	2.453
19	2.423
20	2.396
21	2.371
22	2.350
23	2.329
24	2.309
25	2.292
30	2.220
35	2.166
40	2.126
45	2.092
50	2.065

Source: Table 2.1 from *Guide for Validation of Nuclear Criticality Safety Computational Methodology* (Ref. 2.2.3)

This method results in the following modification to Eq. 1 for the USL;

$$\text{USL} = K_L - \Delta k_{EROA} - \Delta k_m \quad (\text{Eq. 10})$$

This method provides no insight into determining either Δk_{EROA} or Δk_m . A defined ROA for the modeled critical benchmarks along with knowledge of the system to which the USL is to be applied are needed in order to define Δk_{EROA} and Δk_m for a system. The need for and values of Δk_{EROA} are discussed in Section 6.3. A value for Δk_m is not determined in this calculation as discussed in Section 4.3

4.3.2 Shapiro-Wilk Test Procedure for Normality

The distribution of the k_{adj} values for the modeled critical experiments is expected to be approximately normal. The normal distribution of the k_{adj} values allows for the single-sided tolerance limit method described in Section 4.3.1. The Shapiro-Wilk test for normality is used to confirm that the k_{adj} values are normally distributed. This test method works for sample sizes of 50 or less.

The test involves determining a value for a test statistic (W_t) based on the set of data of size n being tested. This is compared to a value of W determined for a normal distribution as given in Table 38 in Attachment 1. If W_t is greater than W then the data is considered normally distributed. The value of W_t is determined using the following equations:

$$W_t = \frac{Y^2}{S^2} \quad (\text{Eq. 11})$$

$$Y = \sum_{j=1}^v \alpha_j (y_{(n+1-j)} - y_j) \quad (\text{Eq. 12})$$

$$S^2 = \sum (y_i - \bar{y})^2 \quad (\text{Eq. 13})$$

Where,

$v = n/2$ for even n , $(n-1)/2$ for odd n

α_j = the coefficients as given in Table 39 through Table 42 in Attachment 1

y_j = the j^{th} k_{adj} value of the k_{adj} values ranked lowest to highest

$\bar{y} = \bar{k}_{\text{adj}}$, weighted mean k_{adj} per Eq. 4

y_i = the i^{th} k_{adj} value

4.3.3 Single-Sided Distribution Free Tolerance Limit

Should the Shapiro-Wilk test for normality presented in Section 4.3.2 show that the data is not normally distributed, a single-sided distribution free tolerance limit will be determined based on the technique described in *Experimental Statistics* (Ref. 2.2.9, p. 2-15). The technique uses a simple look up table that provides a value m such that it may be asserted with a confidence (γ) that 100P percent of the population of the k_{adj} values for critical configurations lies above the m^{th} smallest value given a random sample of n from that population. The values for m for γ of 0.95 and 0.90 and P of 0.95 are given in Table 2 for various values of n .

Table 2. Values of m for a Single-Sided Distribution Free Tolerance Limit

number of critical benchmarks modeled (n)	m^{th} smallest value for P of 0.95 (m)	
	$\gamma=0.90$	$\gamma=0.95$
50	1	--
55	1	--
60	1	1
65	1	1
70	1	1
75	1	1
80	2	1
85	2	1
90	2	1
95	2	2
100	2	2

Source: Table A-31 from *Experimental Statistics* (Ref. 2.2.9)

The values in Table 2 indicate that a minimum of 50 critical benchmarks would need to be modeled with MCNP in order to have 90% confidence that 95% of all critical configurations modeled with MCNP would give a k_{eff} result greater than the smallest k_{eff} value from the 50 modeled critical benchmarks. The table also shows that a minimum of 60 critical benchmarks would need to be modeled in order to make a similar statement with an increased confidence of 95%.

A similar and related approach is suggested in the *Guide for Validation of Nuclear Criticality Safety Computational Methodology* (Ref. 2.2.3, p.14) except that an equation is given to determine the confidence (given as β versus γ) that a given fraction (given as q versus P) of MCNP determined k_{adj} values for critical configurations will lie above smallest k_{adj} value of n number of sampled MCNP determined k_{adj} values for critical configurations. This equation is:

$$\beta = 1 - q^n \quad (\text{Eq. 14})$$

For $q=0.95$ and $n=50$ Eq. 14 results in a β value of 0.92 which is in good agreement with the values presented in Table 2.

From the *Guide for Validation of Nuclear Criticality Safety Computational Methodology* (Ref. 2.2.3, p.14) the value of K_L is given as;

$$K_L = k_{\text{small}} - \sigma_{\text{small}} \cdot \text{NPM} \quad (\text{Eq. 15})$$

Where,

k_{small} = smallest MCNP determined k_{adj} (Eq. 2) for the critical benchmarks modeled

σ_{small} = uncertainty for k_{small} (σ_t per Eq. 3)

NPM = Non-parametric Margin (NPM)

The *Guide for Validation of Nuclear Criticality Safety Calculational Methodology* (Ref. 2.2.3) provided values for the NPM. These values are reproduced in Table 3.

Table 3. Non-Parametric Margins

Degree of Confidence for 95% of the Population	Non-Parametric Margin (NPM)
>90%	0.0
>80%	0.01
>70%	0.02
>60%	0.03
>50%	0.04
>40%	0.05
≤40%	Additional data needed. (This corresponds to less than 10 data points.)

Source: Table 2.2 from *Guide for Validation of Nuclear Criticality Safety Calculational Methodology* (Ref. 2.2.3), Table 2.2

Based on Eq. 14 the minimum number of critical benchmarks that need to be modeled by MCNP in order for the confidence (β) to exceed 90% for 95% of the population is 45. This results in an NPM of 0.

5. LIST OF ATTACHMENTS

Attachment #	Title	Number of Pages
1	Tables of Statistics Values	4
2	Critical Benchmark Pin Maps for LEU-COMP-THERM-007	2
3	Critical Benchmark Pin Maps for LEU-COMP-THERM-011	9
4	Critical Benchmark Pin Maps for LEU-COMP-THERM-021	2
5	List of Files on the Attachment 6 CD	1
6	One CD	N/A

6. BODY OF CALCULATION

6.1 BENCHMARK DESCRIPTIONS

The following benchmark descriptions all come from the Nuclear Energy Agency (NEA) Nuclear Science Committee's *International Handbook of Evaluated Criticality Safety Benchmark Experiments* (Ref. 2.2.6). The section headings utilized in this section are the benchmark identifiers used in the *International Handbook of Evaluated Criticality Safety Benchmark Experiments* (Ref. 2.2.6). These sections do not describe in detail the experimental setups but focus on providing sufficient detail to understand the benchmark model. Further detail on the experimental setups, methods, and analysis of experimental uncertainties can be found in the *International Handbook of Evaluated Criticality Safety Benchmark Experiments* (Ref. 2.2.6).

6.1.1 LEU-COMP-THERM-001

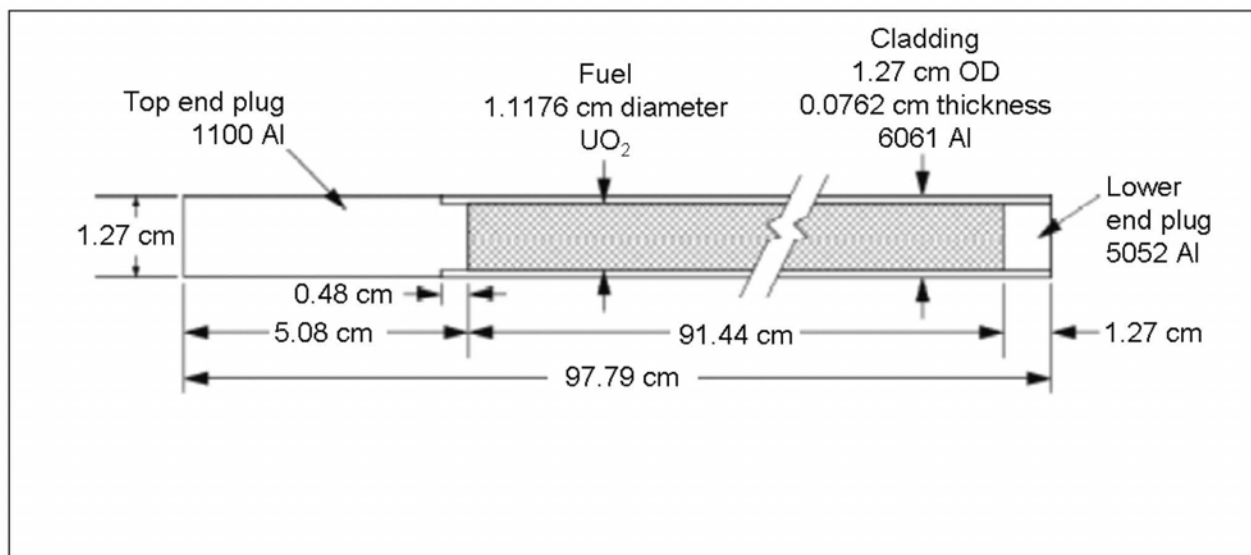
This benchmark report includes critical benchmarks that were developed based upon the results of a series of critical approach experiments with clusters of aluminum clad, 2.35 wt.% ^{235}U enriched UO_2 fuel pins in a large water-filled tank performed over the course of several years at the Critical Mass Laboratory at the Pacific Northwest Laboratories (PNL). These experiments included rectangular, square-pitched lattice clusters, with pitches of 2.032 cm or 1.684 cm. The experiments that are part of this benchmark are of square-pitched lattice clusters with a pin pitch of 2.032 cm.

6.1.1.1 Geometry Description

Detailed geometry description of the experiment and the recommended benchmark model can be found in the LEU-COMP-THERM-001 benchmark report from the *International Handbook of Evaluated Criticality Safety Benchmark Experiments* (Ref. 2.2.6). A basic description only is provided herein.

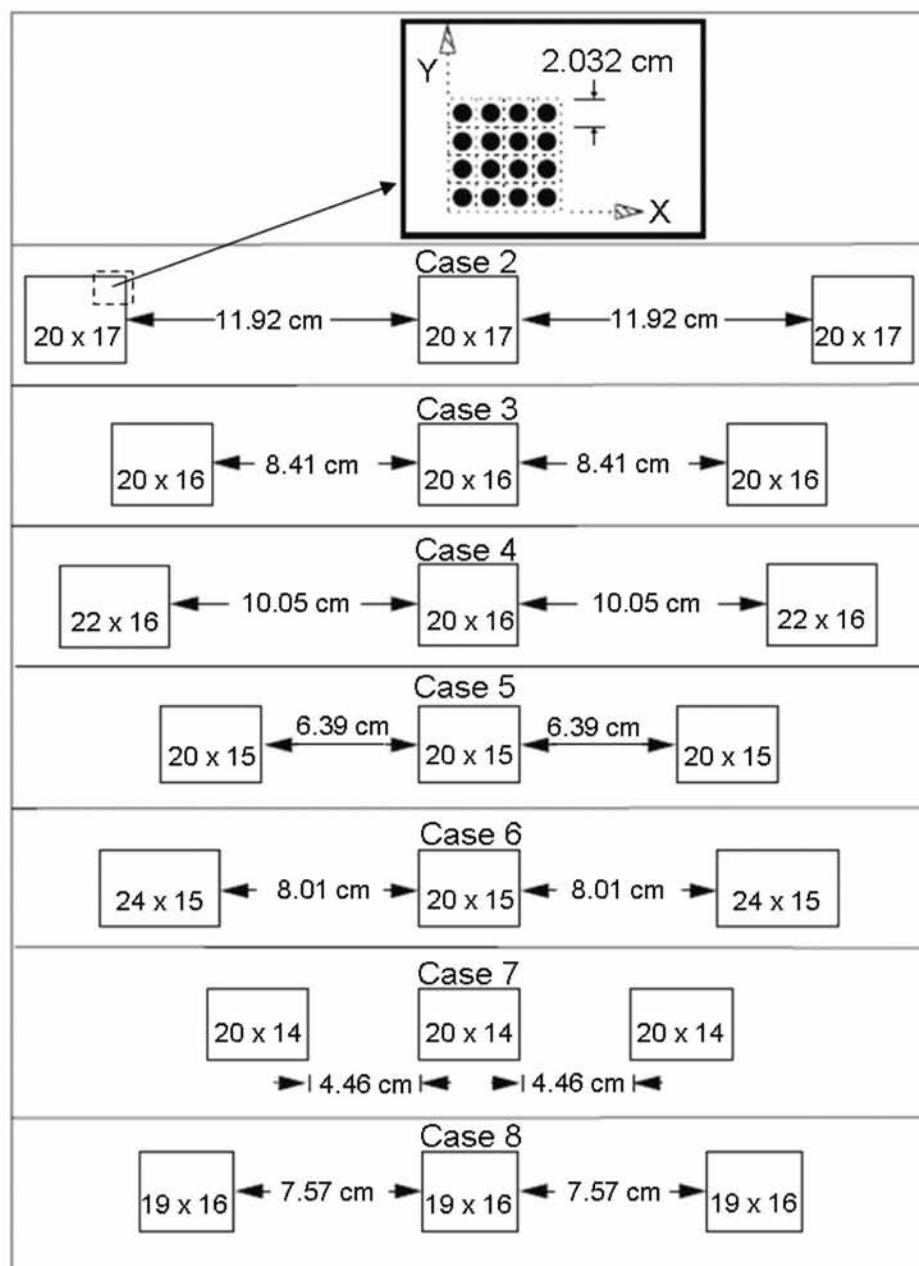
The as modeled fuel pin dimensions per Figure 6 from the LEU-COMP-THERM-001 benchmark report from the *International Handbook of Evaluated Criticality Safety Benchmark Experiments* (Ref. 2.2.6) are shown in Figure 2. The arrangements of the fuel pin clusters per Figure 5 from the LEU-COMP-THERM-001 benchmark report from the *International Handbook of Evaluated Criticality Safety Benchmark Experiments* (Ref. 2.2.6) are provided in Figure 3.

The bottom reflector is a single 2.54-cm-thick acrylic plate, which extends horizontally to the outermost cell-boundary edges of the clusters, followed by 15.3 cm of water. The four side reflectors are 30-cm-thick water. The top reflector is 9.92 cm of water.



Source: Figure 6 from LEU-COMP-THERM-001 benchmark report from the *International Handbook of Evaluated Criticality Safety Benchmark Experiments* (Ref. 2.2.6)

Figure 2. Depiction of Fuel Pin Model for LEU-COMP-THERM-001 Benchmark



Source: Adapted from Figure 5 of LEU-COMP-THERM-001 benchmark report from the *International Handbook of Evaluated Criticality Safety Benchmark Experiments* (Ref. 2.2.6)

Figure 3. Arrangement of Fuel Pin Clusters for Critical Benchmarks from the LEU-COMP-THERM-001 Benchmark

6.1.1.2 Material Descriptions

6.1.1.2.1 Fuel Pin Materials

The fuel region was reported to consist of 825 g of UO_2 per the LEU-COMP-THERM-001 benchmark report from the *International Handbook of Evaluated Criticality Safety Benchmark Experiments* (Ref. 2.2.6). The isotopic composition of the uranium was reported as 0.0137 wt.% ^{234}U , 2.35 wt.% ^{235}U , 0.0171 wt.% ^{236}U , and 97.6192 wt.% ^{238}U . The rest of the fuel pin is 6061 aluminum clad with a 5052 aluminum lower end plug and a 1100 aluminum top end plug as shown in Figure 2.

The weight percents for the material specifications of the uranium and the weight percents and densities of the aluminum materials are taken directly from Table 9 of the LEU-COMP-THERM-001 benchmark report from the *International Handbook of Evaluated Criticality Safety Benchmark Experiments* (Ref. 2.2.6) and are presented in Table 4. The atom densities presented in Table 4 and their determinations are detailed in *Commercial Benchmark Materials.xls* spreadsheet of Attachment 6.

Table 4. Fuel Pin Material Specifications for LEU-COMP-THERM-001 Benchmark

Material	Isotope/ Element	Wt. % ⁽³⁾	MCNP Library ID (ZAID)	Atom Density (atoms/barn-cm)
U(2.35)O_2	^{234}U	0.0137 ⁽¹⁾	92234.50c	2.8579E-06
	^{235}U	2.35 ⁽¹⁾	92235.50c	4.8813E-04
	^{236}U	0.0171 ⁽¹⁾	92236.50c	3.5369E-06
	^{238}U	97.62 ⁽¹⁾	92238.50c	2.0021E-02
	O		8016.50c	4.1031E-02
			Total:	6.1546E-02
1100 Aluminum (top end plug; 2.70 g/cm ^{3 (3)})	Al	99.0	13027.50c	5.9659E-02
	Cu	0.12		
	^{63}Cu		29063.60c	2.1238E-05
	^{65}Cu		29065.60c	9.4661E-06
	Mn	0.025	25055.50c	7.3990E-06
	Zn ⁽²⁾	0.05	29063.60c	1.2429E-05
	Si	0.4025	14000.50c	2.3302E-04
	Fe	0.4025		
	^{54}Fe		26054.60c	6.8497E-06
	^{56}Fe		26056.60c	1.0753E-04
	^{57}Fe		26057.60c	2.4832E-06
	^{58}Fe		26058.60c	3.3047E-07
			Total:	6.0059E-02
5052 Aluminum (lower end plug; 2.69 g/cm ^{3 (3)})	Al	96.65	13027.50c	5.8028E-02
	Cr	0.25		
	^{50}Cr		24050.60c	3.3842E-06
	^{52}Cr		24052.60c	6.5262E-05

Material	Isotope/ Element	Wt. % ⁽³⁾	MCNP Library ID (ZAIID)	Atom Density (atoms/barn-cm)
	⁵³ Cr		24053.60c	7.4002E-06
	⁵⁴ Cr		24054.60c	1.8421E-06
	Cu	0.05		
	⁶³ Cu		29063.60c	8.8166E-06
	⁶⁵ Cu		29065.60c	3.9297E-06
	Mg	2.5	12000.50c	1.6663E-03
	Mn	0.05	25055.50c	1.4743E-05
	Zn ⁽²⁾	0.05	29063.60c	1.2383E-05
	Si	0.225	14000.50c	1.2978E-04
	Fe	0.225		
	⁵⁴ Fe		26054.60c	3.8149E-06
	⁵⁶ Fe		26056.60c	5.9886E-05
	⁵⁷ Fe		26057.60c	1.3830E-06
	⁵⁸ Fe		26058.60c	1.8406E-07
			Total	6.0007E-02
6061 Aluminum (cladding; 2.69 g/cm ³ ⁽³⁾)	Al	97.325	13027.50c	5.8433E-02
	Cr	0.2		
	⁵⁰ Cr		24050.60c	2.7074E-06
	⁵² Cr		24052.60c	5.2209E-05
	⁵³ Cr		24053.60c	5.9201E-06
	⁵⁴ Cr		24054.60c	1.4736E-06
	Cu	0.25		
	⁶³ Cu		29063.60c	4.4083E-05
	⁶⁵ Cu		29065.60c	1.9648E-05
	Mg	1.0	12000.50c	6.6651E-04
	Mn	0.075	25055.50c	2.2115E-05
	Ti	0.075	22000.50c	2.5382E-05
	Zn ⁽²⁾	0.125	29063.60c	3.0958E-05
	Si	0.6	14000.50c	3.4608E-04
	Fe	0.35		
	⁵⁴ Fe		26054.60c	5.9343E-06
	⁵⁶ Fe		26056.60c	9.3153E-05
	⁵⁷ Fe		26057.60c	2.1514E-06
	⁵⁸ Fe		26058.60c	2.8631E-07
			Total:	5.9752E-02

Source: Original to document except as noted.

Notes: ⁽¹⁾ Weight percents of the uranium only..

⁽²⁾ No cross section library available for Zn. ⁶³Cu cross-section utilized. See Assumption 3.2.1.

⁽³⁾ LEU-COMP-THERM-001 benchmark report from the *International Handbook of Evaluated Criticality Safety Benchmark Experiments* (Ref. 2.2.6), Table 9

6.1.1.2.2 Moderator and Reflector Materials

The main moderator/reflector is water at a temperature of 22°C per the LEU-COMP-THERM-001 benchmark report from the *International Handbook of Evaluated Criticality Safety Benchmark Experiments* (Ref. 2.2.6). Water is modeled simply as H₂O in the MCNP models using the atomic fraction variation for material input. The density used is 0.997773 g/cm³ based on water at 22 °C (*CRC Handbook of Chemistry and Physics*, Ref. 2.2.8, p. 6-5). The specification for water is provided in Table 5. The S(α,β) treatment for light water (lwtr.01t) is used in the MCNP models in conjunction with the water material.

Table 5. Water Material Specification

Element/ Isotope	ZAID	Atoms per Molecule
¹ H	1001.50c	2
¹⁶ O	8016.50c	1
Density: 1.0006E-01 atoms/barn-cm (See spreadsheet <i>Commercial Benchmark Materials.xls</i> from Attachment 6 for detailed determination)		

Source: Original to this document.

The fuel pins rest on an acrylic support plate and acts as a minor axial reflector. The acrylic has a density of 1.185 g/cm³ and a composition of 8 wt.% hydrogen, 60 wt.% carbon, and 32 wt.% oxygen per the LEU-COMP-THERM-001 benchmark report from the *International Handbook of Evaluated Criticality Safety Benchmark Experiments* (Ref. 2.2.6). The specification for acrylic is provided in Table 6. See spreadsheet *Commercial Benchmark Materials.xls* from Attachment 6 for additional details. The S(α,β) treatment for polyethylene (poly.01t) is used in the MCNP models in conjunction with the acrylic material.

Table 6. Acrylic Material Specification for LEU-COMP-THERM-001

Element/Isotope	Wt.% ⁽¹⁾	MCNP Library ID (ZAID)	Atom Density (atoms/barn-cm)
H	8	1001.50c	5.6640E-02
C	60	6000.50c	3.5649E-02
O	32	8016.50c	1.4273E-02
		Total:	1.0656E-01

Source: Original to document except as noted.

Notes: ⁽¹⁾ Per the LEU-COMP-THERM-001 Benchmark report from the *International Handbook of Evaluated Criticality Safety Benchmark Experiments* (Ref. 2.2.6)

6.1.1.3 Benchmark k_{eff} Values and Experimental Uncertainties

The benchmark report recommends an adjusted k_{eff} value of 0.9998. A value of 1.0 for the expected k_{eff} value is conservatively used here (See Section 6.1.1.4). An uncertainty on k_{eff} of ± 0.0031 is recommended in the benchmark report based on an analysis of the various experimental uncertainties. This recommended uncertainty will be used here.

6.1.1.4 Variations from Recommended Benchmark Model

The recommended model in the benchmark report did not include the acrylic lattice plates. The exact dimensions and placement of these support plates was not well known. The benchmark report demonstrated that the inclusion of these plates would add a small amount of positive reactivity to the system (0.02 %) and recommended an adjusted k_{eff} value of 0.9998. For the purpose of this validation, the acrylic lattice plates are not modeled but the k_{eff} for the benchmark is maintained at 1.0. The effect of this small variation on the bias determination will be small in comparison to other larger effects (e.g., experimental uncertainties). Further, not accounting for the negative reactivity effect on the benchmark k_{eff} due to the exclusion of the lattice plates is conservative.

6.1.2 LEU-COMP-THERM-002

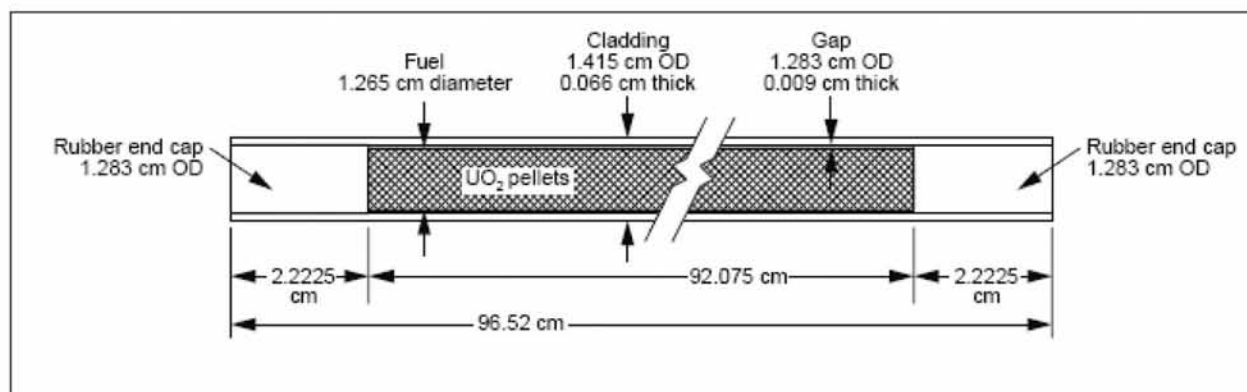
A series of critical approach experiments with clusters of aluminum clad, 4.31 wt.% ^{235}U enriched UO_2 fuel pins in a large water-filled tank was performed over the course of several years at the Critical Mass Laboratory at the Pacific Northwest Laboratories. The critical benchmarks described in the LEU-COMP-THERM-002 benchmark report from the *International Handbook of Evaluated Criticality Safety Benchmark Experiments* (Ref. 2.2.6) included rectangular, square-pitched lattice clusters of fuel pins with pitches of 2.54 cm. The clusters were water-reflected. Two of the five critical benchmarks described in LEU-COMP-THERM-002 are used herein.

6.1.2.1 Geometry Description

A detailed geometry description of the experiment and the recommended benchmark model can be found in the LEU-COMP-THERM-002 benchmark report from the *International Handbook of Evaluated Criticality Safety Benchmark Experiments* (Ref. 2.2.6). A basic description only is provided herein of the benchmark model.

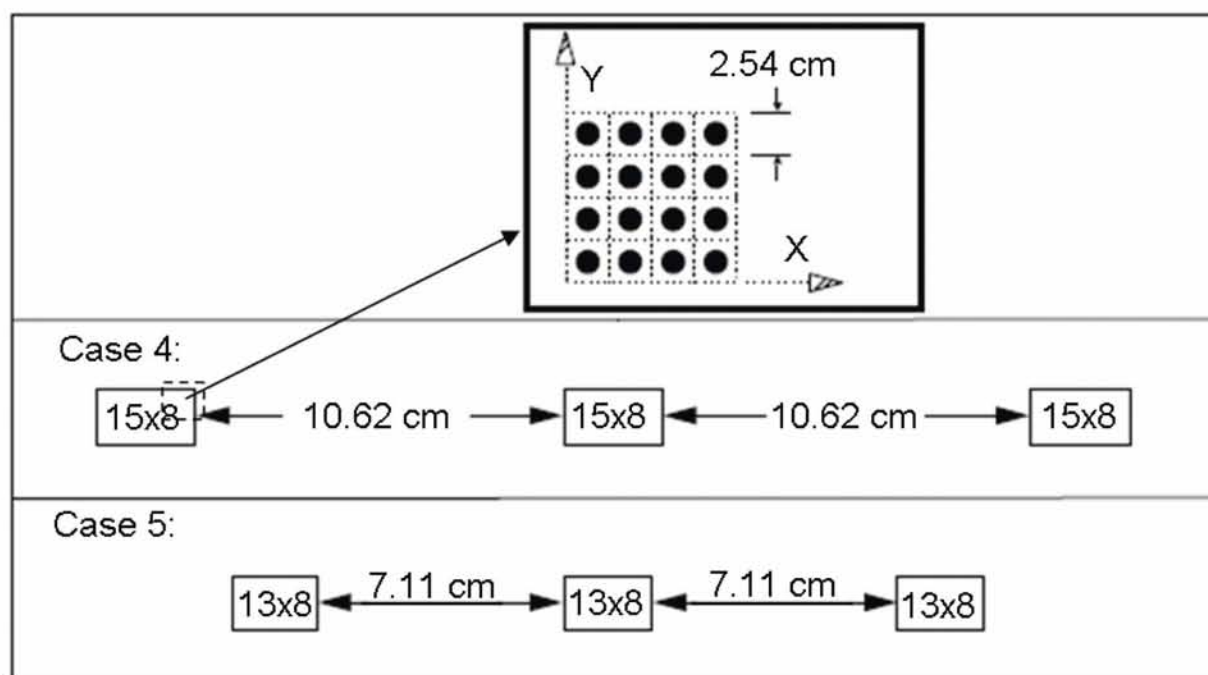
The as-modeled fuel pin dimensions per Figure 5 from the LEU-COMP-THERM-002 benchmark report from the *International Handbook of Evaluated Criticality Safety Benchmark Experiments* (Ref. 2.2.6) are shown in Figure 4. The arrangements of the fuel pin clusters per Figure 4 from the LEU-COMP-THERM-002 benchmark report from the *International Handbook of Evaluated Criticality Safety Benchmark Experiments* (Ref. 2.2.6) are provided in Figure 5.

The bottom reflector is a single 2.54-cm-thick acrylic plate, which extends horizontally to the outermost cell-boundary edges of the clusters, followed by 15.3 cm of water. The four side reflectors are 30-cm-thick water. The top reflector is 12.7775 cm of water.



Source: Figure 5 from LEU-COMP-THERM-002 benchmark report from the *International Handbook of Evaluated Criticality Safety Benchmark Experiments* (Ref. 2.2.6)

Figure 4. Fuel Pin Model for LEU-COMP-THERM-002



Source: Adapted from Figure 4 of LEU-COMP-THERM-001 benchmark report from the *International Handbook of Evaluated Criticality Safety Benchmark Experiments* (Ref. 2.2.6)

Figure 5. Arrangement of Fuel Pin Clusters for Critical Benchmarks from the LEU-COMP-THERM-002 Benchmark

6.1.2.2 Material Descriptions

6.1.2.2.1 Fuel Pin Materials

The fuel region consists of 1203.38 g of UO_2 . The isotopic composition of the uranium is taken directly from the LEU-COMP-THERM-002 benchmark report in the *International Handbook of Evaluated Criticality Safety Benchmark Experiments* (Ref. 2.2.6) and is presented in Table 7. The atom densities presented in Table 7 are determined in spreadsheet *Commercial Benchmark Materials.xls* from Attachment 6.

The fuel pins have 6061 aluminum clad and compressed rubber end plugs with a density of 1.498 g/cm³ per the LEU-COMP-THERM-002 benchmark report from the *International Handbook of Evaluated Criticality Safety Benchmark Experiments* (Ref. 2.2.6). The 6061 aluminum material specification is the same as given in Table 4. The atom densities and density for the compressed rubber material of the end plugs are taken directly from Table 8 of the LEU-COMP-THERM-002 benchmark report in the *International Handbook of Evaluated Criticality Safety Benchmark Experiments* (Ref. 2.2.6) and are presented in Table 7.

Table 7. Fuel Pin Material Specifications for LEU-COMP-THERM-002 Benchmark

Material	Isotope/Element	Wt. % ⁽¹⁾	MCNP Library ID (ZAID)	Atom Density (atoms/barn-cm)
U(4.306)O ₂	²³⁴ U	0.022	92234.50c	5.1888E-06
	²³⁵ U	4.306	92235.50c	1.0113E-03
	²³⁶ U	0.022	92236.50c	5.1448E-06
	²³⁸ U	95.65	92238.50c	2.2180E-02
	O	--	8016.50c	4.6402E-02
			Total:	6.9604E-02
Rubber End Plug ⁽²⁾ (1.498 g/cm ³)	C	--	6000.50c	4.3562E-02
	H	--	1001.50c	5.8178E-02
	Ca	--	20000.50c	2.5660E-03
	S	--	16032.50c	4.7820E-04
	Si	--	14000.50c	9.6360E-05
	O	--	8016.50c	1.2461E-02
			Total:	1.1734E-01

Source: Original to document except as noted.

Notes: ⁽¹⁾ Per the LEU-COMP-THERM-002 benchmark report from the *International Handbook of Evaluated Criticality Safety Benchmark Experiments* (Ref. 2.2.6).

⁽²⁾ Atom densities for the rubber end plug material are taken directly from Table 8 of the LEU-COMP-THERM-002 benchmark report from the *International Handbook of Evaluated Criticality Safety Benchmark Experiments* (Ref. 2.2.6).

6.1.2.2.2 Moderator and Reflector Materials

The fuel pins rest on an acrylic support plate which acts a minor axial reflector. The acrylic has a density of 1.185 g/cm³ and a composition of 8 wt.% hydrogen, 60 wt.% carbon, and 32 wt.% oxygen per the LEU-COMP-THERM-002 benchmark report from the *International Handbook of Evaluated Criticality Safety Benchmark Experiments* (Ref. 2.2.6). This is exactly the same as the acrylic material used in the LEU-COMP-THERM-001 benchmark as given in Table 6.

The main moderator/reflector is water at a temperature of 22°C per the LEU-COMP-THERM-002 benchmark report from the *International Handbook of Evaluated Criticality Safety Benchmark Experiments* (Ref. 2.2.6). This is exactly the same as the water material used in the LEU-COMP-THERM-001 benchmark as given in Table 5.

6.1.2.3 Benchmark k_{eff} Values and Experimental Uncertainties

The benchmark report recommended an adjusted k_{eff} value of 0.9997 for the critical benchmarks. A value of 1.0 for the expected k_{eff} value is conservatively used here (See Section 6.1.2.4). An uncertainty on k_{eff} of ± 0.0020 is recommended in the benchmark report based on an analysis of the various experimental uncertainties. This recommended uncertainty will be used here.

6.1.2.4 Variations from Recommended Benchmark Model

The recommended model in the LEU-COMP-THERM-002 benchmark report from the *International Handbook of Evaluated Criticality Safety Benchmark Experiments* (Ref. 2.2.6) did not include the acrylic lattice plates. The exact dimensions and placement of these support plates was not well known. The LEU-COMP-THERM-002 benchmark report from the *International Handbook of Evaluated Criticality Safety Benchmark Experiments* (Ref. 2.2.6) demonstrated that the inclusion of these plates would add a small amount of positive reactivity to the system (0.03 %) and recommended an adjusted k_{eff} value of 0.9997. For the purpose of this validation, the acrylic lattice plates are not modeled but the k_{eff} values for the critical benchmarks are maintained at 1.0. The effect of this small variation on the bias determination will be small in comparison to other larger effects (e.g., experimental uncertainties). Further, not accounting for the negative reactivity effect of not including the lattice plates on the benchmark k_{eff} is conservative.

6.1.3 LEU-COMP-THERM-007

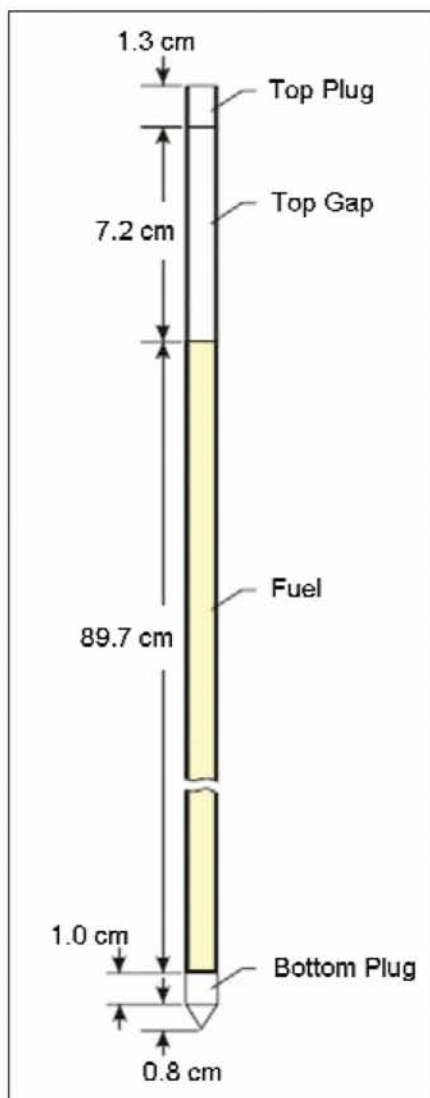
The critical benchmarks described in this section are based upon the LEU-COMP-THERM-007 benchmark report from the *International Handbook of Evaluated Criticality Safety Benchmark Experiments* (Ref. 2.2.6). The benchmarks are based on a series of sub-critical experiments conducted at the experimental criticality facility of Institut de Protection et de Sûreté Nucléaire (IPSN) at Service de Recherche en Sûreté Criticité (SRSC) Valduc, Commissariat à l’Energie Atomique (CEA), France in 1978.

The LEU-COMP-THERM-007 benchmark report from the *International Handbook of Evaluated Criticality Safety Benchmark Experiments* (Ref. 2.2.6) described ten critical benchmarks consisting of fuel pins of 4.738 wt.% ^{235}U enriched UO_2 arranged in square and hexagonal lattices. These lattices are water moderated and reflected.

6.1.3.1 Geometry Description

Detailed geometry descriptions of the experiment and the recommended benchmark models can be found in the LEU-COMP-THERM-007 benchmark report from the *International Handbook of Evaluated Criticality Safety Benchmark Experiments* (Ref. 2.2.6). A basic description only is provided herein of the benchmark models.

The as-modeled fuel pin characteristics per Figure 9 and Table 14 of the LEU-COMP-THERM-007 benchmark report from the *International Handbook of Evaluated Criticality Safety Benchmark Experiments* (Ref. 2.2.6) are shown in Figure 6 and Table 8.



Source: Adapted from Figure 9 of LEU-COMP-THERM-007 benchmark report from the *International Handbook of Evaluated Criticality Safety Benchmark Experiments* (Ref. 2.2.6)

Figure 6. Fuel Pin Model for LEU-COMP-THERM-007

Table 8. Fuel Pin Model Geometry Data for LEU-COMP-THERM-007

Parameter	Dimension (cm)
Fuel diameter	0.7892
Clad inner diameter	0.82
Clad outer diameter	0.94
Fuel height	89.7
Pin height	100.0
Top plug height	1.3
Top gap thickness	7.2
Bottom plug height	1.0
Conical bottom height	0.8

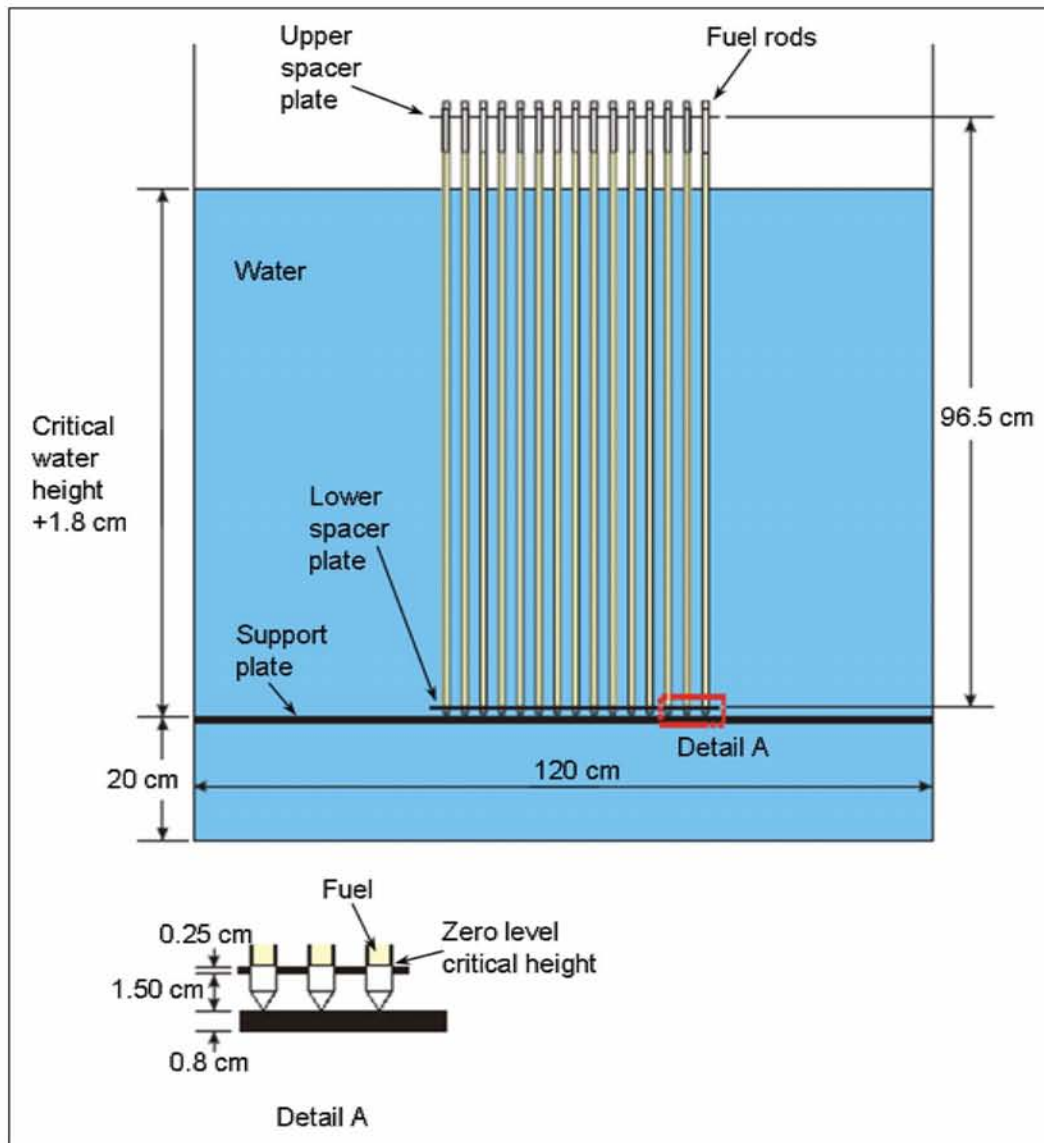
Source: Table 14 from LEU-COMP-THERM-007 benchmark report from the *International Handbook of Evaluated Criticality Safety Benchmark Experiments* (Ref. 2.2.6)

The fuel pins are arranged in a number of square and hexagonal pitched arrays and shown in Figure 16 and Figure 17 in Attachment 2. The fuel pins rest upon a 95 cm x 95 cm steel support plate 0.8-cm thick. The fuel pin spacing and array geometry were maintained by two spacer plates (upper and lower). The spacer plates are 0.25-cm thick. For cases 1 – 5 and 8, the spacer plates are 60 cm x 60 cm. For cases 6 and 9, the spacer plates are 72 cm x 72 cm. For cases 7 and 10, the spacer plates are 92.5 cm x 92.5 cm. The holes in the spacer plates have a diameter of 1.0 cm. The holes are only modeled in the fuel array. The effect of these holes on the benchmark reactivity was shown to be negligible in the LEU-COMP-THERM-007 benchmark report from the *International Handbook of Evaluated Criticality Safety Benchmark Experiments* (Ref. 2.2.6). The axial location of the two grids per Figure 9 from the LEU-COMP-THERM-007 benchmark report from the *International Handbook of Evaluated Criticality Safety Benchmark Experiments* (Ref. 2.2.6) is shown in Figure 7.

The main moderator and reflector is water. The length and width of the water block is 120 cm. The water height above the fuel support plate is equal to the critical water depth (measured from the bottom of the active fuel region) plus 1.8 cm (accounts for the plug at the bottom of the fuel pin). The bottom water reflector is 19.2 cm thick. The critical water depth and other benchmark information for each case per Table 13 of the LEU-COMP-THERM-007 benchmark report from the *International Handbook of Evaluated Criticality Safety Benchmark Experiments* (Ref. 2.2.6) are presented in Table 9.

Table 9. Critical Benchmark Model Information for LEU-COMP-THERM-007

Case	Pitch Type	Pitch (cm)	Fuel Pins	Pin Map (Attachment 2)	Critical Water Height (cm)
1	square	1.26	484	Figure 16	90.69
2	square	1.60	272	Figure 16	73.53
3	square	2.10	225	Figure 16	77.98
4	square	2.52	306	Figure 16	79.85
5	triangular	1.35	547	Figure 16	60.93
6	triangular	1.72	271	Figure 16	68.06
7	triangular	2.26	217	Figure 17	79.50
8	triangular	1.35	484	Figure 17	85.21
9	triangular	1.72	277	Figure 17	61.99
10	triangular	2.26	225	Figure 17	70.44
Source: Adapted from Table 13 of LEU-COMP-THERM-007 benchmark report from the <i>International Handbook of Evaluated Criticality Safety Benchmark Experiments</i> (Ref. 2.2.6)					



Source: Adapted from Figure 9 of LEU-COMP-THERM-007 benchmark report from the *International Handbook of Evaluated Criticality Safety Benchmark Experiments* (Ref. 2.2.6)

Figure 7. Elevation View of Basic Benchmark Model for LEU-COMP-THERM-007

6.1.3.2 Material Descriptions

6.1.3.2.1 Fuel Pin Materials

The fuel consists of UO_2 with a density of 10.38 g/cm^3 per the LEU-COMP-THERM-007 benchmark report in the *International Handbook of Evaluated Criticality Safety Benchmark Experiments* (Ref. 2.2.6). The isotopic composition of the uranium is taken directly from the LEU-COMP-THERM-007 benchmark report in the *International Handbook of Evaluated Criticality Safety Benchmark Experiments* (Ref. 2.2.6) and is presented in Table 10. The atom densities for the UO_2 material presented in Table 10 are determined in spreadsheet *Commercial Benchmark Materials.xls* from Attachment 6.

Aluminum, silicon, and iron impurities were explicitly included in the fuel specification. These impurities are a part of the overall UO_2 density of 10.38 g/cm^3 . The values are listed in Table 10. In addition to these three impurities, boron is added to the material specification to account for other impurities. The atom densities presented in Table 10 are determined in spreadsheet *Commercial Benchmark Materials.xls* from Attachment 6.

The clad and end plug material for the fuel is aluminum alloy AGS. The ‘AGS’ designation is not further defined in the LEU-COMP-THERM-007 benchmark report in the *International Handbook of Evaluated Criticality Safety Benchmark Experiments* (Ref. 2.2.6). The material specification for aluminum alloy AGS was taken from the LEU-COMP-THERM-007 benchmark report in the *International Handbook of Evaluated Criticality Safety Benchmark Experiments* (Ref. 2.2.6). The determined atom densities used in MCNP models are shown in Table 10. Details on the determinations of the atom densities can be found in the spreadsheet *Commercial Benchmark Materials.xls* from Attachment 6.

Table 10. Fuel Material Specifications for LEU-COMP-THERM-007

Material	Element/ Isotope	Atom % ⁽³⁾	g/1E6 g UO ₂ ⁽⁴⁾	Wt.% ⁽²⁾	MCNP Library ID (ZAID)	Atom density (atoms/barn-cm)
UO ₂ Fuel	²³⁴ U	0.0307			92234.50c	7.1087E-06
density=10.38 g/cm ³	²³⁵ U	4.79525			92235.50c	1.1104E-03
	²³⁶ U	0.1373			92236.50c	3.1793E-05
	²³⁸ U	95.03675			92238.50c	2.2006E-02
	O				8016.50c	4.6311E-02
	Al		18		13027.50c	4.1702E-06
	Si		85		14000.50c	2.2480E-05
	Fe		101			
	⁵⁴ Fe				26054.60c	5.5612E-07
	⁵⁶ Fe				26056.60c	8.7299E-06
	⁵⁷ Fe				26057.60c	2.0161E-07
	⁵⁸ Fe				26058.60c	2.6831E-08
	Equivalent B		0.6			
	¹⁰ B				5010.50c	6.9038E-08
	¹¹ B				5011.50c	2.7789E-07
					Total	6.9503E-02
Aluminum Alloy AGS Clad	Al			98.85	13027.50c	5.9570E-02
density=2.7g/cm ³	Mg			0.47	12000.50c	3.1442E-04
	Si			0.43	14000.50c	2.4894E-04
	Fe			0.22		
	⁵⁴ Fe				26054.60c	3.7440E-06
	⁵⁶ Fe				26056.60c	5.8773E-05
	⁵⁷ Fe				26057.60c	1.3573E-06
	⁵⁸ Fe				26058.60c	1.8064E-07
	Zn ⁽¹⁾			0.03	29063.60c	7.4576E-06
					Total:	6.0204E-02

Source: Original to document except as noted.

Notes: ⁽¹⁾ No cross section library available for Zn. ⁶³Cu cross-section utilized. See Assumption 3.2.1.

⁽²⁾ From Table 2 of LEU-COMP-THERM-007 benchmark report from the *International Handbook of Evaluated Criticality Safety Benchmark Experiments* (Ref. 2.2.6)

⁽³⁾ From Table 4 of LEU-COMP-THERM-007 benchmark report from the *International Handbook of Evaluated Criticality Safety Benchmark Experiments* (Ref. 2.2.6)

⁽⁴⁾ Section 2.2 from LEU-COMP-THERM-007 benchmark report from the *International Handbook of Evaluated Criticality Safety Benchmark Experiments* (Ref. 2.2.6)

6.1.3.2.2 Other Materials

The moderator and main reflector for this benchmark is water. Per the LEU-COMP-THERM-007 benchmark report in the *International Handbook of Evaluated Criticality Safety Benchmark Experiments* (Ref. 2.2.6) the experiments were performed at 22 °C (room temperature). The material specification for water at 22 °C is given in Table 5.

The support plate and the two spacer plates are all made of Z2CN18-10 stainless steel. The material specification for Z2CN18-10 stainless steel as defined in the LEU-COMP-THERM-007 benchmark report in the *International Handbook of Evaluated Criticality Safety Benchmark Experiments* (Ref. 2.2.6) is shown in Table 11 along with the determined atom densities. The density of Z2CN18-10 stainless steel is given as 7.9 g/cm³ per Table 2 of the LEU-COMP-THERM-007 benchmark report in the *International Handbook of Evaluated Criticality Safety Benchmark Experiments* (Ref. 2.2.6). Details of the atom density determinations can be found in spreadsheet *Commercial Benchmark Materials.xls* from Attachment 6.

Table 11. Material Specification for Z2CN18-10 Stainless Steel for LEU-COMP-THERM-007

Element/Isotope	Wt.%(¹)	MCNP Library ID (ZAID)	Atom density (atoms/barn-cm)
C	0.015	6000.50c	5.9416E-05
Cr	18		
⁵⁰ Cr		24050.60c	7.1560E-04
⁵² Cr		24052.60c	1.3800E-02
⁵³ Cr		24053.60c	1.5648E-03
⁵⁴ Cr		24054.60c	3.8950E-04
Ni	10		
⁵⁸ Ni		28058.60c	5.5181E-03
⁶⁰ Ni		28060.60c	2.1256E-03
⁶¹ Ni		28061.60c	9.2397E-05
⁶² Ni		28062.60c	2.9460E-04
⁶⁴ Ni		28064.60c	7.5026E-05
Mn	1	25055.50c	8.6597E-04
Si	0.5	14000.50c	8.4697E-04
P	0.02	15031.50c	3.0719E-05
S	0.015	16032.50c	2.2256E-05
Fe	70.45		
⁵⁴ Fe		26054.60c	3.5080E-03
⁵⁶ Fe		26056.60c	5.5068E-02
⁵⁷ Fe		26057.60c	1.2718E-03
⁵⁸ Fe		26058.60c	1.6925E-04
		Total:	8.6418E-02

Source: Original to document except as noted.

Notes: ⁽¹⁾ From Table 2 and Section 2.2.2 from LEU-COMP-THERM-007 benchmark report from the *International Handbook of Evaluated Criticality Safety Benchmark Experiments* (Ref. 2.2.6)

6.1.3.3 Benchmark k_{eff} Values and Experimental Uncertainties

The as modeled critical benchmarks all have an expected k_{eff} value of 1.0 per the *International Handbook of Evaluated Criticality Safety Benchmark Experiments* (Ref. 2.2.6). The estimated experimental uncertainties for each case per the *International Handbook of Evaluated Criticality Safety Benchmark Experiments* (Ref. 2.2.6) are shown in Table 12.

Table 12. Expected k_{eff} and Estimated Experimental Uncertainties for LEU-COMP-THERM-007

Case	k_{eff}	Uncertainty ($\pm 1\sigma$)
1,5,8	1.0000	0.0014
2,6,9	1.0000	0.0008
3,7,10	1.0000	0.0007
4	1.0000	0.0008

Source: Section 3.5 from LEU-COMP-THERM-007 benchmark report from the *International Handbook of Evaluated Criticality Safety Benchmark Experiments* (Ref. 2.2.6)

6.1.4 LEU-COMP-THERM-011

The critical benchmarks described in this section are based upon the LEU-COMP-THERM-011 benchmark report from the *International Handbook of Evaluated Criticality Safety Benchmark Experiments* (Ref. 2.2.6). The benchmarks are based on a series of slightly super-critical experiments conducted at the Babcock and Wilcox's Lynchburg Research Center between November 1977 and March 1978.

The LEU-COMP-THERM-011 benchmark report from the *International Handbook of Evaluated Criticality Safety Benchmark Experiments* (Ref. 2.2.6) described fifteen critical benchmarks consisting of fuel pins with 2.459 wt.% ^{235}U enriched UO_2 arranged in square lattices with a pitch of 1.636 cm. The lattice structure is maintained by upper and lower aluminum spacer grids. The benchmarks are water moderated. The benchmarks included variations of the fuel arrangement in the grids, boron concentration in the water, water height, and/or number of B_4C pins.

6.1.4.1 Geometry Description

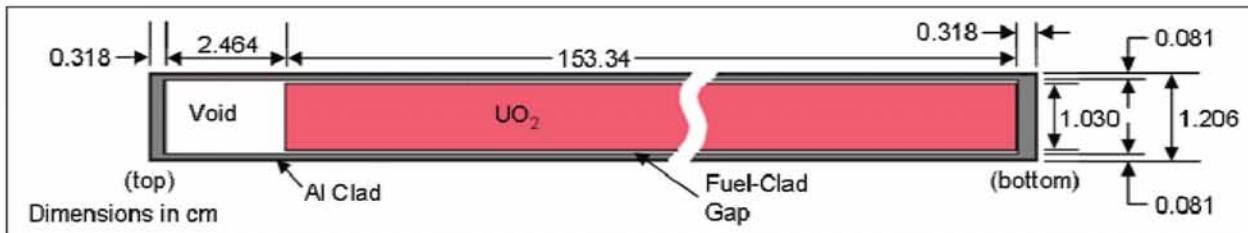
Detailed geometry descriptions of the experiment and the recommended benchmark models can be found in the LEU-COMP-THERM-011 benchmark report from the *International Handbook of Evaluated Criticality Safety Benchmark Experiments* (Ref. 2.2.6). A basic description only is provided herein of the benchmark models.

The as modeled dimensions of the fuel pin per Figure 14, Table 1, and Table 33 of the LEU-COMP-THERM-011 benchmark report from the *International Handbook of Evaluated Criticality Safety Benchmark Experiments* (Ref. 2.2.6) are shown in Figure 8 and Table 13.

Table 13. Fuel Pin Model Geometry Data for LEU-COMP-THERM-011

Parameter	Dimension (cm)
Fuel diameter	1.030
Clad inner diameter	1.044
Clad outer diameter	1.206
Active fuel length	153.34
Total pin length	156.44
Top plug thickness	0.318
Top gap thickness	2.464
Bottom plug thickness	0.318

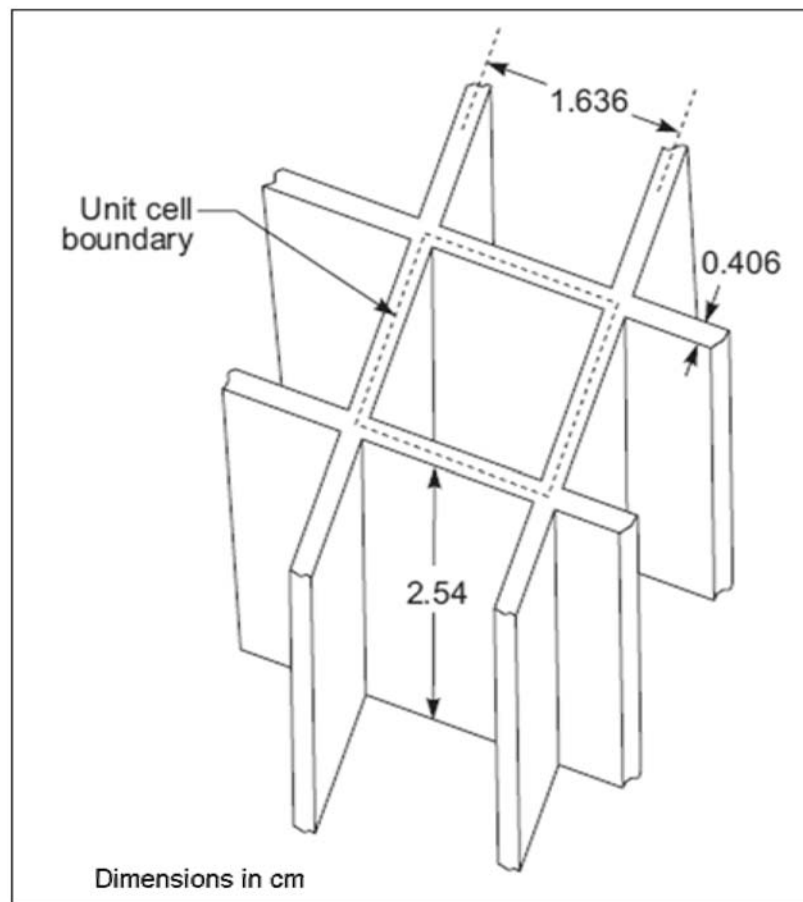
Source: Table 1 and Table 33 of the LEU-COMP-THERM-011 benchmark report from the *International Handbook of Evaluated Criticality Safety Benchmark Experiments* (Ref. 2.2.6)



Source: Adapted from Figure 14, Table 1, and Section 1.2.8 of LEU-COMP-THERM-011 benchmark report from the *International Handbook of Evaluated Criticality Safety Benchmark Experiments* (Ref. 2.2.6)

Figure 8. Fuel Pin Dimensions for LEU-COMP-THERM-011 Benchmark Model

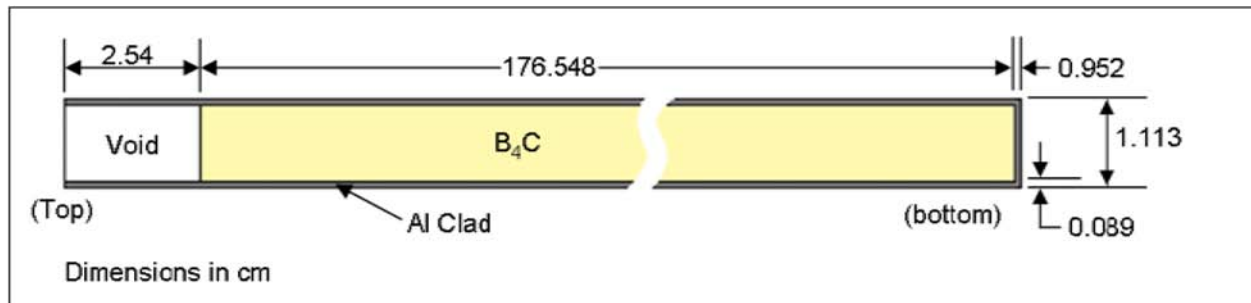
The upper and lower aluminum spacer grids consist of 2.54-cm-wide slotted aluminum strips interlocked to form a square matrix. The strips are 0.406 cm thick and are spaced 1.636 cm center-to-center. The basic grid structure is shown in Figure 9. For convenience, the modeled spacer grids are limited to the dimensions of the pin array. The Case 1 model is an exception to this with the spacer grids modeled as a square such that it bounds the approximately circular shape of the core. The LEU-COMP-THERM-011 benchmark report from the *International Handbook of Evaluated Criticality Safety Benchmark Experiments* (Ref. 2.2.6) demonstrated that the aluminum spacer grids modeled outside the confines of the pin array has a negligible effect on the reactivity of the system.



Source: Figure 16 from LEU-COMP-THERM-011 benchmark report from the *International Handbook of Evaluated Criticality Safety Benchmark Experiments* (Ref. 2.2.6)

Figure 9. Basic Dimensions of the Spacer Grids for LEU-COMP-THERM-011 Benchmark

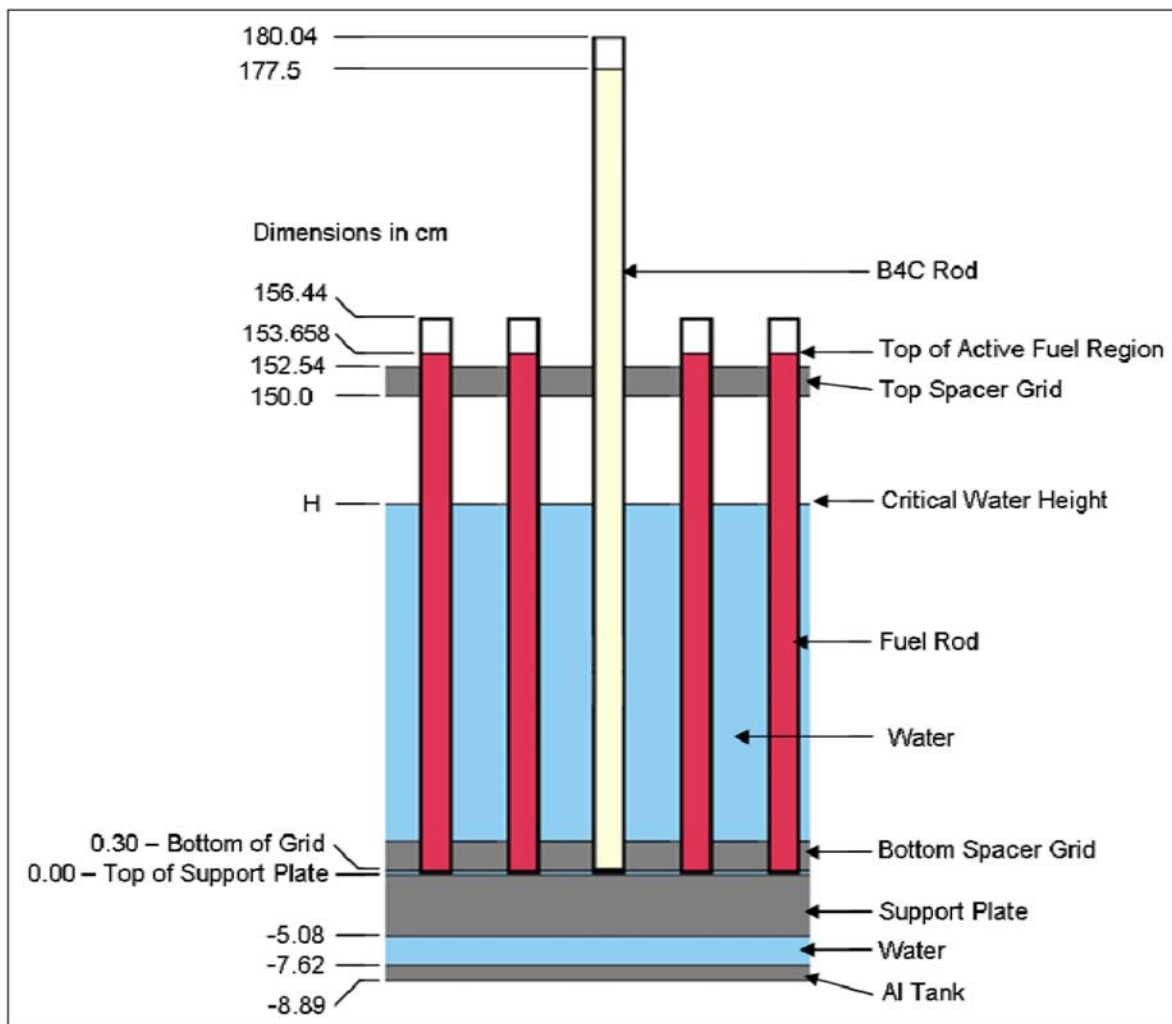
For some of the cases, absorber rods of B_4C are included. The as modeled dimensions are shown in Figure 10. The top of the absorber rods are plugged with cork. This is modeled as void. This is considered a reasonable simplification given that this is well above the active fuel region of the core and the water moderator and would, therefore, not have a significant impact on the system reactivity.



Source: Adapted from Figure 15 and Section 1.2.7 of LEU-COMP-THERM-011 benchmark report from the *International Handbook of Evaluated Criticality Safety Benchmark Experiments* (Ref. 2.2.6)

Figure 10. As Modeled Dimensions of the B₄C Absorber Rods for LEU-COMP-THERM-011

The basic axial arrangement of the as modeled core is shown in Figure 11. This figure shows both the fuel and B₄C rods. The B₄C rods are not present in all benchmarks. The core layout of each case is shown in Attachment 3. The critical water height, soluble boron concentration, recommended benchmark k_{eff} values, and estimated experimental uncertainties for each case are given in Table 14.



Source: Adapted from Figure 13 of LEU-COMP-THERM-011 benchmark report from the *International Handbook of Evaluated Criticality Safety Benchmark Experiments* (Ref. 2.2.6)

Figure 11. Basic Axial Configuration of Benchmark Models for LEU-COMP-THERM-011

The air above the critical water height is modeled as water with a reduced density of 0.0001 g/cm^3 per the recommendation from the LEU-COMP-THERM-011 benchmark report from the *International Handbook of Evaluated Criticality Safety Benchmark Experiments* (Ref. 2.2.6).

Table 14. Benchmark Model Critical Information for LEU-COMP-THERM-011

Case	Core Layout Diagram Figure	Soluble Boron Concentration (g/1E6 cm ³ water at 25°C) ⁽²⁾	Moderator Temperature ⁽²⁾ (°C)	Moderator Height ⁽¹⁾⁽²⁾ (cm)	Recommended Experimental $k_{\text{eff}} \pm 1\sigma$ ⁽³⁾
1	Figure 18	0	21.0	143.88	1.0010 \pm 0.0018
2	Figure 19	1037	18.5	144.29	1.0009 \pm 0.0032
3	Figure 20	769	18.0	148.63	1.0009 \pm 0.0032
4	Figure 20	764	18.0	144.88	1.0009 \pm 0.0032
5	Figure 20	762	18.0	140.38	1.0009 \pm 0.0032
6	Figure 20	753	18.5	131.32	1.0009 \pm 0.0032
7	Figure 20	739	18.0	120.64	1.0009 \pm 0.0032
8	Figure 20	721	18.0	110.04	1.0009 \pm 0.0032
9	Figure 20	702	18.5	100.32	1.0009 \pm 0.0032
10	Figure 21	0	17.0	145.68	1.0010 \pm 0.0017
11	Figure 22	0	17.5	144.75	1.0010 \pm 0.0017
12	Figure 23	0	17.5	107.67	1.0010 \pm 0.0017
13	Figure 24	0	17.5	146.15	1.0010 \pm 0.0017
14	Figure 25	0	17.5	111.49	1.0010 \pm 0.0017
15	Figure 26	0	17.5	129.65	1.0010 \pm 0.0018

Source: Original to document except as noted.

Notes: ⁽¹⁾ Measured from top of base plate

⁽²⁾ Table 4 from LEU-COMP-THERM-011 benchmark report from the *International Handbook of Evaluated Criticality Safety Benchmark Experiments* (Ref. 2.2.6)

⁽³⁾ Section 3.5 from LEU-COMP-THERM-011 benchmark report from the *International Handbook of Evaluated Criticality Safety Benchmark Experiments* (Ref. 2.2.6)

The actual experimental k_{eff} was 1.0 since the benchmarks were actually taken to critical and slightly super-critical. The reason for the slightly higher values for the recommended k_{eff} associated with the benchmark model in Table 14 is due to the small amount of positive reactivity introduced into the benchmark model due to some simplifications of the model involving the exclusion of the fuel impurities from the model and some non-random dimensional uncertainties (See the LEU-COMP-THERM-011 benchmark report from the *International Handbook of Evaluated Criticality Safety Benchmark Experiments* (Ref. 2.2.6) for additional detail.). As a result of this, the MCNP determined k_{eff} (k_{MCNP}) values will need to be rescaled relative to 1.0 based on Eq. 2.

6.1.4.2 Material Descriptions

6.1.4.2.1 Fuel Pin Materials

The fuel consists of UO₂ with an enrichment of 2.459 wt.% ²³⁵U and a mass of 1305.5 g per fuel pin per the LEU-COMP-THERM-011 benchmark report from the *International Handbook of Evaluated Criticality Safety Benchmark Experiments* (Ref. 2.2.6). The isotopic composition of the uranium is taken directly from the LEU-COMP-THERM-011 benchmark report from the *International Handbook of Evaluated Criticality Safety Benchmark Experiments* (Ref. 2.2.6) and is presented in Table 15. The atom densities for the UO₂ fuel material are presented in Table 15.

These values were determined in spreadsheet *Commercial Benchmark Materials.xls* from Attachment 6.

The fuel clad and end plugs are made of 6061-T6 aluminum with a density of 2.7 g/cm^3 . The weight percents are taken from the LEU-COMP-THERM-011 benchmark report from the *International Handbook of Evaluated Criticality Safety Benchmark Experiments* (Ref. 2.2.6) and are presented in Table 15. The atom densities for the fuel clad material are presented in Table 15. These values were determined in spreadsheet *Commercial Benchmark Materials.xls* from Attachment 6.

Table 15. Fuel Pin Material Specifications for LEU-COMP-THERM-011 Benchmark

Material	Isotope/Element	Wt. %	MCNP Library ID (ZAID)	Atom Density (atoms/barn-cm)
U(2.459)O ₂	²³⁴ U	0.021 ⁽²⁾	92234.50c	4.8668E-06
	²³⁵ U	2.459 ⁽²⁾	92235.50c	5.6745E-04
	²³⁶ U	0.00954 ⁽²⁾	92236.50c	2.1922E-06
	²³⁸ U	97.51046 ⁽²⁾	92238.50c	2.2218E-02
	O	--	8016.50c	4.5584E-02
			Total:	6.8377E-02
6061-T6 Aluminum (cladding; 2.7 g/cm ³)	Al	97.3 ⁽³⁾	13027.50c	5.8636E-02
	Cr	0.2 ⁽⁴⁾		
	⁵⁰ Cr		24050.60c	2.7175E-06
	⁵² Cr		24052.60c	5.2404E-05
	⁵³ Cr		24053.60c	5.9421E-06
	⁵⁴ Cr		24054.60c	1.4791E-06
	Cu	0.2 ⁽⁴⁾		
	⁶³ Cu		29063.60c	3.5398E-05
	⁶⁵ Cu		29065.60c	1.5777E-05
	Mg	1.0 ⁽⁴⁾	12000.50c	6.6899E-04
	Mn	0.1 ⁽⁴⁾	25055.50c	2.9597E-05
	Ti	0.1 ⁽⁴⁾	22000.50c	3.3969E-05
	Zn ⁽¹⁾	0.15 ⁽⁴⁾	29063.60c	3.7288E-05
	Si	0.6 ⁽⁴⁾	14000.50c	3.4736E-04
	Fe	0.35 ⁽⁴⁾		
	⁵⁴ Fe		26054.60c	5.9564E-06
	⁵⁶ Fe		26056.60c	9.3503E-05
	⁵⁷ Fe		26057.60c	2.1594E-06
	⁵⁸ Fe		26058.60c	2.8737E-07
			Total:	5.9968E-02

Source: Original to document except as noted.

Notes: ⁽¹⁾ No cross section library available for Zn. ⁶³Cu cross-section utilized. See Assumption 3.2.1

⁽²⁾ Per Sections 2.1.4 and 2.1.5 from LEU-COMP-THERM-011 benchmark report from the *International Handbook of Evaluated Criticality Safety Benchmark Experiments* (Ref. 2.2.6)

⁽³⁾ This is given as 97.25 per Table 15 from LEU-COMP-THERM-011 benchmark report from the *International Handbook of Evaluated Criticality Safety Benchmark Experiments* (Ref. 2.2.6). This specification, however, did not sum to 100%. Given that Al was meant to be the remainder in the specification, it was increased by 0.05 to 97.3 which is used herein.

⁽⁴⁾ From Table 15 of LEU-COMP-THERM-011 benchmark report from the *International Handbook of Evaluated Criticality Safety Benchmark Experiments* (Ref. 2.2.6).

6.1.4.2.2 Moderator and Reflector Materials

The moderator and reflector materials consist of the aluminum base plate and tank and the water/borated water moderator/reflector. The aluminum of the base plate and tank are of the same material as the fuel clad and are given in Table 15. The water and borated water

compositions are dependent upon the temperature of the water and the amount, if any, of boric acid added to the water. The moderator temperature for each experiment is given in the LEU-COMP-THERM-011 benchmark report from the *International Handbook of Evaluated Criticality Safety Benchmark Experiments* (Ref. 2.2.6, Table 4). The boron concentration is also given in units of grams of boron per $1\text{E}6\text{ cm}^3$ of water at a temperature of $25\text{ }^{\circ}\text{C}$. This information is provided in Table 14. The atom densities determined for the water/borated water compositions are given in Table 16. The atom densities presented in Table 16 are determined in spreadsheet *Commercial Benchmark Materials.xls* from Attachment 6.

Table 16. Atom Densities for the Water/Borated Water Moderator for LEU-COMP-THERM-011

Case	Atom Densities (atoms/barn-cm)				
	H	O	^{10}B	^{11}B	Total
1	6.6722E-02	3.3361E-02			1.0008E-01
2	6.6883E-02	3.3528E-02	1.1512E-05	4.6337E-05	1.0047E-01
3	6.6857E-02	3.3493E-02	8.5377E-06	3.4365E-05	1.0039E-01
4	6.6856E-02	3.3492E-02	8.4822E-06	3.4142E-05	1.0039E-01
5	6.6856E-02	3.3492E-02	8.4599E-06	3.4052E-05	1.0039E-01
6	6.6848E-02	3.3487E-02	8.3592E-06	3.3647E-05	1.0038E-01
7	6.6853E-02	3.3488E-02	8.2046E-06	3.3025E-05	1.0038E-01
8	6.6851E-02	3.3486E-02	8.0048E-06	3.2220E-05	1.0038E-01
9	6.6842E-02	3.3480E-02	7.7931E-06	3.1368E-05	1.0036E-01
10	6.6774E-02	3.3387E-02			1.0016E-01
11	6.6768E-02	3.3384E-02			1.0015E-01
12	6.6768E-02	3.3384E-02			1.0015E-01
13	6.6768E-02	3.3384E-02			1.0015E-01
14	6.6768E-02	3.3384E-02			1.0015E-01
15	6.6768E-02	3.3384E-02			1.0015E-01

Source: Original to this document.

6.1.4.2.3 B₄C Absorber Rods

For some cases B₄C absorber rods are present. The B₄C has a density of 1.28 g/cm^3 per the *International Handbook of Evaluated Criticality Safety Benchmark Experiments* (Ref. 2.2.6, Section 3.3.3). This information is used to determine the atom densities for the B₄C material specification shown in Table 17. Details of the atom density determination can be found in the spreadsheet *Commercial Benchmark Materials.xls* from Attachment 6.

Table 17. Material Specification for B₄C for LEU-COMP-THERM-011

Element/Isotope	MCNP Library ID (ZAID)	atoms/barn-cm
B10	5010.50c	1.1041E-02
B11	5011.50c	4.4440E-02
C	6000.50c	1.3351E-02
Total:		6.8832E-02

Source: Original to document

6.1.4.2.4 Other Materials

Water at a reduced density of 0.0001 g/cm³ is recommended for the benchmark model from the LEU-COMP-THERM-011 benchmark report from the *International Handbook of Evaluated Criticality Safety Benchmark Experiments* (Ref. 2.2.6) as air for the region above the water level.

6.1.4.3 Benchmark k_{eff} Values and Experimental Uncertainties

The estimated experimental k_{eff} (k_{exp}) and uncertainties for each case are shown in Table 18.

Table 18. Expected Experimental k_{eff} and Estimated Experimental Uncertainties for LEU-COMP-THERM-011

Cases	k_{eff}	Uncertainty ($\pm 1\sigma$)
1	1.0010	0.0018
2 - 9	1.0009	0.0032
10 - 14	1.0010	0.0017
15	1.0010	0.0018

Source: Section 3.5 from LEU-COMP-THERM-011 benchmark report from the *International Handbook of Evaluated Criticality Safety Benchmark Experiments* (Ref. 2.2.6).

6.1.4.4 Variations from Recommended Benchmark Model

The 0.318 cm thick aluminum bottom plug in the fuel pin is justifiably ignored in the recommended benchmark model described in the LEU-COMP-THERM-011 benchmark report from the *International Handbook of Evaluated Criticality Safety Benchmark Experiments* (Ref. 2.2.6). While considered a minor detail, it is not difficult to model this feature and provides another simple check that helps to ensure that the active fuel region is started at the proper height above the base plate. It is therefore included for completeness.

The active fuel length is given as 153.34 cm in the experimental description from the LEU-COMP-THERM-011 benchmark report from the *International Handbook of Evaluated Criticality Safety Benchmark Experiments* (Ref. 2.2.6) but is given as 153.36 cm in the benchmark model description of the LEU-COMP-THERM-011 benchmark report from the *International Handbook of Evaluated Criticality Safety Benchmark Experiments* (Ref. 2.2.6). The active fuel length is modeled as 153.34 cm herein. This is considered a minor detail that would not affect the modeled system reactivity significantly but the 153.34 cm value is considered to be a more accurate representation of the actual experimental setup.

The total fuel pin length is given as 156.44 cm in the experimental description from the LEU-COMP-THERM-011 benchmark report from the *International Handbook of Evaluated Criticality Safety Benchmark Experiments* (Ref. 2.2.6). This results in a void space at the top of the fuel pin of 2.464 cm versus the 2.5 cm given in the benchmark model description of the LEU-COMP-THERM-011 benchmark report from the *International Handbook of Evaluated*

Criticality Safety Benchmark Experiments (Ref. 2.2.6). Given that this void region sits above the moderated fuel region and is a small variation in the model, it is not considered to be a significant change. It does however more accurately reflect the experimental setup and is therefore modeled as 2.464 cm versus 2.5 cm.

The 0.952 cm thick aluminum bottom plug in the absorber rod is justifiably ignored in the recommended benchmark model described in the LEU-COMP-THERM-011 benchmark report from the *International Handbook of Evaluated Criticality Safety Benchmark Experiments* (Ref. 2.2.6). While considered a minor detail, it is not difficult to model this feature and helps to ensure that the starting location of the B₄C relative to the active fuel region is correct in comparison to the actual experiment. It is therefore included for completeness.

6.1.5 LEU-COMP-THERM-021

The critical benchmarks described in this section are based upon the benchmark report LEU-COMP-THERM-021 from the *International Handbook of Evaluated Criticality Safety Benchmark Experiments* (Ref. 2.2.6). The benchmarks are based on a series of critical experiments conducted at the Russian Research Center (Kurchatov Institute) in 1961.

The LEU-COMP-THERM-021 benchmark report from the *International Handbook of Evaluated Criticality Safety Benchmark Experiments* (Ref. 2.2.6) described six critical benchmarks consisting of fuel pins with ~5 wt.% ²³⁵U enriched UO₂ arranged in hexagonal lattices. Lattice pitches of 10 and 13 mm were examined with boric acid concentrations of 3.15 g/L and 2.36 g/L, respectively, in the water moderator.

6.1.5.1 Geometry Description

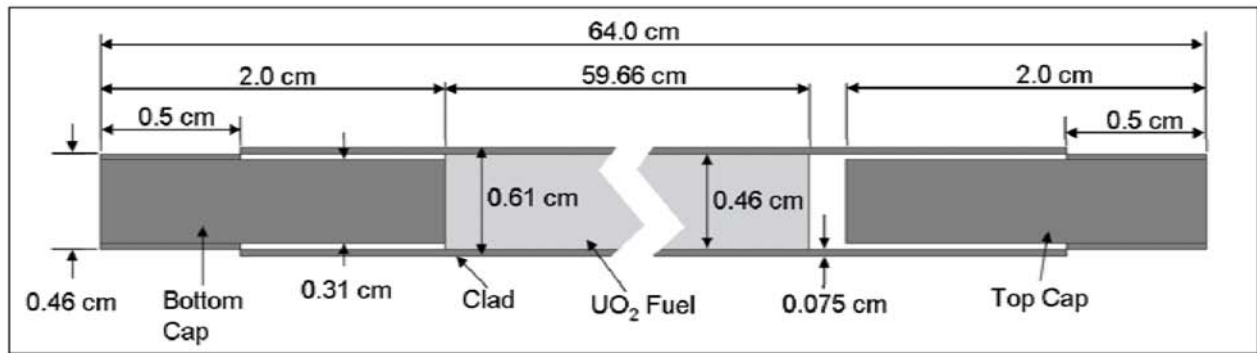
Detailed geometry description of the experiment and the recommended benchmark model can be found in the LEU-COMP-THERM-021 benchmark report from the *International Handbook of Evaluated Criticality Safety Benchmark Experiments* (Ref. 2.2.6). A basic description only is provided herein of the benchmark model.

The as modeled dimensions of the fuel pin are shown in Figure 12 and Table 19. The fuel fit tightly within the clad with essentially no fuel/clad gap. An air gap of 0.34 cm exists between the top of the active fuel region and the top cap.

Table 19. Fuel Pin Model Geometry Data for LEU-COMP-THERM-021

Parameter	Dimension (cm)
Fuel diameter	0.46
Clad outer diameter	0.61
Clad thickness	0.075
Active fuel length	59.66
Top/Bottom cap diameter	0.31
Top/Bottom cap length	2.0

Source: Figure 10 from LEU-COMP-THERM-021 benchmark report from the *International Handbook of Evaluated Criticality Safety Benchmark Experiments* (Ref. 2.2.6).



Source: Figure 10 from LEU-COMP-THERM-021 benchmark report from the *International Handbook of Evaluated Criticality Safety Benchmark Experiments* (Ref. 2.2.6)

Figure 12. Fuel Pin Dimensions for LEU-COMP-THERM-021 Benchmark Model

The fuel is supported by a 3.5 cm thick steel support plate. The actual size of the steel support plate is not given but it is noted in the LEU-COMP-THERM-021 benchmark report from the *International Handbook of Evaluated Criticality Safety Benchmark Experiments* (Ref. 2.2.6, p. 1) that the support plate is held in place by stainless steel rods that are more than 40 cm from the core. The Case 4 core has the largest radius at ~40 cm. Therefore the support plate is modeled with a diameter of 160 cm.

The pitch of the fuel pins was maintained by two aluminum D1 alloy lattice plates. The bottom 0.5 cm thick plate was placed 0.5 cm above the steel support plate. The top 1.0 cm thick plate was placed 60.0 cm above the bottom lattice plate. These plates are not modeled beyond the confines of the fuel lattice and their presence outside the core region was considered negligible per the LEU-COMP-THERM-021 benchmark report from the *International Handbook of Evaluated Criticality Safety Benchmark Experiments* (Ref. 2.2.6, p. 14). For Cases 1 through 3 the lattice plates maintained a pin pitch of 1.0 cm. For Cases 4 through 6 the lattice plates maintained a pin pitch of 1.3 cm. The holes through the lattice plates were 0.02 cm larger than the diameter of the fuel pin or 0.63 cm and are modeled as such.

The LEU-COMP-THERM-021 benchmark report from the *International Handbook of Evaluated Criticality Safety Benchmark Experiments* (Ref. 2.2.6, p. 14) noted that the side reflection provided by the tank and lattice support structures (excluding the support plate) were inconsequential to the system reactivity and are therefore not included in the benchmark model. The experiments were performed in a large steel tank with the experiment raised ~1 m above the bottom of the tank. The tank radius is sufficient to ensure that the radial borated water reflection was greater than 50 cm thick. The tank shell is not modeled. The borated water reflector is modeled as a cylinder with a diameter of 180 cm which is the reported tank diameter from the LEU-COMP-THERM-021 benchmark report from the *International Handbook of Evaluated Criticality Safety Benchmark Experiments* (Ref. 2.2.6).

A 30 cm thick borated water reflector is modeled below the support plate which is more than sufficient to account for the ~1 meter of borated water present in the actual experiment. The borated water cylinder extends to the critical water height as given in Table 20. The values presented in Table 20 are relative to the top of the support plate or bottom of the fuel pin. This reference point is different from the benchmark which used the bottom of the active fuel region for its zero water level reference. The top of the support plate is 2 cm lower and is a more convenient reference from a modeling perspective.

The air surrounding the portion of the core above the critical water height is modeled as void. The air above the core would not be expected to provide a measurable contribution to the reactivity of the system and is therefore considered reasonable to ignore.

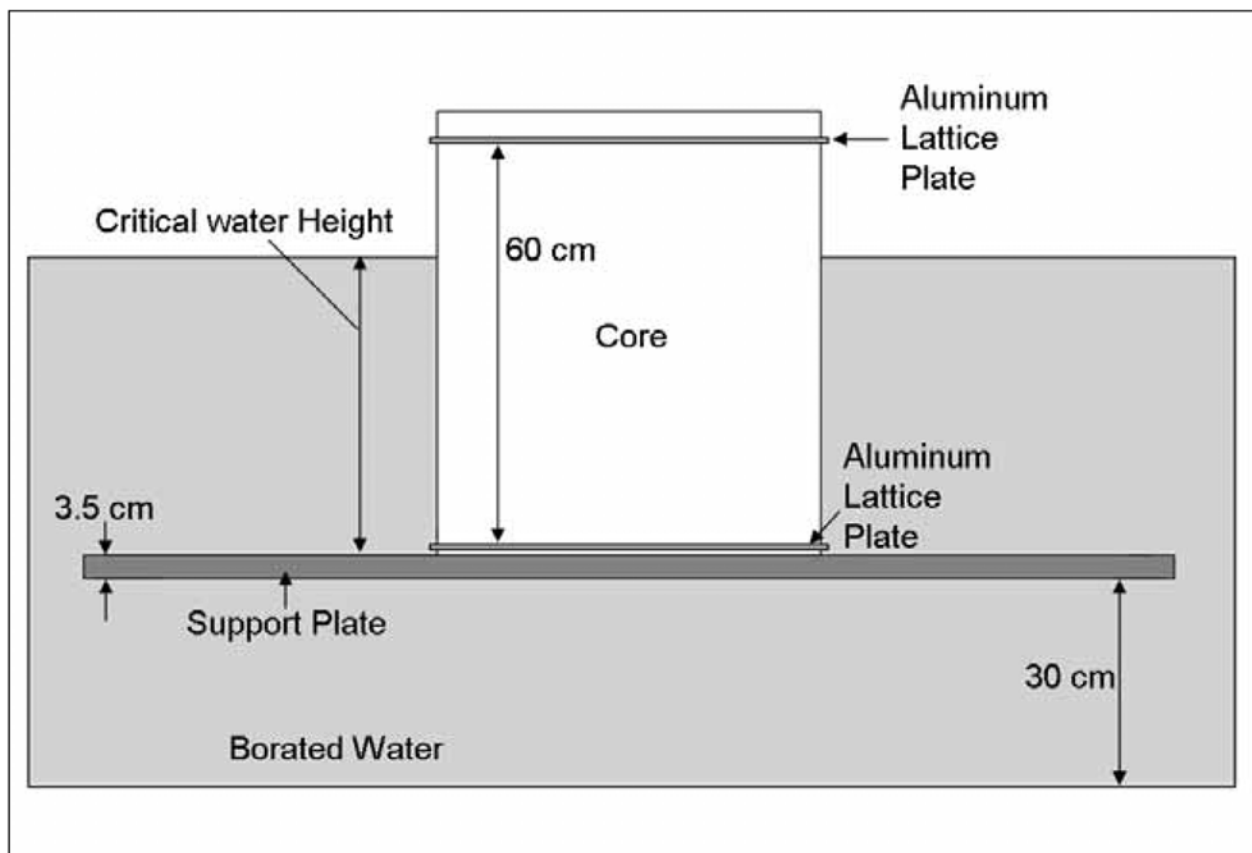
Table 20. Benchmark Model Critical Parameters for LEU-COMP-THERM-021

Case	Boric Acid Concentration (gH ₃ BO ₃ /L)	Pin Pitch (cm)	Critical Water Height ⁽¹⁾ (cm)	Critical Number of Fuel Pins
1	3.15	1.0	42.52	2612
2	3.15	1.0	47.47	2300
3	3.15	1.0	51.74	2128
4	2.36	1.3	42.59	3267
5	2.36	1.3	45.40	2865
6	2.36	1.3	51.93	2307

Source: Table 1 from LEU-COMP-THERM-021 benchmark report from the *International Handbook of Evaluated Criticality Safety Benchmark Experiments* (Ref. 2.2.6).

Notes: ⁽¹⁾ Critical water height relative to the top of the support plate

An axial view of the basic model arrangement is given in Figure 13. The pin maps for the various cases can be found in Attachment 4.



Source: Original to document.

Figure 13. Axial Depiction of Benchmark Model for LEU-COMP-THERM-021

6.1.5.2 Material Descriptions

6.1.5.2.1 Fuel Pin Materials

The fuel consists of UO_2 with an enrichment of 5.059 atom % ^{235}U and a mass of 91.63 g per fuel pin per the LEU-COMP-THERM-021 benchmark report from the *International Handbook of Evaluated Criticality Safety Benchmark Experiments* (Ref. 2.2.6). The isotopic composition of the uranium is taken directly from the LEU-COMP-THERM-021 benchmark report from the *International Handbook of Evaluated Criticality Safety Benchmark Experiments* (Ref. 2.2.6) and is presented in Table 21. The atom densities for the UO_2 fuel material are presented in Table 21. These values were determined in spreadsheet *Commercial Benchmark Materials.xls* from Attachment 6.

The fuel clad and end plugs are made of Zirconium Alloy 110 with a density of 6.44 g/cm^3 . The weight percents are taken from the LEU-COMP-THERM-021 benchmark report from the *International Handbook of Evaluated Criticality Safety Benchmark Experiments* (Ref. 2.2.6) and are presented in Table 21. The atom densities for the fuel clad material are presented in Table 21. These values were determined in spreadsheet *Commercial Benchmark Materials.xls* from Attachment 6.

Table 21. Fuel Pin Material Specifications for LEU-COMP-THERM-021 Benchmark

Material	Isotope/Element	atom %	Wt. %	MCNP Library ID (ZAIID)	Atom Density (atoms/barn-cm)
UO ₂	²³⁴ U	0.031 ⁽¹⁾		92234.50c	6.3924E-06
	²³⁵ U	5.059 ⁽¹⁾		92235.50c	1.0432E-03
	²³⁶ U	0.031 ⁽¹⁾		92236.50c	6.3924E-06
	²³⁸ U	94.879 ⁽¹⁾		92238.50c	1.9565E-02
	O	--		8016.50c	4.1241E-02
				Total:	6.1862E-02
Zirconium Alloy 110 (cladding; 6.44 g/cm ³⁽²⁾)	Zr		98.96 ⁽²⁾	40000.60c	4.2071E-02
	Nb		1 ⁽²⁾	41093.50c	4.1744E-04
	Hf		0.04 ⁽²⁾	72000.50c	8.6913E-06
				Total:	4.2498E-02

Source: Original to document except as noted.

Notes: ⁽¹⁾ Per Section 1.3.1 of LEU-COMP-THERM-021 benchmark report from the *International Handbook of Evaluated Criticality Safety Benchmark Experiments* (Ref. 2.2.6).

⁽²⁾ Based on information presented in Sections 1.3.1 and 2.0 of LEU-COMP-THERM-021 benchmark report from the *International Handbook of Evaluated Criticality Safety Benchmark Experiments* (Ref. 2.2.6).

6.1.5.2.2 Moderator and Reflector Materials

The experiment is moderated and reflected by borated water with boric acid (H₃BO₃) concentrations of either 2.36 g/L or 3.15 g/L. The temperature of the critical assemblies was stated as ranging between 18 – 20 °C (LEU-COMP-THERM-021 benchmark report from the *International Handbook of Evaluated Criticality Safety Benchmark Experiments* (Ref. 2.2.6, p. 4)). A temperature of 20 °C is used here as the water temperature for all the benchmark models which better represents the actual water density of the experiments. The benchmark model's temperature for all zones was given as 300 K (26.85 °C). It is unclear if this temperature was used to define the density of the water in the borated water material or if this may refer to some other aspect of the model (e.g., the temperature to which the cross-section data is evaluated). The determined borated water atom densities are determined with a density based on 20 °C and are compared with the atom densities provided in the LEU-COMP-THERM-021 benchmark report from the *International Handbook of Evaluated Criticality Safety Benchmark Experiments* (Ref. 2.2.6, p. 16). These are presented below in Table 22 with those determined here. The comparison shows only minor variations and it is concluded that these small variations would have no significant impact on the MCNP determined k_{eff} .

Water at 20 °C has a density of 0.9982063 g/cm³ per *CRC Handbook of Chemistry and Physics* (Ref. 2.2.8, p. 6-5). The density of boric acid is given as 1.5 g/cm³ per *CRC Handbook of Chemistry and Physics* (Ref. 2.2.8, p. 4-53). The atom densities for the borated material are presented in Table 22. These values were determined in spreadsheet *Commercial Benchmark Materials.xls* from Attachment 6.

Table 22: Material Specification for Borated Water for LEU-COMP-THERM-021

Element	MCNP Library ID (ZAID)	Atom Densities (atoms/barn-cm)			
		3.15 g/L Boric Acid		2.36 g/L Boric Acid	
		Based on 20 °C water	From benchmark report ⁽¹⁾	Based on 20 °C water	From benchmark report ⁽¹⁾
B10	5010.50c	6.1051E-06	6.1051E-06	4.5740E-06	4.5740E-06
B11	5011.50c	2.4574E-05	2.4574E-05	1.8411E-05	1.8411E-05
H	1001.50c	6.6688E-02	6.6718E-02	6.6700E-02	6.6722E-02
O	8016.50c	3.3390E-02	3.3405E-02	3.3384E-02	3.3396E-02
Total		1.0011E-01		1.0011E-01	

Source: Original to document except as noted.

Notes: ⁽¹⁾ From page 16 of the LEU-COMP-THERM-021 benchmark report from the *International Handbook of Evaluated Criticality Safety Benchmark Experiments* (Ref. 2.2.6)

6.1.5.2.3 Other Materials

The support plate for the fuel pins is made of Steel 3 type steel with a density of 8 g/cm³ per the LEU-COMP-THERM-021 benchmark report from the *International Handbook of Evaluated Criticality Safety Benchmark Experiments* (Ref. 2.2.6). The material specification from the LEU-COMP-THERM-021 benchmark report from the *International Handbook of Evaluated Criticality Safety Benchmark Experiments* (Ref. 2.2.6) and the determined atom densities are presented in Table 23. The atom densities were determined in spreadsheet *Commercial Benchmark Materials.xls* from Attachment 6.

Table 23. Material Specification for Steel 3 for LEU-COMP-THERM-021

Isotope/Element	Weight % ⁽¹⁾	MCNP Library ID (ZAID)	Atom Density (atoms/barn-cm)
C	0.25	6000.50c	1.0028E-03
Si	0.17	14000.50c	2.9161E-04
Al	0.1	13027.50c	1.7856E-04
Mn	0.14	25055.50c	1.2277E-04
Ti	0.46	22000.60c	4.6298E-04
Fe	98.853	--	
⁵⁴ Fe		26054.60c	4.9846E-03
⁵⁶ Fe		26056.60c	7.8248E-02
⁵⁷ Fe		26057.60c	1.8071E-03
⁵⁸ Fe		26058.60c	2.4049E-04
Total:			8.7339E-02

Source: Original to document except as noted.

Notes: ⁽¹⁾ From Table 3.c of the LEU-COMP-THERM-021 benchmark report from the *International Handbook of Evaluated Criticality Safety Benchmark Experiments* (Ref. 2.2.6).

The lattice plates are made of aluminum alloy D1 with a density of 2.7 g/cm³ per the LEU-COMP-THERM-021 benchmark report from the *International Handbook of Evaluated Criticality Safety Benchmark Experiments* (Ref. 2.2.6). The material specification from the LEU-COMP-THERM-021 benchmark report from the *International Handbook of Evaluated Criticality Safety Benchmark Experiments* (Ref. 2.2.6) and the determined atom densities are presented in Table 24. The atom densities were determined in spreadsheet *Commercial Benchmark Materials.xls* from Attachment 6.

Table 24. Material Specification for Aluminum D1 Alloy for LEU-COMP-THERM-021

Isotope/Element	Weight % ⁽¹⁾	MCNP Library ID (ZAID)	Atom Density (atoms/barn-cm)
Al	93.8	13027.50c	5.6526E-02
Cu	4.3	--	--
⁶³ Cu		29063.60c	7.6105E-04
⁶⁵ Cu		29065.60c	3.3921E-04
Mn	0.6	25055.50c	1.7758E-04
Mg	0.6	12000.50c	4.0139E-04
Fe	0.7	--	--
⁵⁴ Fe		26054.60c	1.1913E-05
⁵⁶ Fe		26056.60c	1.8701E-04
⁵⁷ Fe		26057.60c	4.3188E-06
⁵⁸ Fe		26058.60c	5.7475E-07
Total			5.8409E-02

Source: Original to document except as noted

Notes: ⁽¹⁾ From Table 9 of LEU-COMP-THERM-021 benchmark report from the *International Handbook of Evaluated Criticality Safety Benchmark Experiments* (Ref. 2.2.6)

6.1.5.3 Benchmark k_{eff} Values and Experimental Uncertainties

The estimated experimental k_{eff} and uncertainties for each case are shown in Table 25.

Table 25. Expected k_{eff} and Estimated Experimental Uncertainties for LEU-COMP-THERM-021

Cases	k_{eff}	Uncertainty ($\pm 1\sigma$)
1 - 3	1.0000	0.0072
4 - 6	1.0000	0.0050

Source: Section 3.5 of LEU-COMP-THERM-021 benchmark report from the *International Handbook of Evaluated Criticality Safety Benchmark Experiments* (Ref. 2.2.6)

6.1.5.4 Variations from Recommended Benchmark Model

The borated water reflector in the recommended model from the LEU-COMP-THERM-021 benchmark report from the *International Handbook of Evaluated Criticality Safety Benchmark Experiments* (Ref. 2.2.6) is given as a 30 cm thick side reflector and a 20 cm thick layer below the support plate. These are both considered reasonable and sufficient to account for the reflection effects of water. The 30 cm thick side reflection is inconvenient from a modeling perspective given the varying sizes of the different cores modeled. Therefore the water is modeled as a simple cylinder with a diameter of 180 cm which is the actual tank diameter from the experiment.

As noted in Section 6.1.5.1 and the LEU-COMP-THERM-021 benchmark report from the *International Handbook of Evaluated Criticality Safety Benchmark Experiments* (Ref. 2.2.6, p. 2), the experiments were performed in a large steel tank with ~1 m of borated water reflection below the experiment which is considered to effectively act as an infinite reflector. The 20 cm thick layer below the support plate is increased to 30 cm which is a more typical full or infinite water reflector thickness. Neither of these changes would be expected to significantly impact the modeled reactivity of the system as compared to the recommended model. They remain consistent with the described experimental setup from the LEU-COMP-THERM-021 benchmark report from the *International Handbook of Evaluated Criticality Safety Benchmark Experiments* (Ref. 2.2.6).

The support plate in the recommended benchmark model is modeled as the full diameter of the water reflector surrounding the core. As discussed in Section 6.1.5.1, the support plate is modeled with a diameter of 160 cm. The modeling of the support plate beyond the recommended model's 30 cm thick side reflector would not contribute significantly to the reactivity of the system but is both convenient from a modeling perspective and consistent with the actual experimental setup described in the LEU-COMP-THERM-021 benchmark report from the *International Handbook of Evaluated Criticality Safety Benchmark Experiments* (Ref. 2.2.6).

The recommended benchmark model is unclear on what water temperature is used for determining the borated water atom densities. Based on the comparison performed in Table 22 it appears that a temperature of 20 °C was likely used as indicated in Section 1.3.3 of the LEU-COMP-THERM-021 benchmark report from the *International Handbook of Evaluated Criticality Safety Benchmark Experiments* (Ref. 2.2.6) versus the 300 K (26.85 °C) indicated in Section 3.4 of the LEU-COMP-THERM-021 benchmark report from the *International Handbook of Evaluated Criticality Safety Benchmark Experiments* (Ref. 2.2.6). A water density based on 20 °C is used here and is reasonable given the reported temperature range of the experimental setups of 18 °C – 20 °C (LEU-COMP-THERM-021 benchmark report from the *International Handbook of Evaluated Criticality Safety Benchmark Experiments* (Ref. 2.2.6, p. 4)).

6.1.6 LEU-COMP-THERM-034

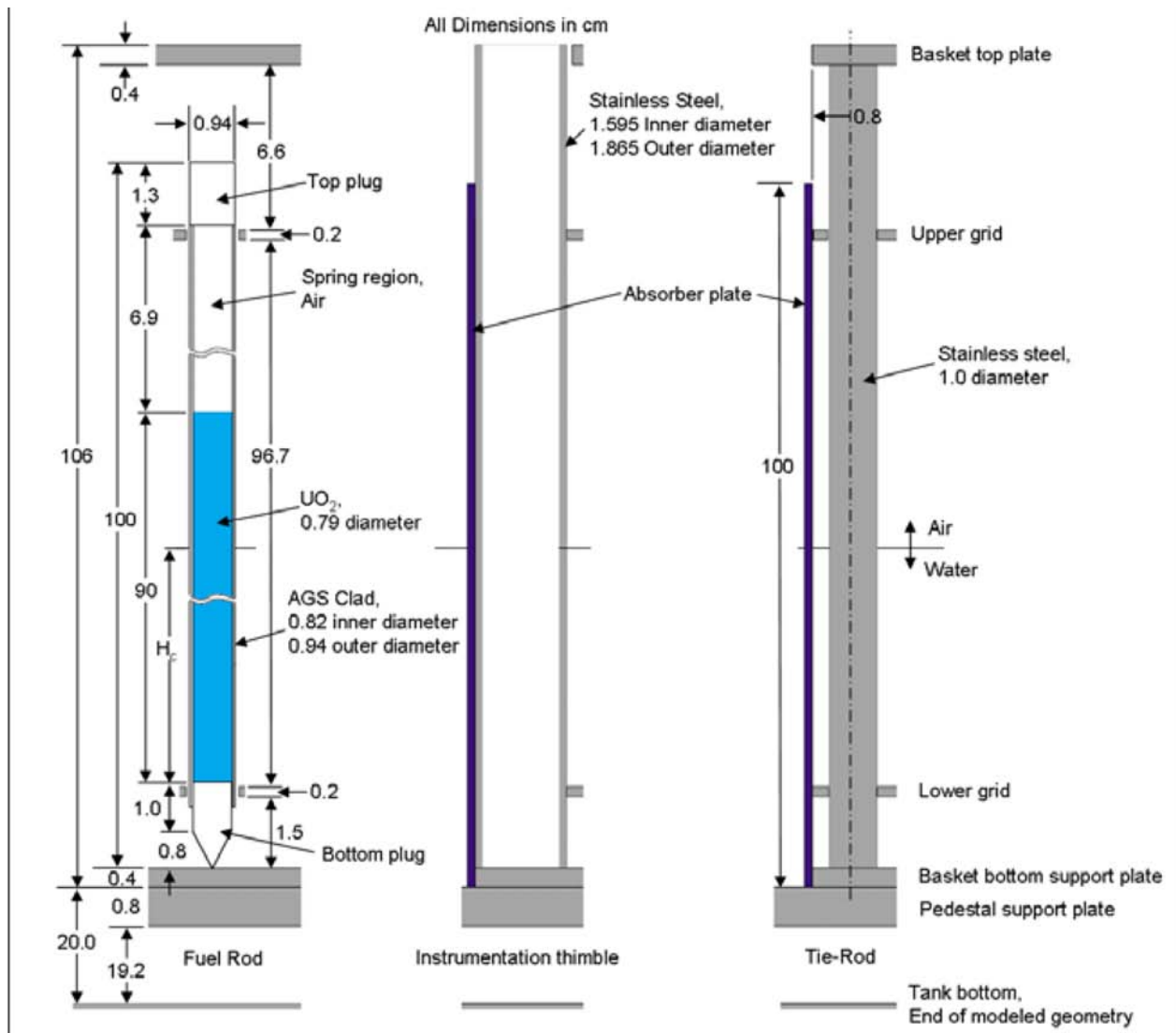
The critical benchmarks described in this section are based upon the LEU-COMP-THERM-034 benchmark report from the *International Handbook of Evaluated Criticality Safety Benchmark Experiments* (Ref. 2.2.6). The benchmarks are based on a series of approach to critical experiments conducted in Apparatus B of the experimental criticality facility at the Service de Recherches et d'Etudes en Criticité in 1979.

The LEU-COMP-THERM-034 benchmark report from the *International Handbook of Evaluated Criticality Safety Benchmark Experiments* (Ref. 2.2.6) described 26 critical benchmarks consisting of fuel pins with 4.738 wt.% ^{235}U enriched UO_2 arranged in square lattices. Of these, 14 are used here. These 14 included absorber plates of either borated stainless steel or Boral. The experiments were water moderated and reflected. The critical water height was determined for each experiment.

6.1.6.1 Geometry Description

Detailed geometry description of the experiment and the recommended benchmark model can be found in the LEU-COMP-THERM-034 benchmark report from the *International Handbook of Evaluated Criticality Safety Benchmark Experiments* (Ref. 2.2.6). A basic description only is provided herein of the benchmark model.

The as-modeled fuel pin characteristics are shown in Figure 14 and Table 26.



Source: Adapted from Figures 8 and 10 from LEU-COMP-THERM-034 benchmark report from the *International Handbook of Evaluated Criticality Safety Benchmark Experiments* (Ref. 2.2.6)

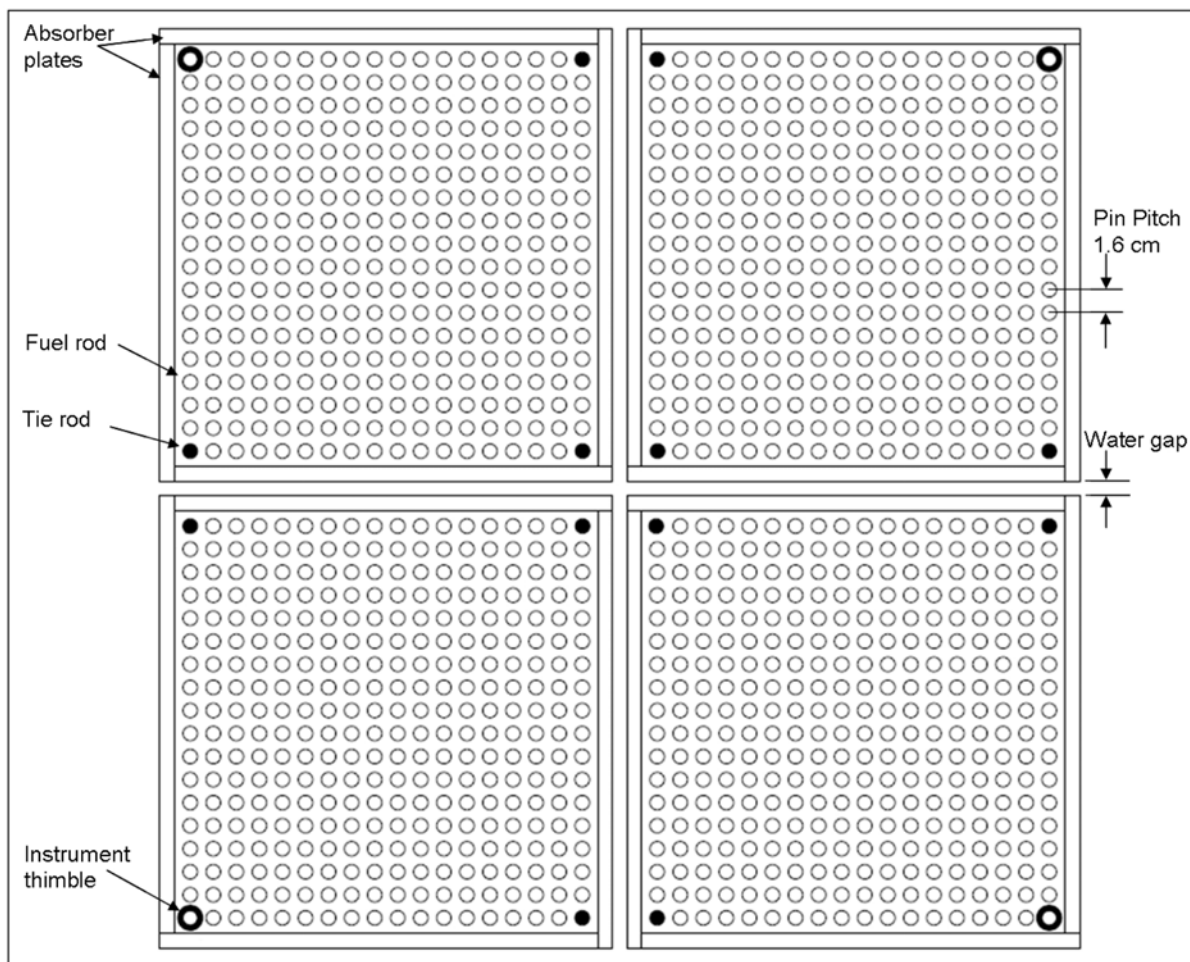
Figure 14. Axial Views of the as-modeled Experimental Setup for LEU-COMP-THERM-034

Table 26. Fuel Pin Model Geometry Data for LEU-COMP-THERM-034

Parameter	Dimension (cm)
Fuel diameter	0.79
Clad inner diameter	0.82
Clad outer diameter	0.94
Fuel height	90.0
Pin height	100.0
Top plug height	1.3
Top gap thickness	6.9
Bottom plug height	1.0
Conical bottom height	0.8
Source: Figures 8 and 10 from LEU-COMP-THERM-034 benchmark report from the <i>International Handbook of Evaluated Criticality Safety Benchmark Experiments</i> (Ref. 2.2.6)	

The fuel pins are arranged into four assemblies with each set of pins arranged in a 1.6 cm square pitched lattice in each assembly. The fuel pin lattice is an 18 x 18 array with the corner positions taken up by either tie rods (3 per assembly) or an instrument thimble (1 per assembly). The fuel is held in position by upper and lower grids. These grids are 0.2 cm thick steel with 1.0 cm diameter holes for the fuel. The instrument thimble hole size is modeled as the same as the outer diameter of the instrument thimble (1.865 cm). The instrument thimble was placed such that its outer diameter was essentially tangent to the grid outer edge. The tie rods are 1.0 cm in diameter. No explicit value for the diameter of the holes in the spacer grids for the tie rods is given in the LEU-COMP-THERM-034 benchmark report from the *International Handbook of Evaluated Criticality Safety Benchmark Experiments* (Ref. 2.2.6) and is modeled the same as the tie rod diameter (1.0 cm). This small simplification over the experiment will not significantly impact the modeled reactivity of the system. Each assembly has a bottom support and top plate that are 28.8 cm square and 0.4 cm thick. The basic axial arrangement can be seen in Figure 14.

The Boral plates used are 29.45 cm wide, 100 cm in height and 0.65 cm thick. The Boral is constructed of a B₄C and aluminum mixture between two 0.11 cm thick aluminum plates. The borated stainless steel plates are 28.955 cm wide, 100 cm in height, and 0.155 cm thick. The basic axial arrangement of the absorber plates is shown in Figure 14. The basic arrangement of the four assemblies is shown in Figure 15. The critical water heights and water gaps between the assemblies for each critical benchmark are given in Table 27.



Source: Adapted from Figure 5 of LEU-COMP-THERM-034 benchmark report from the *International Handbook of Evaluated Criticality Safety Benchmark Experiments* (Ref. 2.2.6)

Figure 15. Fuel Pin Assembly Arrangement for LEU-COMP-THERM-034

Table 27. Benchmark Critical Parameters for LEU-COMP-THERM-034

Case	Absorber Plate Material	Water Gap (cm)	Water Critical Height (cm)
1	borated steel	0.6	34.33
2	borated steel	1.0	36.54
3	borated steel	2.0	41.40
4	borated steel	3.0	47.15
5	borated steel	4.0	53.87
6	borated steel	5.0	62.86
7	borated steel	6.0	70.73
8	borated steel	7.0	80.66
10	Boral	0.3	50.74
11	Boral	0.5	53.01
12	Boral	1.0	57.43
13	Boral	1.5	66.15
14	Boral	2.0	72.96
15	Boral	2.5	84.15

Source: Table 1 from of LEU-COMP-THERM-034 benchmark report from the *International Handbook of Evaluated Criticality Safety Benchmark Experiments* (Ref. 2.2.6)

The four assemblies sit on a 95 cm x 95 cm steel support plate that is part of a pedestal which raises the fuel assemblies off the bottom of the steel tank in which the experiments were conducted. The pedestal support plate is 0.8 cm thick. Its axial location is shown in Figure 14.

The experimental setup was placed inside a square 120 cm x 120 cm steel tank. The height of the tank was 140 cm. The recommended model from the LEU-COMP-THERM-034 benchmark report from the *International Handbook of Evaluated Criticality Safety Benchmark Experiments* (Ref. 2.2.6) did not model the tank walls or bottom due to the thickness of the water reflectors on the sides and bottom of the assemblies. The worth of the portion of the fuel above the water was considered sufficiently small as to be able to ignore the reflection effects of the tank's steel wall. Therefore the four assemblies are modeled in the center of 120 cm x 120 cm block of water. The water extends up to the given critical height and extends 19.2 cm below the pedestal support plate.

6.1.6.2 Material Descriptions

6.1.6.2.1 Fuel Pin Materials

The fuel consists of UO_2 with a density of 10.38 g/cm^3 per the LEU-COMP-THERM-034 benchmark report in the *International Handbook of Evaluated Criticality Safety Benchmark Experiments* (Ref. 2.2.6). The isotopic composition of the uranium is taken directly from the LEU-COMP-THERM-034 benchmark report in the *International Handbook of Evaluated Criticality Safety Benchmark Experiments* (Ref. 2.2.6) and is presented in Table 28.

Aluminum, silicon, and iron impurities were explicitly included in the fuel specification. These impurities are a part of the overall UO_2 density of 10.38 g/cm^3 . The values are listed in Table 28.

In addition to these three impurities, boron is added to the material specification to account for other impurities. The atom densities presented in Table 28 are determined in spreadsheet *Commercial Benchmark Materials.xls* from Attachment 6.

The clad and end plug material for the fuel is AGS. The material specification for AGS was taken from the LEU-COMP-THERM-034 benchmark report in the *International Handbook of Evaluated Criticality Safety Benchmark Experiments* (Ref. 2.2.6). The determined atom densities to be used in MCNP are shown in Table 28. Details on the determinations of the atom densities can be found in the spreadsheet *Commercial Benchmark Materials.xls* from Attachment 6.

Table 28. Fuel Material Specifications for LEU-COMP-THERM-034

Material	Element/ Isotope	Concentration (g/cm ³)	Wt.%	MCNP Library ID (ZAID)	Atom density (atoms/barn-cm)
UO ₂ Fuel	²³⁴ U		0.0303 ⁽²⁾	92234.50c	7.1333E-06
density=10.38 g/cm ³⁽²⁾	²³⁵ U		4.738 ⁽²⁾	92235.50c	1.1107E-03
	²³⁶ U		0.1364 ⁽²⁾	92236.50c	3.1839E-05
	²³⁸ U		95.0953 ⁽²⁾	92238.50c	2.2011E-02
	O			8016.50c	4.6320E-02
	Equivalent B	5.19E-06 ⁽²⁾			
	¹⁰ B			5010.50c	5.7531E-08
	¹¹ B			5011.50c	2.3157E-07
				Total:	6.9481E-02
AGS Alloy Clad	Al		98.85 ⁽³⁾	13027.50c	5.9570E-02
density=2.7g/cm ³⁽³⁾	Mg		0.47 ⁽³⁾	12000.50c	3.1442E-04
	Si		0.43 ⁽³⁾	14000.50c	2.4894E-04
	Fe		0.22 ⁽³⁾		
	⁵⁴ Fe			26054.60c	3.7440E-06
	⁵⁶ Fe			26056.60c	5.8773E-05
	⁵⁷ Fe			26057.60c	1.3573E-06
	⁵⁸ Fe			26058.60c	1.8064E-07
	Zn ⁽¹⁾		0.03 ⁽³⁾	29063.60c	7.4576E-06
				Total:	6.0204E-02

Source: Original to document except as noted.

Notes: ⁽¹⁾ No cross section library available for Zn. ⁶³Cu cross-section utilized. See Assumption 3.2.1.

⁽²⁾ Per Table 1 and Section 1.3 from the LEU-COMP-THERM-034 benchmark report in the *International Handbook of Evaluated Criticality Safety Benchmark Experiments* (Ref. 2.2.6)

⁽³⁾ Per Table 4 from the LEU-COMP-THERM-034 benchmark report in the *International Handbook of Evaluated Criticality Safety Benchmark Experiments* (Ref. 2.2.6)

6.1.6.2.2 Other Materials

The moderator and main reflector for this benchmark is water. Per the LEU-COMP-THERM-034 benchmark report in the *International Handbook of Evaluated Criticality Safety Benchmark Experiments* (Ref. 2.2.6) the experiments were performed at 21 °C. The density of water at 21 °C per *CRC Handbook of Chemistry and Physics* (Ref. 2.2.8, p. 6-5) is 0.9979948 g/cm³. This value was used to determine the material specification for water at 21 °C as given in Table 29.

Details of this determination may be found in spreadsheet *Commercial Benchmark Materials.xls* from Attachment 6.

Table 29. Water Material Specification

Element/ Isotope	MCNP Library ID (ZAID)	Atoms per Molecule
¹ H	1001.50c	2
¹⁶ O	8016.50c	1
Density: 1.0008E-01 atoms/barn-cm (See spreadsheet <i>Commercial Benchmark Materials.xls</i> from Attachment 6 or detailed determination)		

Source: Original to this document.

The support plate and the two spacer plates are all made of Z2CN18-10 stainless steel. This is the same material as that used in the LEU-COMP-THERM-007 benchmark report in the *International Handbook of Evaluated Criticality Safety Benchmark Experiments* (Ref. 2.2.6) for stainless steel and detailed in Section 6.1.3.2.2 with the determined atom densities shown in Table 11.

The Boral plates were described in the LEU-COMP-THERM-034 benchmark report in the *International Handbook of Evaluated Criticality Safety Benchmark Experiments* (Ref. 2.2.6) as a mixture of B₄C and aluminum between two plates of pure aluminum. The aluminum density is given as 2.651 g/cm³. The overall density of the B₄C and aluminum mixture is given as 2.6189 g/cm³. The boron is defined as natural boron with an areal density of 250 mg/cm² with a thickness of 0.43 cm. The aluminum plate information (the 2.651 g/cm³ density) is used directly in the MCNP models with the MCNP aluminum library 13027.50c. The B₄C and aluminum mixture information is used to determine the atom densities which are presented in Table 30. Details on the atom density determinations can be found in spreadsheet *Commercial Benchmark Materials.xls* from Attachment 6.

Table 30. Boral B₄C+Al Material Specification for LEU-COMP-THERM-034

Element/Isotope	MCNP Library ID (ZAID)	Atom Densities (atoms/barn-cm)
B10	5010.50c	6.4448E-03
B11	5011.50c	2.5941E-02
C	6000.50c	8.0965E-03
Al	13027.50c	4.1872E-02
Total:		8.2354E-02

Source: Original to document.

The borated steel material specification for the borated steel plates was given in terms of an overall density and weight percents for each of the elements. This specification was used to determine the atom densities used in the MCNP models. These are presented in Table 31. Details on the atom density determinations can be found in spreadsheet *Commercial Benchmark Materials.xls* from Attachment 6. The density of borated steel was given as 8.033 g/cm³ per the

LEU-COMP-THERM-034 benchmark report in the *International Handbook of Evaluated Criticality Safety Benchmark Experiments* (Ref. 2.2.6, p. 13).

Table 31. Borated Steel Material Specification for LEU-COMP-THERM-034

Element/Isotope	Wt.%(¹)	MCNP Library ID (ZAID)	Atom density (atoms/barn-cm)
B	1.1		
¹⁰ B		5010.50c	9.7951E-04
¹¹ B		5011.50c	3.9426E-03
C	0.036	6000.50c	1.4500E-04
Cr	18.49		
⁵⁰ Cr		24050.60c	7.4745E-04
⁵² Cr		24052.60c	1.4414E-02
⁵³ Cr		24053.60c	1.6344E-03
⁵⁴ Cr		24054.60c	4.0684E-04
Ni	12.99		
⁵⁸ Ni		28058.60c	7.2887E-03
⁶⁰ Ni		28060.60c	2.8076E-03
⁶¹ Ni		28061.60c	1.2204E-04
⁶² Ni		28062.60c	3.8913E-04
⁶⁴ Ni		28064.60c	9.9100E-05
Mn	0.68	25055.50c	5.9878E-04
Si	0.61	14000.50c	1.0507E-03
P	0.03	15031.50c	4.6855E-05
S	0.006	16032.50c	9.0521E-06
Fe	66.058		
⁵⁴ Fe		26054.60c	3.3447E-03
⁵⁶ Fe		26056.60c	5.2504E-02
⁵⁷ Fe		26057.60c	1.2126E-03
⁵⁸ Fe		26058.60c	1.6137E-04
		Total:	9.1905E-02

Source: Original to document except as noted.

Notes: ⁽¹⁾ Per Table 3 of the LEU-COMP-THERM-034 benchmark report in the *International Handbook of Evaluated Criticality Safety Benchmark Experiments* (Ref. 2.2.6).

6.1.6.3 Benchmark k_{eff} Values and Experimental Uncertainties

The estimated experimental k_{eff} and uncertainties for each case are shown in Table 32.

Table 32. Expected k_{eff} and Estimated Experimental Uncertainties for LEU-COMP-THERM-034

Cases	k_{eff}	Uncertainty ($\pm 1\sigma$)
1 and 2	1.0000	0.0047
3 – 8	1.0000	0.0039
10 – 11	1.0000	0.0048

Source: Table 17 from the LEU-COMP-THERM-034 benchmark report in the *International Handbook of Evaluated Criticality Safety Benchmark Experiments* (Ref. 2.2.6)

6.1.6.4 Variations from Recommended Benchmark Model

The conical portion of the bottom plug is modeled in the LEU-COMP-THERM-034 benchmark report from the *International Handbook of Evaluated Criticality Safety Benchmark Experiments* (Ref. 2.2.6) as a simple cylinder with a height that conserves the plug mass. This is a reasonable simplification but the true conical shape of the plug is a relatively simple geometry for MCNP. Therefore, the conical portion of the bottom plug is modeled as described for the actual fuel pin per the LEU-COMP-THERM-034 benchmark report from the *International Handbook of Evaluated Criticality Safety Benchmark Experiments* (Ref. 2.2.6).

The recommended model from the LEU-COMP-THERM-034 benchmark report from the *International Handbook of Evaluated Criticality Safety Benchmark Experiments* (Ref. 2.2.6) modeled the instrument thimble as 1.6 cm x 1.6 cm square tube with a wall thickness such that mass is preserved. This was done to simplify the model. This feature is modeled as described in Figure 14. This is the actual geometry from the experiment and is a relatively simple feature to model in MCNP. This is considered to be a minor feature and modeling it as described in the LEU-COMP-THERM-034 benchmark report from the *International Handbook of Evaluated Criticality Safety Benchmark Experiments* (Ref. 2.2.6) or as done herein would not be expected to result in a significant impact on the MCNP determined reactivity of the system.

The LEU-COMP-THERM-034 benchmark report from the *International Handbook of Evaluated Criticality Safety Benchmark Experiments* (Ref. 2.2.6) based the material specification for Z2CN18-10 Stainless Steel on a national standard. The assumptions made regarding the exact composition of this steel are slightly different from those used in the LEU-COMP-THERM-007 benchmark report from the *International Handbook of Evaluated Criticality Safety Benchmark Experiments* (Ref. 2.2.6). The material specification for Z2CN18-10 Stainless Steel as presented in the LEU-COMP-THERM-007 benchmark report from the *International Handbook of Evaluated Criticality Safety Benchmark Experiments* (Ref. 2.2.6) is used here for the stainless steel.

6.2 DETERMINATION OF CRITICAL LIMIT (K_L)

6.2.1 Benchmark Results

Based upon the benchmark models described in Section 6.1 a total of 51 critical benchmarks were modeled using MCNP (Ref. 2.2.11). The normalized k_{eff} results with the combined uncertainties are presented in Table 33. Additional results and details of the determination of the various quantities presented in Table 33 can be found in spreadsheet *Commercial Validation Results.xls* from Attachment 6.

Table 33. Benchmark Results

Benchmark	Case	MCNP Output File	$k_{\text{adj}}^{(1)}$	Combined uncertainty ⁽²⁾
LEU-COMP-THERM-001	2	LCT001bo	0.99675	0.00313
LEU-COMP-THERM-001	3	LCT001co	0.99568	0.00313
LEU-COMP-THERM-001	4	LCT001do	0.99625	0.00313
LEU-COMP-THERM-001	5	LCT001eo	0.99374	0.00313
LEU-COMP-THERM-001	6	LCT001fo	0.99591	0.00313
LEU-COMP-THERM-001	7	LCT001go	0.99603	0.00312
LEU-COMP-THERM-001	8	LCT001ho	0.99471	0.00313
LEU-COMP-THERM-002	4	LCT002do	0.99611	0.00205
LEU-COMP-THERM-002	5	LCT002eo	0.99412	0.00206
LEU-COMP-THERM-007	1	LCT007ao	0.99389	0.00149
LEU-COMP-THERM-007	2	LCT007bo	0.99648	0.00096
LEU-COMP-THERM-007	3	LCT007co	0.99360	0.00084
LEU-COMP-THERM-007	4	LCT007do	0.99402	0.00090
LEU-COMP-THERM-007	5	LCT007eo	0.99321	0.00149
LEU-COMP-THERM-007	6	LCT007fo	0.99660	0.00094
LEU-COMP-THERM-007	7	LCT007go	0.99858	0.00083
LEU-COMP-THERM-007	8	LCT007ho	0.99403	0.00149
LEU-COMP-THERM-007	9	LCT007io	0.99639	0.00094
LEU-COMP-THERM-007	10	LCT007jo	0.99908	0.00084
LEU-COMP-THERM-011	1	LCT011ao	0.99332	0.00185
LEU-COMP-THERM-011	2	LCT011bo	0.99627	0.00323
LEU-COMP-THERM-011	3	LCT011co	0.99569	0.00323
LEU-COMP-THERM-011	4	LCT011do	0.99645	0.00323
LEU-COMP-THERM-011	5	LCT011eo	0.99538	0.00323
LEU-COMP-THERM-011	6	LCT011fo	0.99635	0.00323
LEU-COMP-THERM-011	7	LCT011go	0.99650	0.00323
LEU-COMP-THERM-011	8	LCT011ho	0.99548	0.00323
LEU-COMP-THERM-011	9	LCT011io	0.99404	0.00323
LEU-COMP-THERM-011	10	LCT011jo	0.99090	0.00176
LEU-COMP-THERM-011	11	LCT011ko	0.99071	0.00175
LEU-COMP-THERM-011	12	LCT011lo	0.99166	0.00176
LEU-COMP-THERM-011	13	LCT011mo	0.99100	0.00175
LEU-COMP-THERM-011	14	LCT011no	0.99109	0.00175

Benchmark	Case	MCNP Output File	$k_{adj}^{(1)}$	Combined uncertainty ⁽²⁾
LEU-COMP-THERM-011	15	LCT011oo	0.99043	0.00185
LEU-COMP-THERM-021	1	LCT021ao	1.01088	0.00722
LEU-COMP-THERM-021	2	LCT021bo	1.01074	0.00722
LEU-COMP-THERM-021	3	LCT021co	1.01041	0.00722
LEU-COMP-THERM-021	4	LCT021do	1.01191	0.00502
LEU-COMP-THERM-021	5	LCT021eo	1.01321	0.00502
LEU-COMP-THERM-021	6	LCT021fo	1.01227	0.00502
LEU-COMP-THERM-034	1	LCT034ao	1.00350	0.00473
LEU-COMP-THERM-034	2	LCT034bo	1.00536	0.00473
LEU-COMP-THERM-034	3	LCT034co	1.00144	0.00393
LEU-COMP-THERM-034	4	LCT034do	1.00010	0.00393
LEU-COMP-THERM-034	5	LCT034eo	0.99955	0.00393
LEU-COMP-THERM-034	6	LCT034fo	1.00160	0.00393
LEU-COMP-THERM-034	7	LCT034go	0.99873	0.00393
LEU-COMP-THERM-034	8	LCT034ho	0.99942	0.00393
LEU-COMP-THERM-034	9	LCT034io	1.00158	0.00393
LEU-COMP-THERM-034	10	LCT034jo	1.00127	0.00483
LEU-COMP-THERM-034	11	LCT034ko	0.99761	0.00483

Source: Original to this document.

Notes: ⁽¹⁾ Per Eq. 2 from Section 4.3.

⁽²⁾ Per Eq. 3 from Section 4.3.

6.2.2 Test for Normality of Benchmark results

The Shapiro-Wilk normality test described in Section 4.3.2 was applied to the data presented in Table 33. The Shapiro-Wilk test can handle no more than 50 data points, therefore the 50 smallest adjusted k_{eff} values from the 51 values presented in Table 33 are used here.

The value for the statistic W_t was determined to be 0.644 for the 50 smallest adjusted k_{eff} values from Table 33 (Details can be found in spreadsheet *Commercial Validation Results.xls* from Attachment 6). The value of W for 50 experiments from Table 38 in Attachment 1 is 0.947. Given that W_t is less than W , the distribution cannot be considered normal. As a result the single-sided distribution free tolerance limit technique described in Section 4.3.3 will be used to determine the value of K_L .

6.2.3 Single-Sided Distribution Free Tolerance Limit Determination

Given that the distribution of the adjusted k_{eff} (k_{adj}) values presented in Table 33 was shown not to be normally distributed (See Section 6.2.2), the single-sided distribution free tolerance limit methodology described in Section 4.3.3 is used to determine the value of K_L . From Table 2 the value of K_L should be based on the smallest value of the adjusted k_{eff} (k_{adj}) values given 51 critical benchmarks for the 90% confidence level ($\gamma=0.90$). The smallest adjusted k_{eff} value from Table 33 is 0.99043 ± 0.00185 .

Based on Eq. 15 from Section 4.3.3 and Table 33 (Case 15 of LEU-COMP-THERM-011), the value of k_{small} is set to 0.99043 and the value of σ_{small} is set to 0.00185. The value of NPM from Eq.15 is based upon the degree of confidence in the population of k_{adj} values which is based on the size of the population (51 in this case). From Table 3 a confidence of greater than 90% for 95% of the population results in a NPM value of 0.0. As discussed in Section 4.3.3 the minimum number of modeled critical benchmarks needed to result in a NPM of 0 is 45. Therefore, given a population size of 51, the value of NPM is set to 0 and the value of K_L per Eq.15 is determined as follows:

$$K_L = 0.99043 - 0.00185 - 0.0$$

$$K_L = 0.988$$

This value of K_L is considered to be a critical limit for MCNP calculations involving similar configurations to those described in Section 6.1. The meaning of this limit is that there is a 90% confidence that 95% of all critical configurations modeled with MCNP will have a k_{eff} value greater than 0.988. This value will be modified into an USL based upon Eq. 10 and the values for Δk_{EROA} and Δk_m . The value of Δk_{EROA} is determined in the following section. The value of Δk_m is left to be determined in an applicable criticality safety analysis that includes an evaluation of operations associated with commercial nuclear fuel.

6.3 RANGE OF APPLICABILITY DETERMINATIONS AND COMPARISONS

The range of applicability (ROA) determination is based upon the examination of parameters associated with the modeled critical benchmarks. The parameters examined for determining the ROA were the following:

- Fissile Material – Fissile Isotope, Enrichment, and Physical form
- Moderator – Moderating Element, Moderating Material, and Moderator Element to Fissile Isotope atom ratio (M/X)
- Reflector Material
- Neutron Absorber – Absorbing Element and Absorber Form (Soluble or Solid)
- Geometry – Basic shapes used (e.g., arrays of cylindrical pins)
- Energy Spectrum – Average Energy of Neutron Causing Fission (AENCF), Energy of Average Lethargy of neutrons causing Fission (EALF), and the percent breakdown of the energy of neutrons causing fissions occurring in the thermal (0 – 0.625 eV), Intermediate (> 0.625 eV – 100 keV), and Fast (>100 keV) energy ranges

The determinations associated with each of the above parameters were based upon the information presented in Section 6.1 and the MCNP model input and output files located on the CD from Attachment 6. The AENCF and EALF are determined based upon the following equations:

$$AENCF = \frac{\sum n_i \times e_i}{\sum n_i} \quad (\text{Eq. 16})$$

$$EALF = \frac{e_0}{\exp \left[\frac{\sum (n_i \times \mu_i)}{\sum n_i} \right]} \quad (\text{Eq. 17})$$

$$\mu_i = \ln \frac{e_0}{e_i} \quad (\text{Eq. 18})$$

where,

n_i = the number of fissions caused by neutrons of the i^{th} energy bin

e_i = the upper energy limit in eV of the i^{th} energy bin

e_0 = 20 MeV

μ_i = lethargy of e_i

The parameter determinations are presented in Table 34.

The values from Table 34 for the critical benchmarks are used to help determine the applicability of the resulting value of K_L to those MCNP modeled configurations involving commercial nuclear fuel that are considered to be significant to the criticality safety of the geologic repository operations area. Of specific interest to this validation are the MCNP modeled configurations of commercial nuclear fuel used to evaluate the reactivity of water moderated configurations associated with operations in the Wet Handling Facility. These configurations are evaluated and documented in *Nuclear Criticality Calculations for the Wet Handling Facility* (Ref. 2.2.14). The output files listed in Table 35 represent the results considered to be the most significant to criticality safety. The output files selected may also be considered representative of many similar MCNP models of commercial nuclear fuel found in *Nuclear Criticality Calculations for the Wet Handling Facility* (Ref. 2.2.14) based upon the range of parameter values determined from these specific output files as summarized in Table 34.

Table 34. Parameter Values and Ranges for the MCNP Modeled Critical Benchmarks and Selected Commercial Nuclear Fuel Models

Parameter		Value(s) or Range from Critical Benchmarks Described in Section 6.1	Value(s) or Range from Commercial Nuclear Fuel Configurations Listed in Table 35
Fissile Isotope		^{235}U	^{235}U
Enrichment (wt% ^{235}U in U)		2.35 - 5.00	5.0
Fissile Material Physical Form		UO ₂	UO ₂
Moderating Element		Hydrogen	Hydrogen
Moderating Material		Water	Water
Moderator Element to fissile isotope atom ratio (H/ ^{235}U)		108.61 - 694.68 ⁽¹⁾	29.13 – 158.13 ⁽³⁾
Reflecting Materials		Water, Steel, Aluminum, Acrylic	Water, Steel, Concrete
Neutron Absorber Element		Boron	Boron
Neutron Absorber Physical Form		Soluble(boric acid), Solid (borated stainless steel, Boral, B ₄ C)	Soluble(boric acid), Solid (borated stainless steel, Boral)
Geometry of Critical Benchmarks (Shape or Form)		Arrays of cylindrical fuel pins	Arrays of cylindrical fuel pins
AENCF (eV)		78,437 - 256,359 ⁽²⁾	172,975 – 577,156 ⁽⁴⁾
EALF (eV)		0.087 - 0.384 ⁽²⁾	0.318 – 34.787 ⁽⁴⁾
Neutrons Causing Fission Spectrum	Thermal % (0 - 0.625 eV)	82.25 - 94.76 ⁽²⁾	40.49 – 80.91 ⁽⁴⁾
	Intermediate % (0.625 eV - 100 keV)	3.16 - 11.81 ⁽²⁾	13.46 – 41.83 ⁽⁴⁾
	Fast % (100 keV - 20 MeV)	2.08 - 6.77 ⁽²⁾	5.63 – 17.68 ⁽⁴⁾

Source: Original to this document

Notes:

- ⁽¹⁾ Determined directly from the critical benchmark input models from the CD of Attachment 6. The determinations were based upon the unit cell consisting of a fuel pin, the interstitial moderator present, and the pin array parameters (e.g., pin pitch and array type (hexagonal or square)). See spreadsheet *Commercial Validation Results.xls* from Attachment 6 and the MCNP critical benchmark models for additional detail.
- ⁽²⁾ Information based upon MCNP tally results taken from the MCNP output files for the modeled critical benchmarks. Additional details and results can be found in spreadsheet *Commercial Validation Results.xls* from Attachment 6 and the MCNP output files from the CD of Attachment 6.
- ⁽³⁾ Determined directly from the MCNP input models from the CD of Attachment 6. The determinations were based upon the unit cell consisting of a fuel pin and the interstitial moderator present pin array parameters (e.g., pin pitch and array type (hexagonal or square)). See spreadsheet *Commercial Validation Results.xls* from Attachment 6 and the MCNP model descriptions from *Nuclear Criticality Calculations for the Wet Handling Facility* (Ref. 2.2.14) for additional detail.
- ⁽⁴⁾ Information based upon MCNP tally results taken from the MCNP output files for the MCNP models. These models are modified from the originals taken from *Nuclear Criticality Calculations for the Wet Handling Facility* (Ref. 2.2.14). The modifications involve the addition of the applicable tallies used to determine these parameters. Additional details and results can be found in spreadsheet *Commercial Validation Results.xls* from Attachment 6 and the MCNP output files from the CD of Attachment 6.

Table 35. Significant MCNP Models of Commercial Nuclear Fuel from the Criticality Safety Analysis

Output File Name	Significance to Criticality Safety
17OFAPinArrayC_0.8_20_37_ino	The results of these and similar MCNP output files from <i>Nuclear Criticality Calculations for the Wet Handling Facility</i> (Ref. 2.2.14) define the minimum required boron concentration associated with WHF pool operations. These models represent simple water moderated square pitched arrays of large numbers of fuel pins (1,681 – 6,561) reflected by water and concrete or steel. See the model descriptions provided in <i>Nuclear Criticality Calculations for the Wet Handling Facility</i> (Ref. 2.2.14) for additional details.
17OFAPinArrayC_0.8_20_40_ino	
17OFAPinArrayS_0.8_20_37_ino	
17OFAPinArrayS_0.8_20_40_ino	
BW15PinArrayC_0.8_20_60_ino	
BW15PinArrayC_0.8_20_70_ino	
BW15PinArrayS_0.8_20_60_ino	
BW15PinArrayS_0.8_20_70_ino	
ANF9PinArrayC_0.9_20_37_ino	
ANF9PinArrayS_0.9_20_37_ino	
GE7PinArrayC_0.9_20_20_ino	
GE7PinArrayC_0.9_20_30_ino	
GE7PinArrayS_0.9_20_20_ino	
GE7PinArrayS_0.9_20_30_ino	
ANF9CW_1.51_ino	The results of these and similar MCNP output files from <i>Nuclear Criticality Calculations for the Wet Handling Facility</i> (Ref. 2.2.14) demonstrate that the modeled condition remains subcritical. These models represent a variety of specific conditions for various fuel assemblies in the WHF pool. These include single assemblies, assemblies in Transport, Aging, and Disposal Canisters, and assemblies in the WHF pool staging racks. See the model descriptions provided in <i>Nuclear Criticality Calculations for the Wet Handling Facility</i> (Ref. 2.2.14) for additional details.
BW15S_1.7_1000_ino	
GE7CW_1.968_ino	
TAD_Array_BW15_B2_0.999_1.525_2500_90_ino	
TAD_Array_BW15_B2_0.999_1.525_2500_91_ino	
TAD_Array_BW15_B2_0.999_1.525_2500_92_ino	
TAD_Array_BW15_B2_0.999_1.525_2500_93_ino	
TAD_Array_BW15_B2_0.999_1.525_2500_94_ino	
rck_17OFA_Assembly_on_topo	
rck_17OFAB_1.2598_5.08_2500_ino	
rck_BW15BnoGap_1.525_2500_ino	

A comparison of the parameter ranges in Table 34 between the critical benchmark and the MCNP models of commercial nuclear fuel shows that the parameter values of the MCNP models of commercial nuclear fuel are within the ROA of the modeled critical benchmarks for the basic physical benchmark parameters such as fissile material, moderator material, neutron absorber materials, and geometry. For the other parameters, the MCNP models of the commercial nuclear fuel are only partially within the ROA. For example, while the ROA explicitly includes water and steel as reflector materials, concrete is not included in the critical benchmarks. Each of the parameters that are either only partially covered or not covered by the ROA defined by Table 34 will be discussed below to determine the need for an additional penalty on the USL for extending the range of applicability.

The areas for which the parameters of the MCNP models of commercial nuclear fuel are outside the ROA can be grouped into two basic categories. The first is the reflector materials and the second is the neutron energy spectrum of neutrons causing fission. The neutron energy spectrum parameters include the obvious direct measures of the spectrum (e.g., AENCF and EALF) and the H/²³⁵U ratio which directly influences these parameters.

Concrete is used as a reflector material in *Nuclear Criticality Calculations for the Wet Handling Facility* (Ref. 2.2.14) but is not a material in any of the modeled critical benchmarks. The most significant elements that make up concrete (oxygen, hydrogen, silicon, iron, and aluminum) are however, all modeled as part of significant materials in the modeled critical benchmarks. Only sodium, calcium, and potassium are not modeled in any of the significant materials of the critical benchmarks. Calcium is modeled in a few of the critical benchmarks (e.g., part of rubber end cap of the fuel rods) but these materials are only considered a minor part of the geometry. The most significant elements that make up concrete are well represented in other materials (water, cladding, and steel) in the modeled critical benchmarks. Those that are not represented would not be expected to have a significant impact on system reactivity based upon their small combined weight percent in concrete (~12% per Table 16 of *Nuclear Criticality Calculations for the Wet Handling Facility* (Ref. 2.2.14)) and their small cross sections as compared to the other elements per *Nuclides and Isotopes* (Ref. 2.2.7). Therefore, the most significant elements of the concrete material used in the MCNP models of commercial nuclear fuel are considered covered by this validation. No additional margin is considered necessary to cover the other minor material constituents of the concrete material as specified in Table 16 of *Nuclear Criticality Calculations for the Wet Handling Facility* (Ref. 2.2.14).

Although the ROA parameters from Table 34 related to the neutron energy spectrum show that the neutrons causing fission are predominantly in the thermal energy range, the intermediate and, to a lesser extent, the fast energy ranges of the fissile material are well exercised. This is not considered sufficient to validate cases that, for example, have little or no thermal fissions (e.g., metal fuel with no moderation) or are otherwise dominated by the fast energy spectrum. However, it is considered reasonable that the critical benchmarks sufficiently exercise the thermal and intermediate ranges that they would be applicable to systems dominated by these regions. Given that the fissile materials, geometric configurations, moderator, significant neutron poisons, and reflector materials (except as noted above) of the MCNP models of commercial nuclear fuel are all either the same or very similar to modeled critical benchmarks, this assertion is considered reasonable. The differences seen in the neutron spectral parameters can be attributed to the over moderated conditions of most of the critical benchmarks as seen in the higher H/²³⁵U ratios and the presence of boron in almost all of the MCNP models of commercial nuclear fuel. This does not, however, preclude the critical benchmarks from being applicable to modeled configurations that are less dominated by the thermal region but are still highly dominated by both the thermal and intermediate regions. Therefore, while there is a difference in the neutron energy spectral parameters as seen in Table 34, they are not considered different enough to preclude the applicability of the modeled critical benchmarks to the MCNP models of commercial nuclear fuels. No additional margin is considered necessary due to these noted differences in the neutron energy spectral parameters.

Although not listed as part of the ROA or ROP, the actual boron concentrations and more importantly the ¹⁰B concentrations used in the MCNP models from *Nuclear Criticality Calculations for the Wet Handling Facility* (Ref. 2.2.14) are considerably higher than the boron concentrations seen in the modeled critical benchmarks. However, given that boron is a very effective neutron poison, its effect on k_{eff} is large in comparison to both the benchmark uncertainties and the MCNP Monte Carlo uncertainties. As a result, even small errors in MCNP's ability to properly model the absorption cross section of boron would be noted even at the relatively low boron concentrations utilized in the modeled critical benchmarks. To show the overall worth of the boron to the system reactivity four of the model critical benchmarks and two

of the MCNP models of commercial nuclear fuels were modified to void out the boron in the borated water. The results are presented in Table 36.

Table 36. Estimated Boron Worth in Selected MCNP Models

Output File with Boron	Output File without Boron	Boron Concentration (mg/L)	$k_{\text{eff}}+2\sigma$ with Boron	$k_{\text{eff}}+2\sigma$ without Boron	Δk /(mg B/L)
LCT011bo	LCT011b-noborono	1038.5	0.99807	1.19211	1.868E-04
LCT011io	LCT011i-noborono	703	0.9958	1.17258	2.515E-04
LCT021ao	LCT021a-nborono	550.8	1.0119	1.13084	2.159E-04
LCT021do	LCT021d-nborono	412.6	1.01281	1.17144	3.845E-04
BW15S_1.7_1000_ino ⁽²⁾	BW15S_1.7_1000_-NoB-ino	1000 ⁽³⁾	0.9337 ⁽¹⁾	1.1054	1.717E-04
ANF9PinArrayC_0.9_20_37_ino ⁽²⁾	ANF9PinArrayC_0.9_20_37_-NoB-ino	2500 ⁽³⁾	0.91513 ⁽¹⁾	1.1617	9.863E-05

Source: Original to document except as noted.

Notes: ⁽¹⁾ From Excel spreadsheet Simple Geometry Results.xls of Attachment 2 from *Nuclear Criticality Calculations for the Wet Handling Facility* (Ref. 2.2.14).

⁽²⁾ MCNP input files from MCNP Files.zip of Attachment 2 from *Nuclear Criticality Calculations for the Wet Handling Facility* (Ref. 2.2.14).

⁽³⁾ Determined from MCNP input file and *Nuclear Criticality Calculations for the Wet Handling Facility* (Ref. 2.2.14).

From the results presented in Table 36 it can be seen that the overall worth of the boron in terms of the change in k_{eff} per milligram of boron per liter of water is similar for both the critical benchmark models and the models of commercial nuclear fuels. It is therefore reasonable to expect that the critical benchmarks containing borated water sufficiently cover and allow for any bias in MCNP's ability to properly predict k_{eff} values as the result of the presence of borated water regardless of the higher concentration of boron in the water of the commercial nuclear fuel configurations.

As a result of the above discussions, no penalties are included as part of the Δk_{EROA} for extending the ROA of the selected benchmark experiments to cover the ROP of the commercial nuclear fuel configurations as given in Table 34.

7. RESULTS AND CONCLUSIONS

This calculation determined the bias plus bias uncertainty for the MCNP modeling of commercial nuclear fuels to result in a critical limit (K_L) of 0.988. This is applicable to commercial nuclear fuels modeled with MCNP that take no burnup credit (i.e., model fresh fuel). The range of applicability (ROA) for this validation is given in Table 37. This limit is expected to be used in the determination of an upper subcritical limit (USL) which also includes an administrative margin (Δk_m) and any additional penalties for extending the range of applicability (Δk_{EROA}). The determination of the administrative margin is left to the applicable analysis of specific operations to which the USL is to be applied. Conclusions related to the extension of the ROA were determined herein for a specific set of MCNP models. They may reasonably be applied to similar models but caution should be exercised to ensure that such application is reasonable and justified.

This calculation compared the range of parameters for a number of the more significant MCNP models of commercial nuclear fuel to the ROA provided in Table 37. This comparison showed that for the physical parameters (e.g., enrichment, moderating material, neutron absorber, etc.) the MCNP models for commercial nuclear fuel were within the ROA. The comparison also determined that while the neutron spectral parameters of the MCNP models did not fall within the ROA, the difference between the MCNP models and the ROA was not significant enough to warrant any additional penalty.

Table 37. Range of Applicability for Commercial Fuel Modeled with MCNP

Parameter		Value(s) or Range
Fissile Isotope		^{235}U
Enrichment (wt% ^{235}U in U)		2.35 - 5.00
Fissile Material Physical Form		UO_2
Moderating Element		Hydrogen
Moderating Material		Water
Moderator Element to fissile isotope atom ratio ($\text{H}/^{235}\text{U}$)		108.61 - 694.68
Reflecting Materials		Water, Steel, Aluminum, Acrylic
Neutron Absorber Element		Boron
Neutron Absorber Physical Form		Soluble(boric acid), Solid (borated stainless steel, Boral, B_4C)
Geometry of Critical Benchmarks (Shape or Form)		Arrays of cylindrical fuel pins
AENCF (eV)		78,437 - 256,359
EALF (eV)		0.087 - 0.384
Neutrons Causing Fission Spectrum	Thermal % (0 - 0.625 eV)	82.25 - 94.76
	Intermediate % (0.625 eV - 100 keV)	3.16 - 11.81
	Fast % (100 keV - 20 MeV)	2.08 - 6.77

Source: Table 34 of this Document

The MCNP models did include concrete as reflector material which is not included in the ROA. The elements making up concrete were determined to be sufficiently represented in other materials utilized in the criticality benchmark models that no additional penalty for concrete reflection was deemed necessary.

The determined critical limit and penalties for extending the range of applicability are considered applicable to MCNP models of moderated commercial nuclear fuel with the same basic parameters as those defined by the ROA. The determined need for additional penalties on the USL determined herein may be applicable to other MCNP models not specifically evaluated in this calculation but their applicability must be justified.

Attachment 1: Tables of Statistics Values

Table 38. Lower Tail Values of W for n experiments at the 95% Confidence Level

n	W	n	W
10	0.842	31	0.929
11	0.850	32	0.930
12	0.859	33	0.931
13	0.866	34	0.933
14	0.874	35	0.934
15	0.881	36	0.935
16	0.887	37	0.936
17	0.892	38	0.938
18	0.897	39	0.939
19	0.901	40	0.940
20	0.905	41	0.941
21	0.908	42	0.942
22	0.911	43	0.943
23	0.914	44	0.944
24	0.916	45	0.945
25	0.918	46	0.945
26	0.920	47	0.946
27	0.923	48	0.947
28	0.924	49	0.947
29	0.926	50	0.947
30	0.927		

Source: Table 5.5 of *Goodness-Of-Fit Techniques* (Ref. 2.2.13).

Table 39. Values of α_j for the Shapiro-Wilks Test for Normality

j	Number of experiments (n)										
	10	11	12	13	14	15	16	17	18	19	20
1	0.5739	0.5601	0.5475	0.5359	0.5251	0.5150	0.5056	0.4968	0.4886	0.4808	0.4734
2	0.3291	0.3315	0.3325	0.3325	0.3318	0.3306	0.3290	0.3273	0.3253	0.3232	0.3211
3	0.2141	0.2260	0.2347	0.2412	0.2460	0.2495	0.2521	0.2540	0.2553	0.2561	0.2565
4	0.1224	0.1429	0.1586	0.1707	0.1802	0.1878	0.1939	0.1988	0.2027	0.2059	0.2085
5	0.0399	0.0695	0.0922	0.1099	0.1240	0.1353	0.1447	0.1524	0.1587	0.1641	0.1686
6		0.0000	0.0303	0.0539	0.0727	0.0880	0.1005	0.1109	0.1197	0.1271	0.1334
7				0.0000	0.0240	0.0433	0.0593	0.0725	0.0837	0.0932	0.1013
8						0.0000	0.0196	0.0359	0.0496	0.0612	0.0711
9								0.0000	0.0163	0.0303	0.0422
10										0.0000	0.0140

Source: Table 5.4 of *Goodness-Of-Fit Techniques* (Ref. 2.2.13).Table 40. Values of α_j for the Shapiro-Wilks Test for Normality

j	Number of experiments (n)									
	21	22	23	24	25	26	27	28	29	30
1	0.4643	0.4590	0.4542	0.4493	0.4450	0.4407	0.4366	0.4328	0.4291	0.4254
2	0.3185	0.3156	0.3126	0.3098	0.3069	0.3043	0.3018	0.2992	0.2968	0.2944
3	0.2578	0.2571	0.2563	0.2554	0.2543	0.2533	0.2522	0.2510	0.2499	0.2487
4	0.2119	0.2131	0.2139	0.2145	0.2148	0.2151	0.2152	0.2151	0.2150	0.2148
5	0.1736	0.1764	0.1787	0.1807	0.1822	0.1836	0.1848	0.1857	0.1864	0.1870
6	0.1399	0.1443	0.1480	0.1512	0.1539	0.1563	0.1584	0.1601	0.1616	0.1630
7	0.1092	0.1150	0.1201	0.1245	0.1283	0.1316	0.1346	0.1372	0.1395	0.1415
8	0.0804	0.0878	0.0941	0.0997	0.1046	0.1089	0.1128	0.1162	0.1192	0.1219
9	0.0530	0.0618	0.0696	0.0764	0.0823	0.0876	0.0923	0.0965	0.1002	0.1036
10	0.0263	0.0368	0.0459	0.0539	0.0610	0.0672	0.0728	0.0778	0.0822	0.0862
11	0.0000	0.0122	0.0228	0.0321	0.0403	0.0476	0.0540	0.0598	0.0650	0.0697
12			0.0000	0.0107	0.0200	0.0284	0.0358	0.0424	0.0483	0.0537
13					0.0000	0.0094	0.0178	0.0253	0.0320	0.0381
14							0.0000	0.0084	0.0159	0.0227
15									0.0000	0.0076

Source: Table 5.4 of *Goodness-Of-Fit Techniques* (Ref. 2.2.13).

Table 41. Values of α_j for the Shapiro-Wilks Test for Normality

j	Number of experiments (n)									
	31	32	33	34	35	36	37	38	39	40
1	0.4220	0.4188	0.4156	0.4127	0.4096	0.4068	0.4040	0.4015	0.3989	0.3964
2	0.2921	0.2898	0.2876	0.2854	0.2834	0.2813	0.2794	0.2774	0.2755	0.2737
3	0.2475	0.2463	0.2451	0.2439	0.2427	0.2415	0.2403	0.2391	0.2380	0.2368
4	0.2145	0.2141	0.2137	0.2132	0.2127	0.2121	0.2116	0.2110	0.2104	0.2098
5	0.1874	0.1878	0.1880	0.1882	0.1883	0.1883	0.1883	0.1881	0.1880	0.1878
6	0.1641	0.1651	0.1660	0.1667	0.1673	0.1678	0.1683	0.1686	0.1689	0.1691
7	0.1433	0.1449	0.1463	0.1475	0.1487	0.1496	0.1505	0.1513	0.1520	0.1526
8	0.1243	0.1265	0.1284	0.1301	0.1317	0.1331	0.1344	0.1356	0.1366	0.1376
9	0.1066	0.1093	0.1118	0.1140	0.1160	0.1179	0.1196	0.1211	0.1225	0.1237
10	0.0899	0.0931	0.0961	0.0988	0.1013	0.1036	0.1056	0.1075	0.1092	0.1108
11	0.0739	0.0777	0.0812	0.0844	0.0873	0.0900	0.0924	0.0947	0.0967	0.0986
12	0.0585	0.0629	0.0669	0.0706	0.0739	0.0770	0.0798	0.0824	0.0848	0.0870
13	0.0435	0.0485	0.0530	0.0572	0.0610	0.0645	0.0677	0.0706	0.0733	0.0759
14	0.0289	0.0344	0.0395	0.0441	0.0484	0.0523	0.0559	0.0592	0.0622	0.0651
15	0.0144	0.0206	0.0262	0.0314	0.0361	0.0404	0.0444	0.0481	0.0515	0.0546
16	0.0000	0.0068	0.0131	0.0187	0.0239	0.0287	0.0331	0.0372	0.0409	0.0444
17			0.0000	0.0062	0.0119	0.0172	0.0220	0.0264	0.0305	0.0343
18					0.0000	0.0057	0.0110	0.0158	0.0203	0.0244
19							0.0000	0.0053	0.0101	0.0146
20									0.0000	0.0049

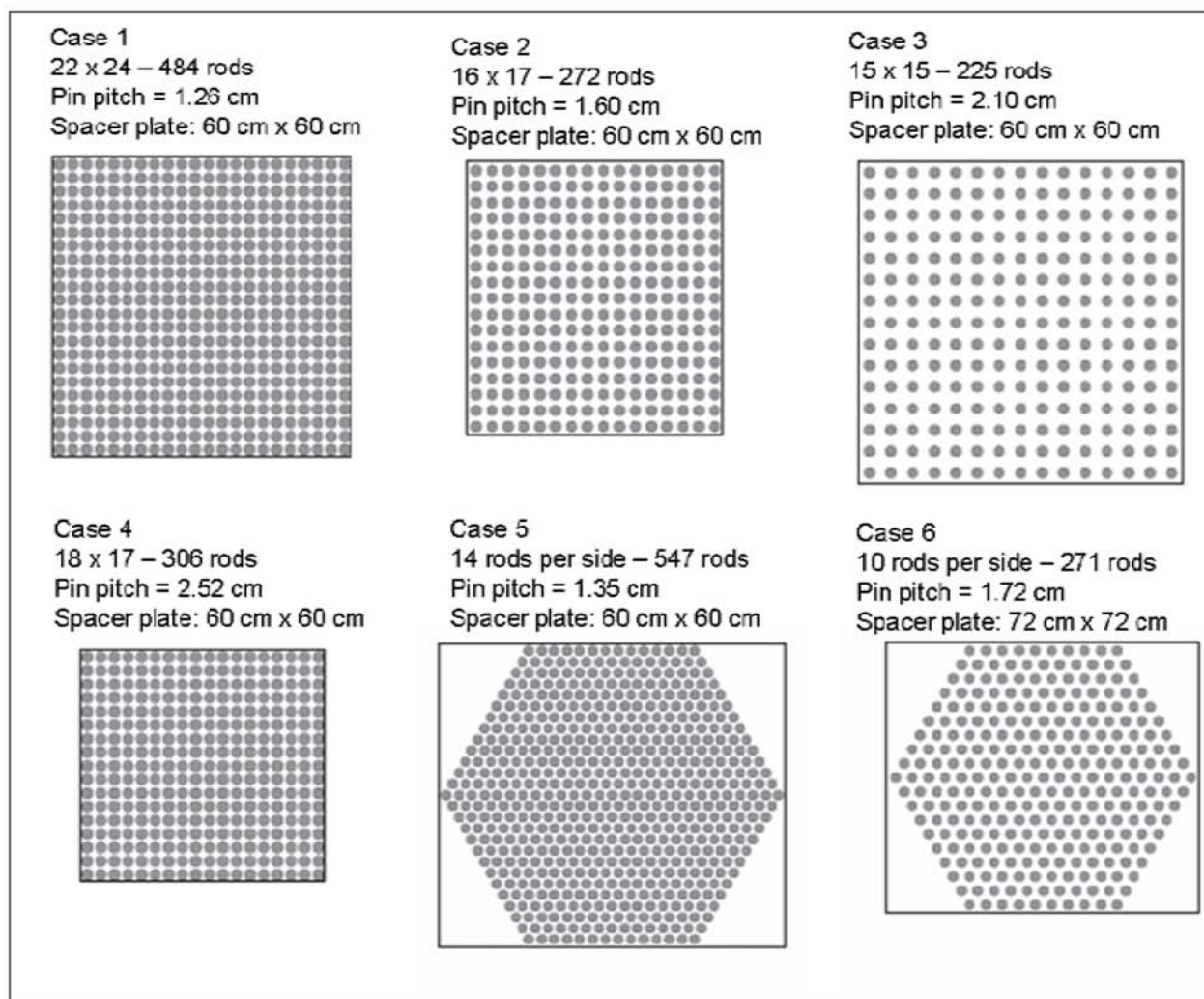
Source: Table 5.4 of *Goodness-Of-Fit Techniques* (Ref. 2.2.13).

Table 42. Values of α_j for the Shapiro-Wilks Test for Normality

j	Number of experiments (n)									
	41	42	43	44	45	46	47	48	49	50
1	0.3940	0.3917	0.3894	0.3872	0.3850	0.3830	0.3808	0.3789	0.3770	0.3751
2	0.2719	0.2701	0.2684	0.2667	0.2651	0.2635	0.2620	0.2604	0.2589	0.2574
3	0.2357	0.2345	0.2334	0.2323	0.2313	0.2302	0.2291	0.2281	0.2271	0.2260
4	0.2091	0.2085	0.2078	0.2072	0.2065	0.2058	0.2052	0.2045	0.2038	0.2032
5	0.1876	0.1874	0.1871	0.1868	0.1865	0.1862	0.1859	0.1855	0.1851	0.1847
6	0.1693	0.1694	0.1695	0.1695	0.1695	0.1695	0.1695	0.1693	0.1692	0.1691
7	0.1531	0.1535	0.1539	0.1542	0.1545	0.1548	0.1550	0.1551	0.1553	0.1554
8	0.1384	0.1392	0.1398	0.1405	0.1410	0.1415	0.1420	0.1423	0.1427	0.1430
9	0.1249	0.1259	0.1269	0.1278	0.1286	0.1293	0.1300	0.1306	0.1312	0.1317
10	0.1123	0.1136	0.1149	0.1160	0.1170	0.1180	0.1189	0.1197	0.1205	0.1212
11	0.1004	0.1020	0.1035	0.1049	0.1062	0.1073	0.1085	0.1095	0.1105	0.1113
12	0.0891	0.0909	0.0927	0.0943	0.0959	0.0972	0.0986	0.0998	0.1010	0.1020
13	0.0782	0.0804	0.0824	0.0842	0.0860	0.0876	0.0892	0.0906	0.0919	0.0932
14	0.0677	0.0701	0.0724	0.0745	0.0765	0.0783	0.0801	0.0817	0.0832	0.0846
15	0.0575	0.0602	0.0628	0.0651	0.0673	0.0694	0.0713	0.0731	0.0748	0.0764
16	0.0476	0.0506	0.0534	0.0560	0.0584	0.0607	0.0628	0.0648	0.0667	0.0685
17	0.0379	0.0411	0.0442	0.0471	0.0497	0.0522	0.0546	0.0568	0.0588	0.0608
18	0.0283	0.0318	0.0352	0.0383	0.0412	0.0439	0.0465	0.0489	0.0511	0.0532
19	0.0188	0.0227	0.0263	0.0296	0.0328	0.0357	0.0385	0.0411	0.0436	0.0459
20	0.0094	0.0136	0.0175	0.0211	0.0245	0.0277	0.0307	0.0335	0.0361	0.0386
21	0.0000	0.0045	0.0087	0.0126	0.0163	0.0197	0.0229	0.0259	0.0288	0.0314
22			0.0000	0.0042	0.0081	0.0118	0.0153	0.0185	0.0215	0.0244
23					0.0000	0.0039	0.0076	0.0111	0.0143	0.0174
24							0.0000	0.0037	0.0071	0.0104
25									0.0000	0.0035

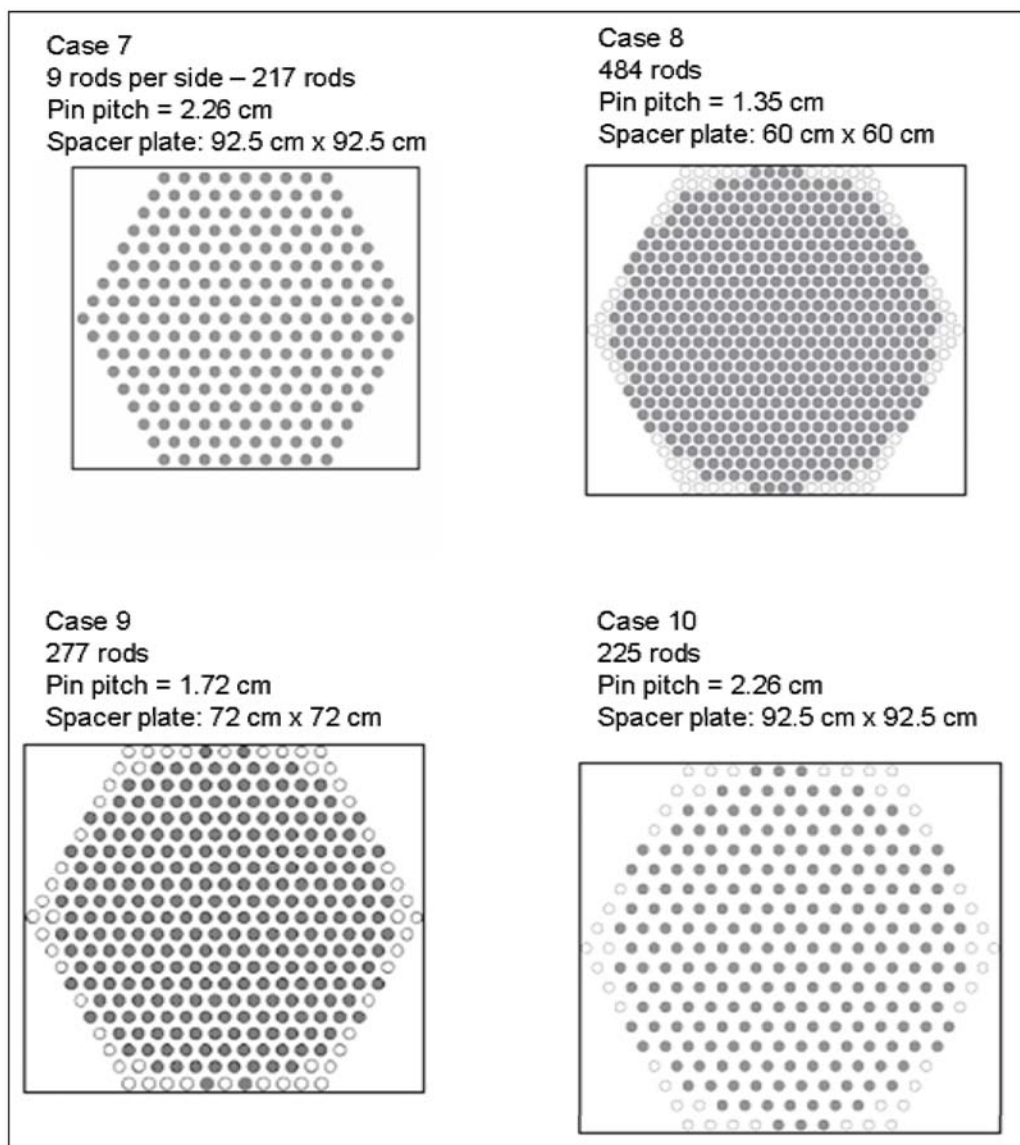
Source: Table 5.4 of *Goodness-Of-Fit Techniques* (Ref. 2.2.13).

Attachment 2: Critical Benchmark Pin Maps for LEU-COMP-THERM-007



Source: Adapted from Figures 3 and 4 of LEU-COMP-THERM-007 benchmark report from the *International Handbook of Evaluated Criticality Safety Benchmark Experiments* (Ref. 2.2.6)

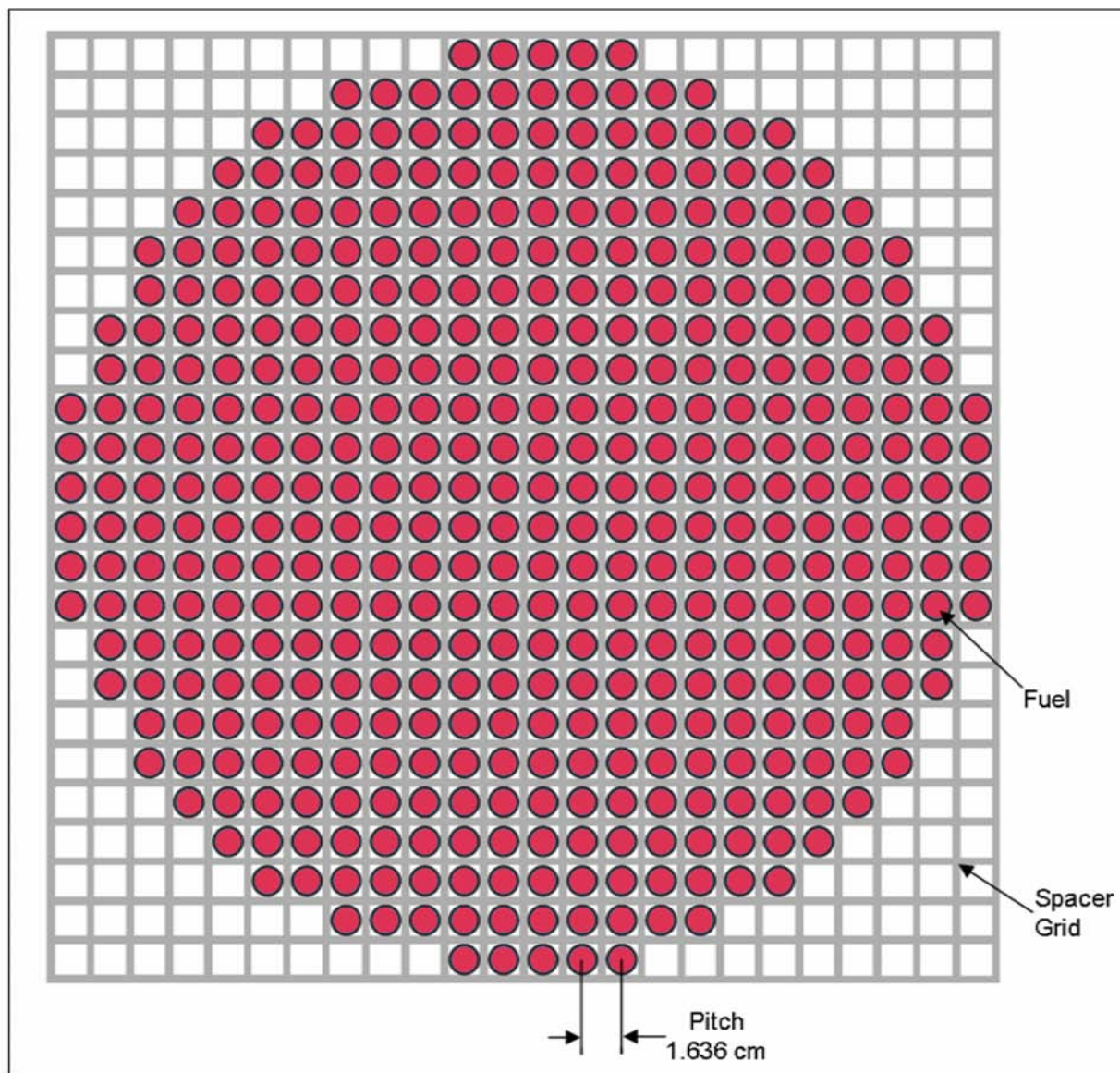
Figure 16. Pin Maps for Cases 1 through 6 for LEU-COMP-THERM-007



Source: Adapted from Figures 4 and 5 of LEU-COMP-THERM-007 benchmark report from the *International Handbook of Evaluated Criticality Safety Benchmark Experiments* (Ref. 2.2.6)

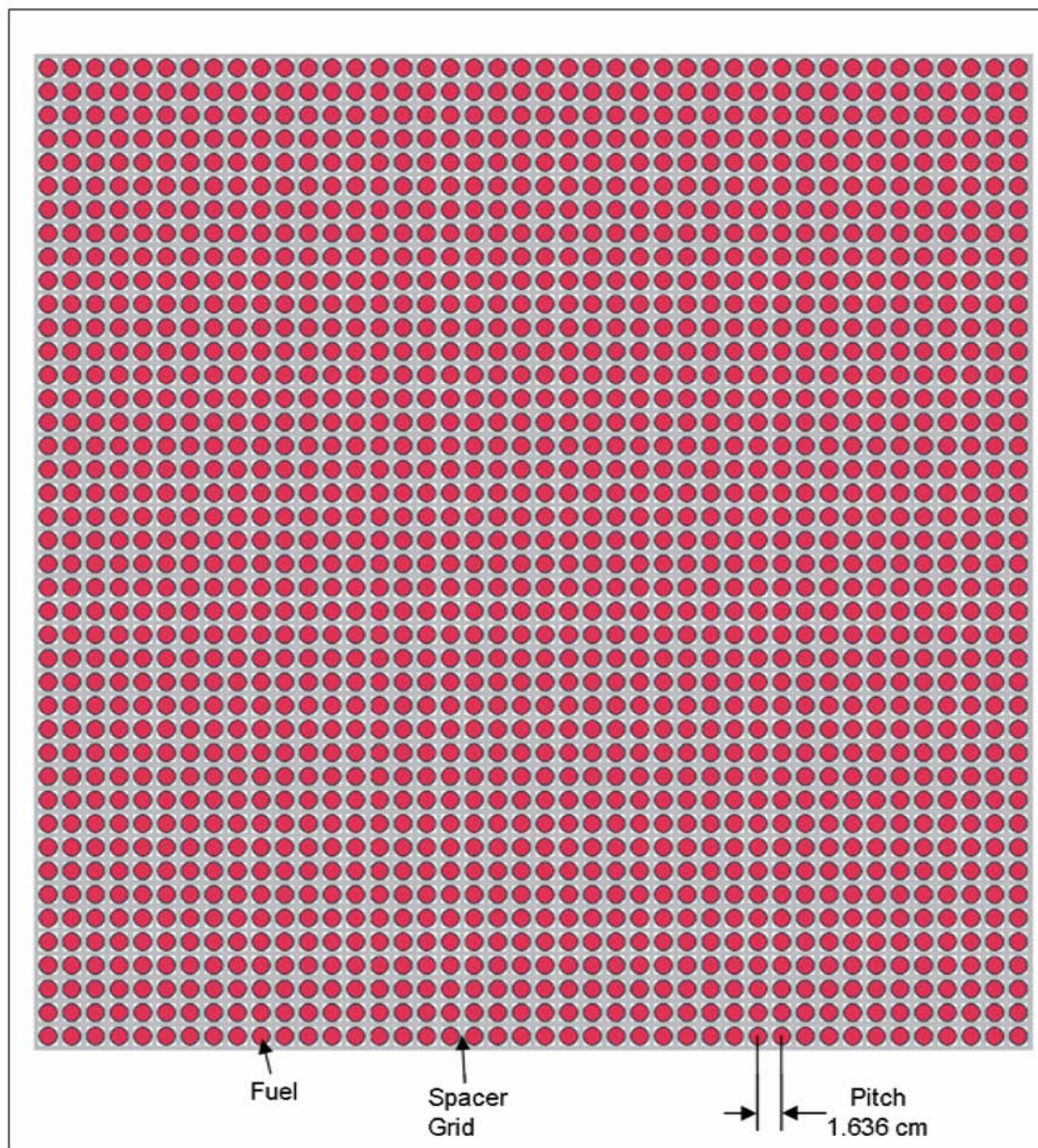
Figure 17. Pin Maps for Cases 7 through 10 for LEU-COMP-THERM-007

Attachment 3: Critical Benchmark Pin Maps for LEU-COMP-THERM-011



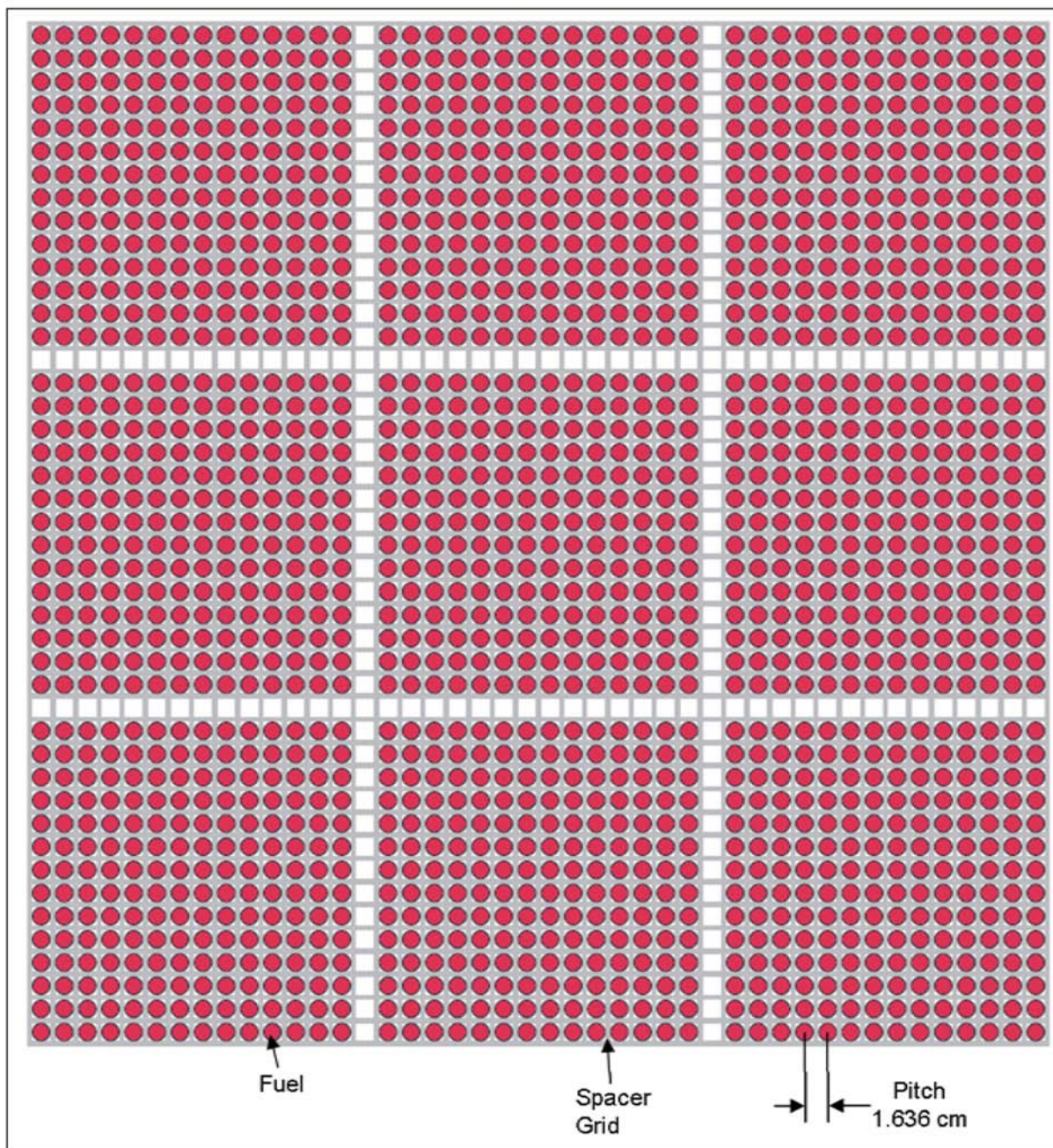
Source: Adapted from Figure 3 of LEU-COMP-THERM-011 benchmark report from the *International Handbook of Evaluated Criticality Safety Benchmark Experiments* (Ref. 2.2.6)

Figure 18. Pin Map for Case 1 of LEU-COMP-THERM-011



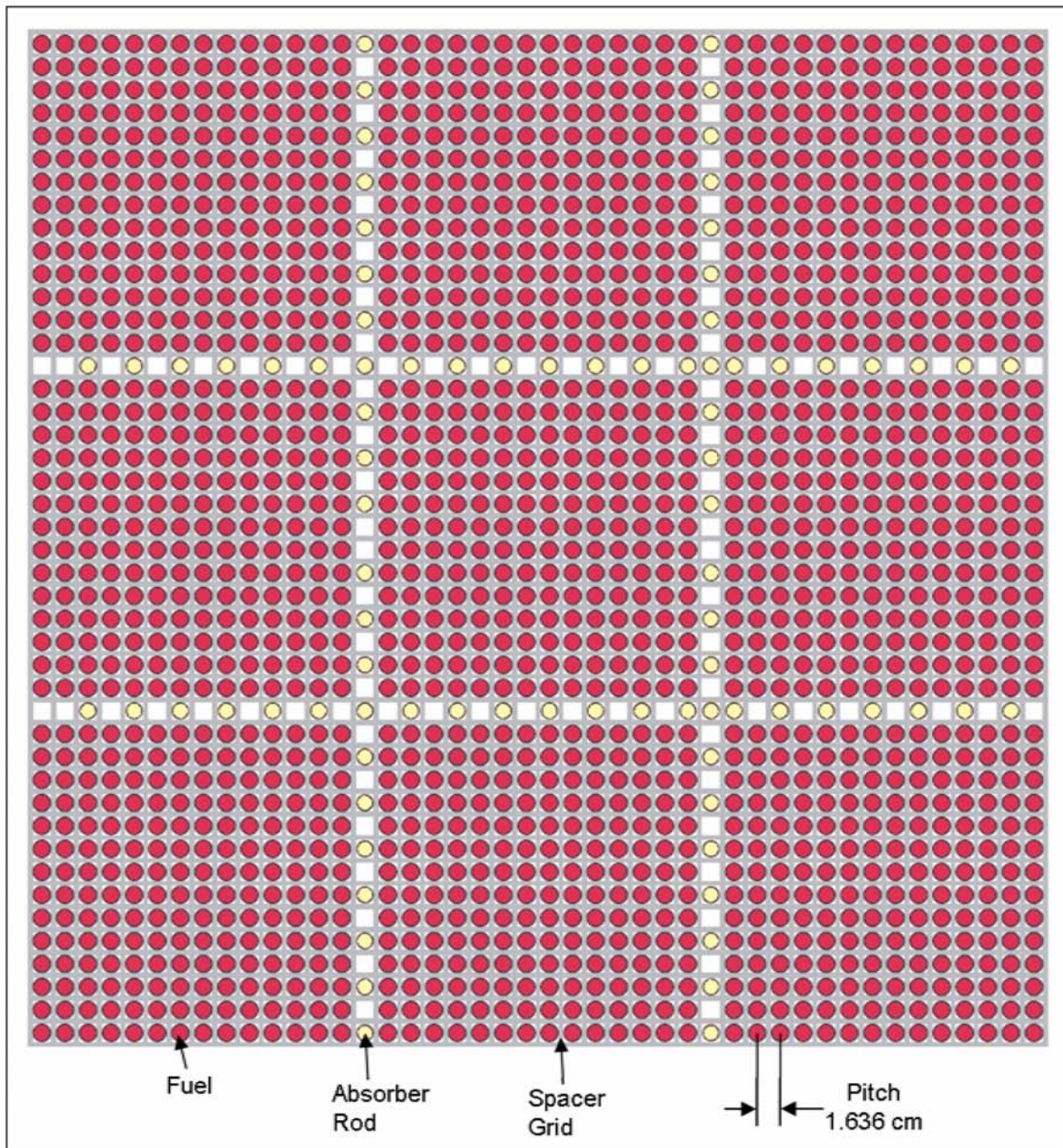
Source: Adapted from Figure 4 of LEU-COMP-THERM-011 benchmark report from the *International Handbook of Evaluated Criticality Safety Benchmark Experiments* (Ref. 2.2.6)

Figure 19. Pin Map for Case 2 of LEU-COMP-THERM-011



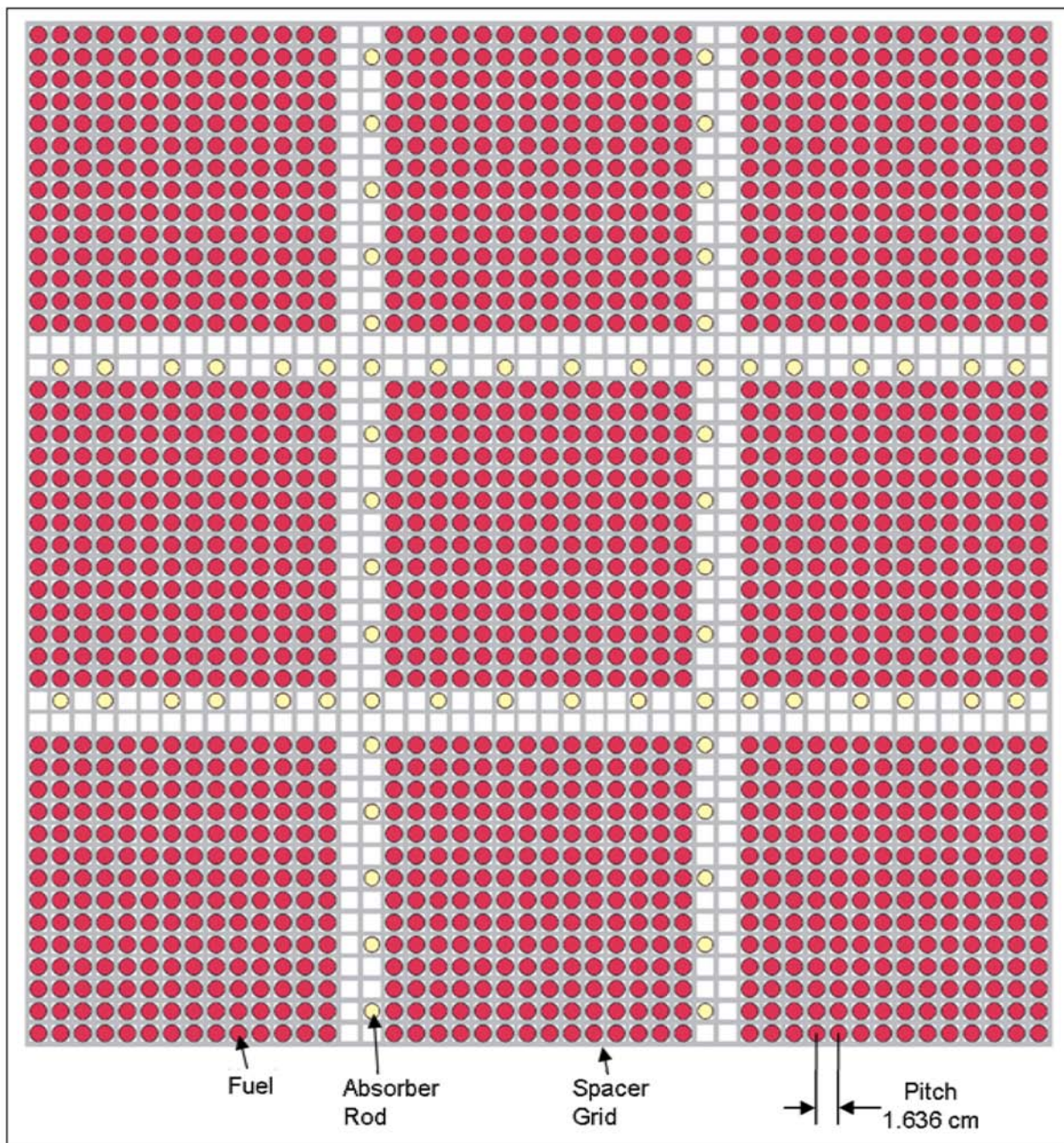
Source: Adapted from Figure 5 of LEU-COMP-THERM-011 benchmark report from the *International Handbook of Evaluated Criticality Safety Benchmark Experiments* (Ref. 2.2.6)

Figure 20. Pin Map for Cases 3 through 9 of LEU-COMP-THERM-011



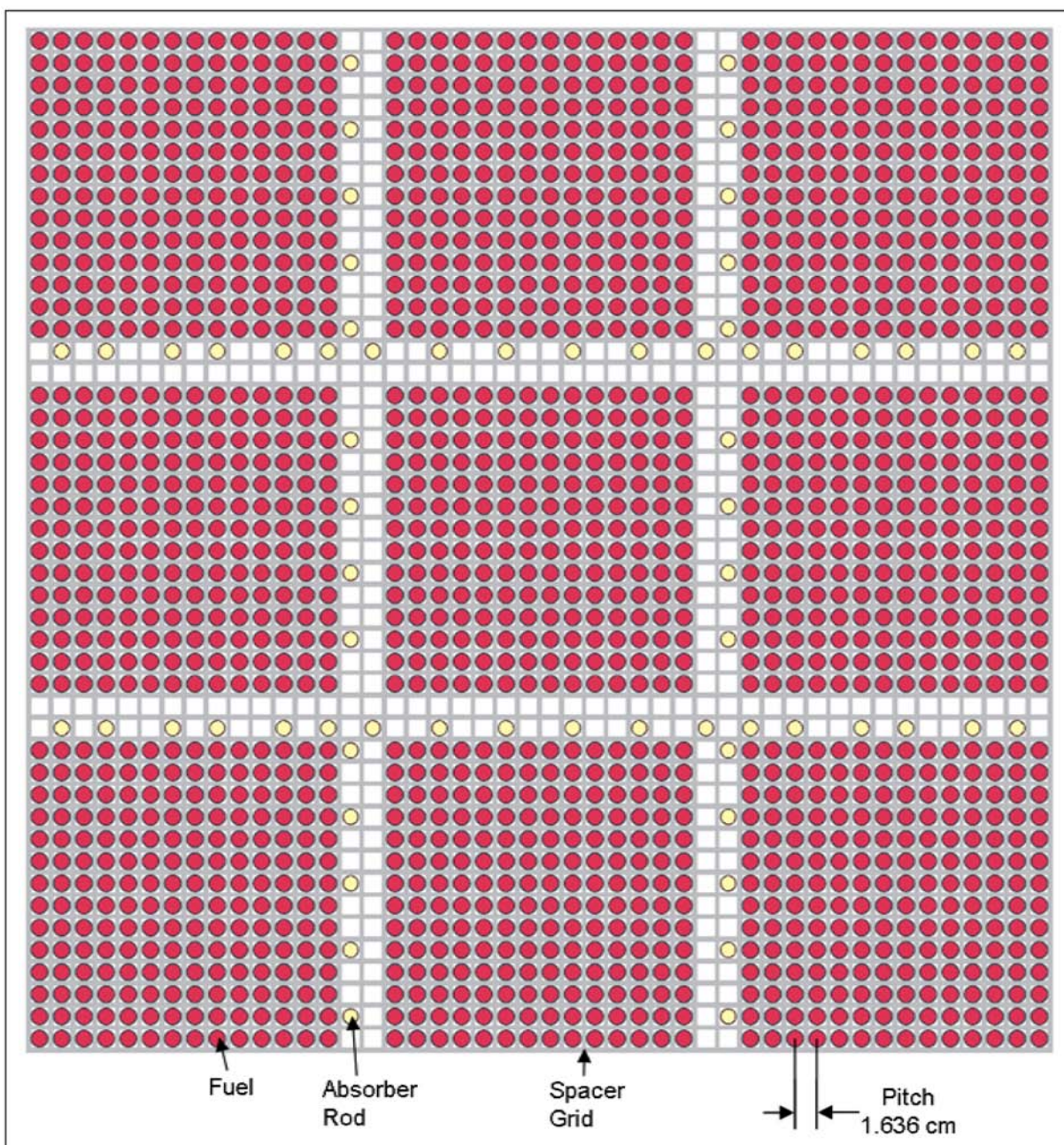
Source: Adapted from Figure 6 of LEU-COMP-THERM-011 benchmark report from the *International Handbook of Evaluated Criticality Safety Benchmark Experiments* (Ref. 2.2.6)

Figure 21. Pin Map for Case 10 of LEU-COMP-THERM-011



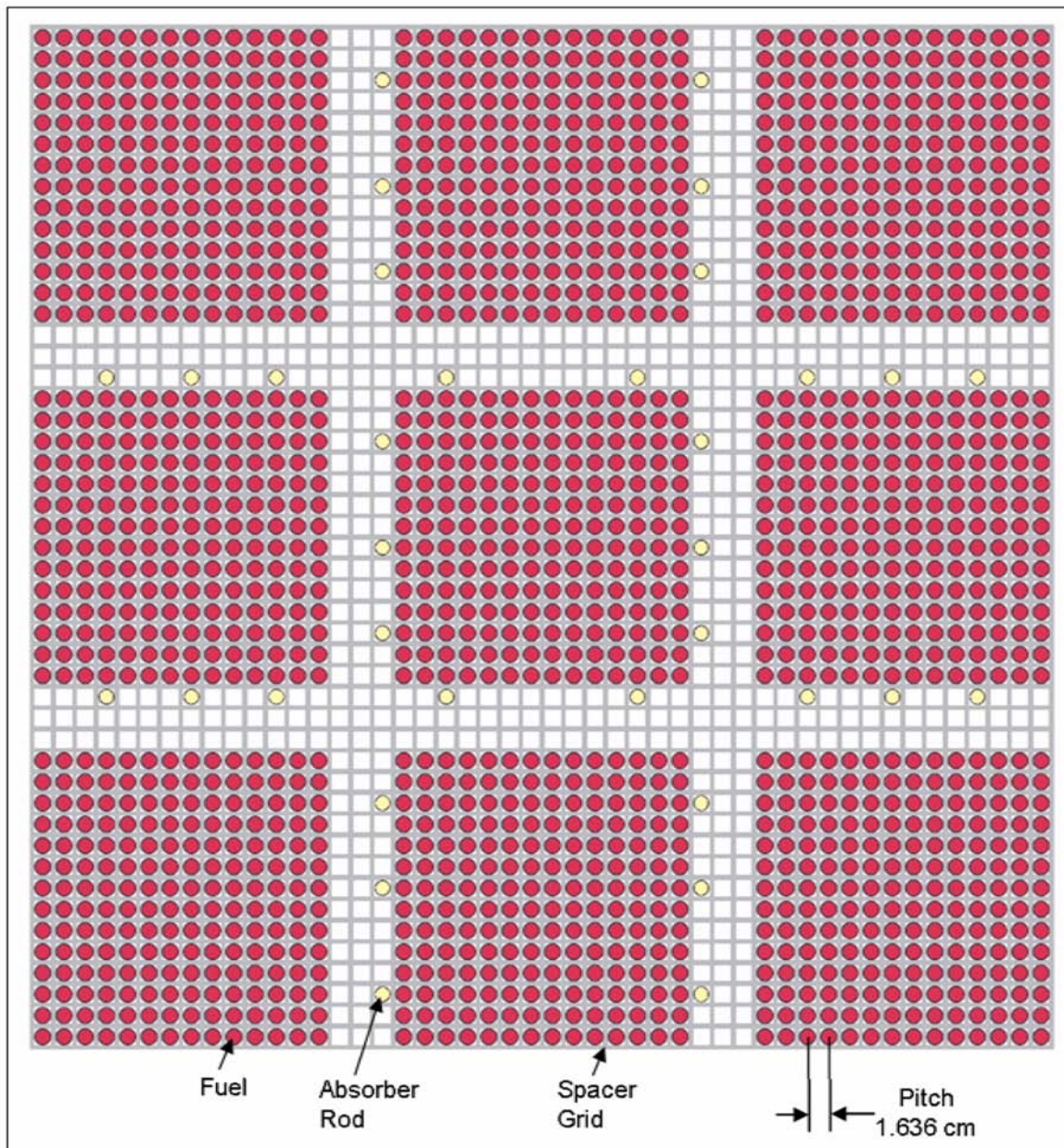
Source: Adapted from Figure 7 of LEU-COMP-THERM-011 benchmark report from the *International Handbook of Evaluated Criticality Safety Benchmark Experiments* (Ref. 2.2.6)

Figure 22. Pin Map for Case 11 of LEU-COMP-THERM-011



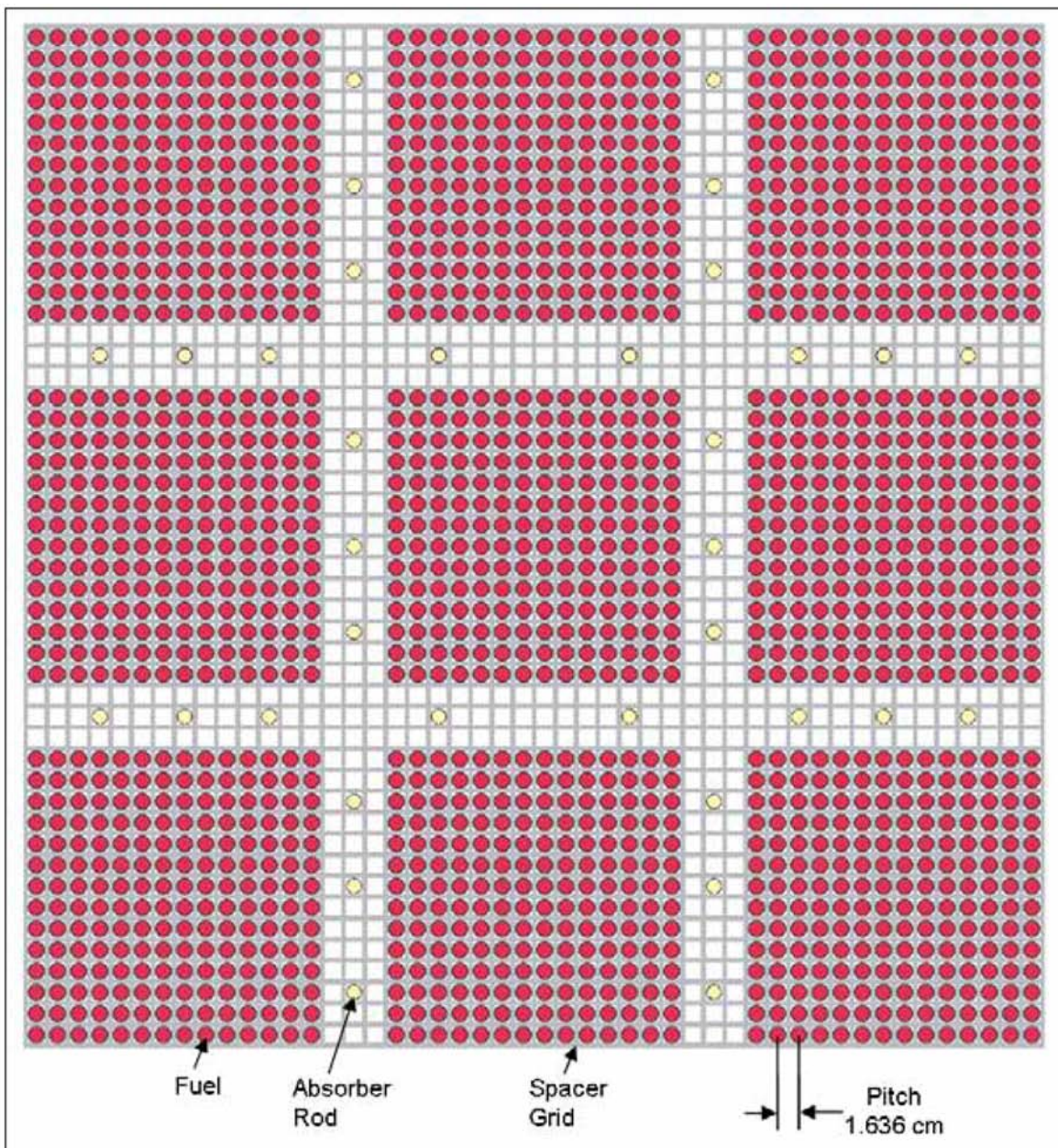
Source: Adapted from Figure 8 of LEU-COMP-THERM-011 benchmark report from the *International Handbook of Evaluated Criticality Safety Benchmark Experiments* (Ref. 2.2.6)

Figure 23. Pin Map for Case 12 of LEU-COMP-THERM-011



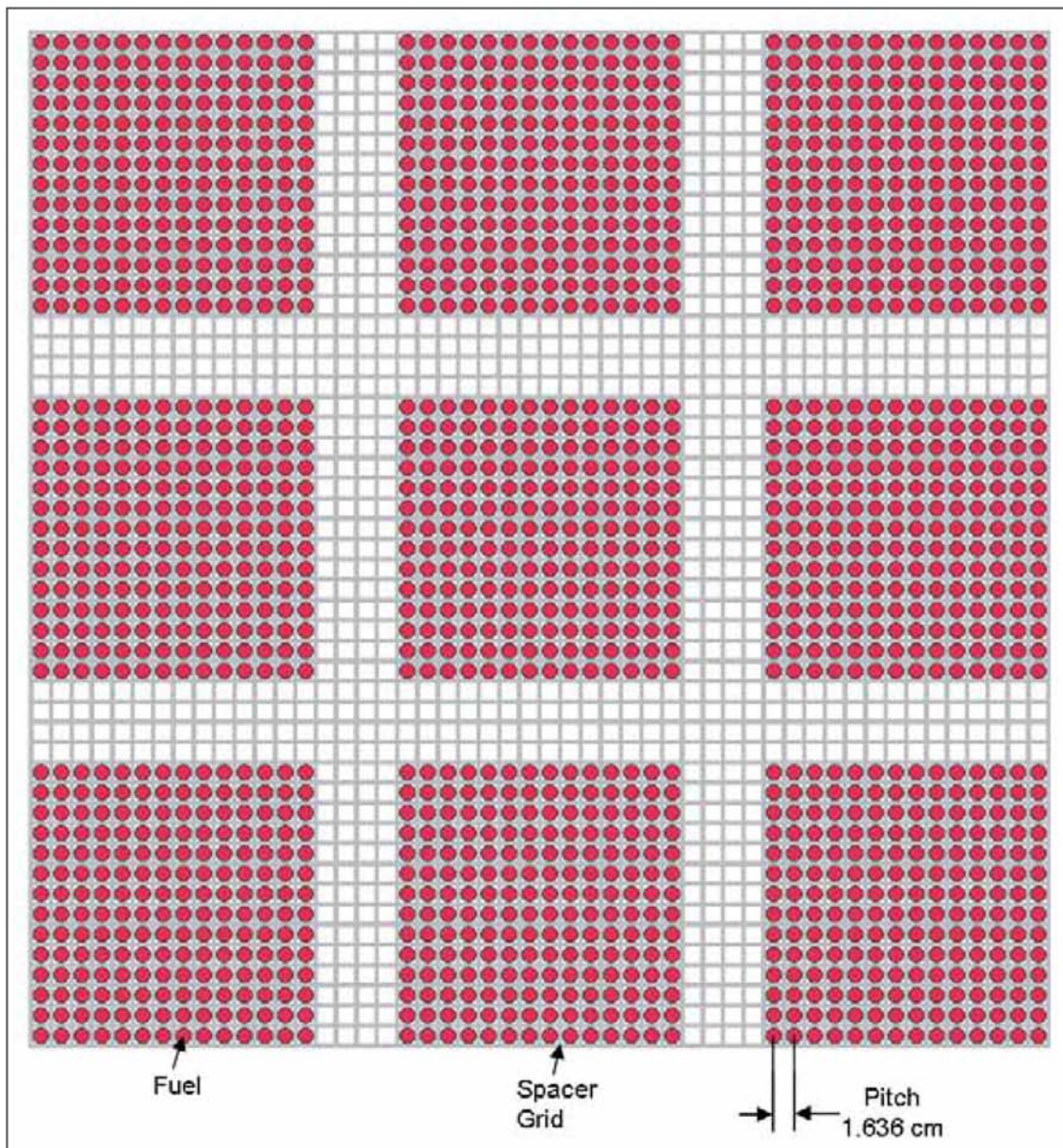
Source: Adapted from Figure 9 of LEU-COMP-THERM-011 benchmark report from the *International Handbook of Evaluated Criticality Safety Benchmark Experiments* (Ref. 2.2.6)

Figure 24. Pin Map for Case 13 of LEU-COMP-THERM-011



Source: Adapted from Figure 10 of LEU-COMP-THERM-011 benchmark report from the *International Handbook of Evaluated Criticality Safety Benchmark Experiments* (Ref. 2.2.6)

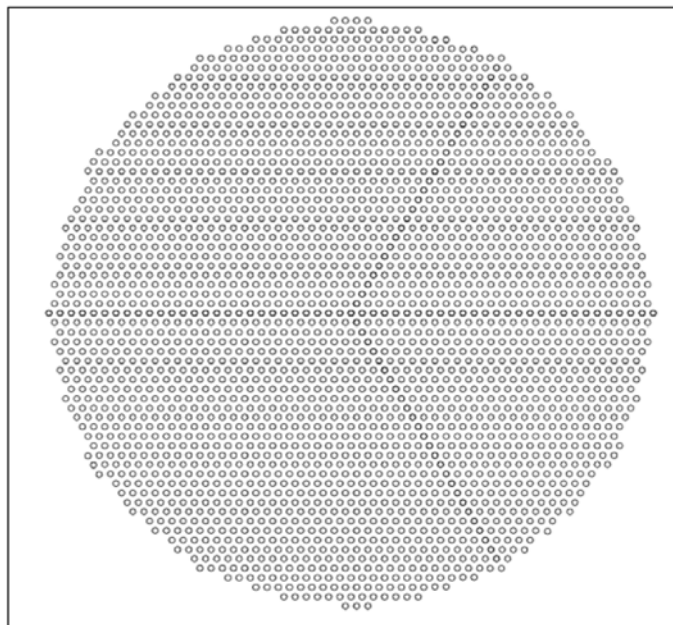
Figure 25. Pin Map for Case 14 of LEU-COMP-THERM-011



Source: Adapted from Figure 11 of LEU-COMP-THERM-011 benchmark report from the *International Handbook of Evaluated Criticality Safety Benchmark Experiments* (Ref. 2.2.6)

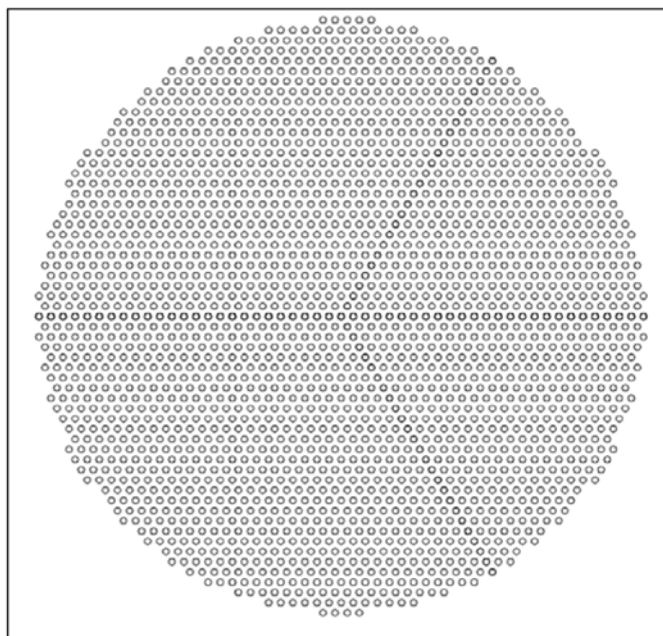
Figure 26. Pin Map for Case 15 of LEU-COMP-THERM-011

Attachment 4: Critical Benchmark Pin Maps for LEU-COMP-THERM-021



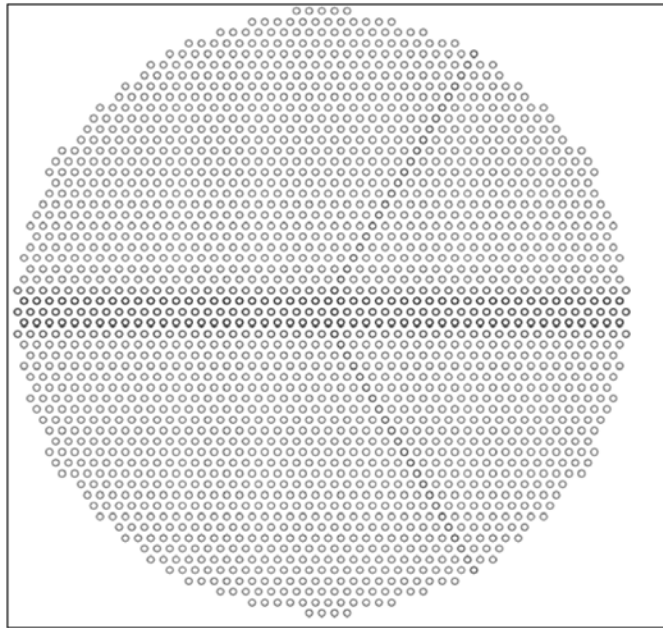
Source: Figure 4 of LEU-COMP-THERM-021 benchmark report from the *International Handbook of Evaluated Criticality Safety Benchmark Experiments* (Ref. 2.2.6)

Figure 27. Case 1 Pin Map for LEU-COMP-THERM-021



Source: Figure 5 of LEU-COMP-THERM-021 benchmark report from the *International Handbook of Evaluated Criticality Safety Benchmark Experiments* (Ref. 2.2.6)

Figure 28. Case 2 Pin Map for LEU-COMP-THERM-021



Source: Figure 6 of LEU-COMP-THERM-021 benchmark report from the *International Handbook of Evaluated Criticality Safety Benchmark Experiments* (Ref. 2.2.6)

Figure 29. Case 3 Pin Map for LEU-COMP-THERM-021

Attachment 5: List of Files on the Attachment 6 CD

This attachment contains a listing and description of the files contained on the attachment CD of this report (Attachment 6). The CD was written using Sonic DigitalMedia Plus v7 installed on DOE M&O Property tag number YMP003943 central processing unit, and can be viewed on most standard CD-ROM drives. The zip archive was created using WINZIP 9.0 SR-1. The file attributes on the CD are as follows:

Filename	File (KB)	Size	File Date	File Time	Description
MCNP Files.zip	11,000		02/12/08	8:48a	Archive containing MCNP files
Commercial Benchmark Materials.xls	240		02/12/08	8:50a	Excel spreadsheet of material determinations
Commercial Validation Results.xls	1,119		02/12/08	8:50a	Excel spreadsheet of results

The archive file (*MCNP Files.zip*) contains a total of 164 files (not including folders) contained in a unique directory structure. Files ending with an “in” are input files, and files ending with an “ino” are output files.